OFFICIAL JOURNAL OF THE SCIENTIFIC SOCIETY OF
ANATOMISTS, HISTOLOGISTS, EMBRYOLOGISTS AND
TOPOGRAPHIC ANATOMISTS OF UKRAINE

DOI: 10.31393
ISSN 1818-1295
eISSN 2616-6194

ВІСНИК МОРФОЛОГІЇ
REPORTS OF MORPHOLOGY

Vol. 26, №2, 2020

Scientific peer-reviewed journal in the fields of normal and pathological anatomy, histology, cytology and embryology, topographical anatomy and operative surgery, biomedical anthropology, ecology, molecular biology, biology of development

Published since 1993
Periodicity: 4 times a year

Vinnytsya • 2020

ВІСНИК МОРФОЛОГІЇ - REPORTS OF MORPHOLOGY

Founded by the "Scientific Society of Anatomists, Histologists, Embryologists, and Topographic Anatomists of Ukraine" and National Pyrogov Memorial Medical University, Vinnytsya in 1993

Certificate of state registration КВ №9310 from 02.11.2004

Professional scientific publication of Ukraine in the field of medical sciences in specialties 221, 222, 228, 229
According to the list of professional scientific publications of Ukraine, approved by the order of the Ministry of Education and Science of Ukraine No. 1188 of 24.09.2020 (Annex 5)

Approved by the Academic Council of National Pyrogov Memorial Medical University, Vinnytsya, protocol №4 від 08.10.2020

Indexation: CrossRef, elibrary.ru, Google Schoolar Metrics, National Library of Ukraine Vernadsky

Address editors and publisher:
Pyrogov Str. 56,
Vinnytsya, Ukraine - 21018
Tel.: +38 (0432) 553959
E-mail: nila@vnmu.edu.ua

Computer page-proofs - Klopotovska L.O.
Translator - Gunas V.I.
Technical support - Levenchuk S.S., Parashuk O.I.
Scientific editing - editorship

The site of the magazine - https://morphology-journal.com

CONTENT

DOI: 10.31393/morphology-journal-2020-26(2)-01 Reports of Morphology, Vol. 26, №2, Pages 5-11

ISSN 1818-1295 eISSN 2616-6194

REPORTS OF MORPHOLOGY

Official Journal of the Scientific Society of Anatomists, Histologists, Embryologists and Topographic Anatomists of Ukraine

journal homepage: https://morphology-journal.com

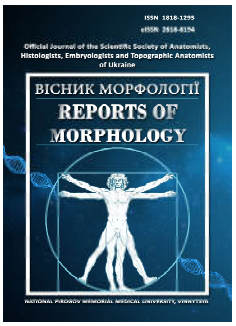

Histological changes of the arterial bed of the hind limbs of the rats under condition of the acute ischemia-reperfusion and correction with the carbacetam

Veresiuk T.O., Selskyy P.R.

I. Horbachevsky Ternopil National Medical University, Ternopil, Ukraine

ARTICLE INFO

Received: 15 June, 2020

Accepted: 20 July, 2020

UDC: 616.137.83/93-091.8:616-005.4:615.214.3]-092.9

CORRESPONDING AUTHOR

e-mail: taras-o@ukr.net

Veresiuk T.O.

The ischemic-reperfusion lesion is a complex multifactorial damage of the primary ischemic tissues as a result of restoration of the arterial blood circulation in them, which is accompanied by local morpho-functional reorganization of the vascular bed of the hind limbs of the rats. One of the promising means in the treatment and prevention of the reperfusion disorders is a carbacetam, which smooths the phenomena of hypo- and hyperperfusion in the post-ischemic period. The aim of the study was to established the manifestations of the morpho-functional remodeling of the vascular bed of the hind limbs of the rats in ischemia-reperfusion and under conditions of correction with carbacetam. Histological examination of the vascular bed of the hind limbs of 30 rats under conditions of ischemia-reperfusion (group I) and 30 rats in the simulation of ischemia-reperfusion, which in the post-ischemic period administered carbacetam once a day (5 mg/kg) for 14 days (group II) were done. There were 6 intact animals in the control group. Simulation of ischemia was performed by applying SWAT rubber tourniquets on the hind limbs for 2 hours, and reperfusion - by removing of the tourniquet. The animals of the experimental groups were divided into 5 subgroups with reperfusion terms after 1, 2 hours and 1 day, as well as after 7 and 14 days. Histological examination was performed according to generally accepted methods. The vascular bed in the middle third of the thigh and the shin below the tourniquet was examined using a Bresser Trino Researcher 40x-1000x microscope. Analyzing of the obtained results, was established that after 1 hour of the reperfusion the histological changes became a systemic, and after 1 day it were more significant. It should be noted that the thickness of the vessel walls increased, and the elastic membranes were partially eligned, thinned and torned. The stepwise clarity of the arterials walls structure was lost. The edema acquired a total nature. The histological examination of the vessels after 7 days revealed that the swelling of the walls decreased and the condition of the elastic frame was improved. There was a proliferation of collagen fibers in the adventitia, which was a response to ischemic effects. It is noted that after 14 days in all wall membranes the proliferative activity of fiboblasts was remained. Under the conditions of the correction with the carbacetam after 2 hours, the structural positive dynamics became more pronounced and increased to a maximum level after 7 days of the experiment. The number of the modified and exfoliated endothelial cells decreased, and the condition of smooth myocytes increased. Histologically, the gradual restoration of endothelial coverage of the intima was established. As follows, ischemia and reperfusion cause vascular remodeling after 1 hour with a peak of the manifestations after 1 day of the reperfusion, which includes edematous syndrome, dystrophic-degenerative changes with an inflammatory response to the damage, and in the late reperfusion period increased a fibroblasts activity. Gradual return of morphological changes occurs after 14 days of the experiment. Under the conditions of correction, the acceleration of the remodeling with stabilization of the process and the most possible structural restoration after 7 days of the study was noted.

Keywords: *artery, remodeling, ischemia-reperfusion, elastic membranes, carbacetam.*

Introduction

Ischemic-reperfusion lesion is a complex multifactorial process of damage and dysfunction of primary ischemic tissues as a result of restoration of arterial blood circulation in conditions of acute or chronic ischemia [9, 11, 13, 15, 19, 22]. Arterial ischemia is one of the main reasons for the deterioration of the quality of life of patients, their early disability and accounts for about 10% of all gunshot wounds in the structure of combat trauma [5, 15]. In 67% of cases of vascular damage at the prehospital stage, a tourniquet is applied, which can induce reperfusion damage [4, 9, 10, 15, 22].

Recently, more and more attention in the treatment and prevention of ischemic disorders is paid to nootropic drugs that have metabolic, neuroprotective, antiplatelet, antioxidant effects, as well as smoothing the phenomena of hypo- and hyperperfusion in the postischemic period, increase microcirculation in tissues. Among the new drugs, carbacetam, an endogenous modulator of the GABA-benzodiazepine receptor complex derived from β-carboline, is markedly secreted [7, 23]. The effectiveness of its use is shown in the work on the restoration of cognitive impairment, reduction of endogenous intoxication and oxidative stress in polytrauma [23].

Literature data indicate that the morphological manifestations of the syndrome of ischemia and reperfusion are impaired hemomicrocirculation, which is histologically manifested by endothelial edema, leukocyte-endothelial adhesion, hemodynamic disorders, reduction of microvascular and arteriovenous shunting, however, morpho-functional changes in arteries of large diameter, their dynamics, as well as the search for means of tissue protection remains open for further research [9, 13].

However, in reviewing the scientific and experimental literature, we did not find any publications on the use of this drug for the treatment and prevention of complications of ischemia-reperfusion, which prompted an attempt to use carbacetam to study the local correction of reperfusion.

The aim of the study was to establish the manifestations of morphofunctional reorganization of the vascular bed of the hind limbs of rats during ischemia-reperfusion and under conditions of correction with carbacetam.

Materials and methods

Histological examination of the vascular bed of 60 rats have been done.

Ischemia was modeled by applying SWAT (Stretch-Wrap-And-Tuck) rubber tourniquets to the right hind limb of the animal at the level of the inguinal fold for 2 hours under thiopental-sodium anesthesia. The reperfusion syndrome was modeled by removing the tourniquet and restoring blood circulation in the previously ischemic limb 2 hours after application. Observations of animals were carried out for 14 days.

During the experiment, the experimental animals were divided into three groups:

- first experimental group (30 rats) - animals with simulation of ischemic-reperfusion injury;
- second experimental group (30 rats) - animals with simulation of ischemic-reperfusion damage, in which 1-oxo-3.3.6-trimethyl-1.2.3.4-tetrahydroindolo [2.3-c] quinolines (carbacetam) was injected intraperitoneally in the reperfusion period for the purpose of correction at a dose of 5 mg per kilogram of body weight 1 time per day for 14 days of the reperfusion period;
- control group (6 rats) - intact animals.

Animals of the first and second experimental groups were divided into 5 subgroups (6 animals each). The model of the early post-ischemic period in both groups was presented by subgroups of animals with reperfusion changes after 1, 2 hours and 1 day, and the model of the late reperfusion period - by subgroups of animals 7 and 14 days after removal of the tourniquet.

All studies were conducted in compliance with the main provisions of the Law of Ukraine № 3447-IV of 21.02.06 "On the protection of animals from cruel treatment" (2006) and Council of Europe Directive 2010/63 EU on animal experiments.

Euthanasia of animals was performed by administration of thiopental-sodium anesthesia (500 mg/kg body weight intraperitoneally), followed by decapitation and collection of biological material. Soft tissue samples, together with the vascular-nervous bundle of the hind limb of the animals, were taken below the level of the tourniquet at the level of the middle third of the thigh, followed by fixation, dehydration and paraffin removal, which were performed according to conventional methods. Prepared a series of sections with a thickness of 4-5 μm, made on a microtome MS-2. The latter, after dewaxing, were stained with hematoxylin and eosin, picrofuchsin by Van Gieson's method, resorcin fuchsin by Weigert's elastic stain method, and Heidenhain's AZAN trichrome stain method [17]. This made it possible to obtain differentiated tissue staining due to the heterogeneity of the perception of different dyes by biological tissues.

Examination of the preparations was performed using a Bresser Trino Researcher 40x-1000x microscope (serial number 0913137). The most demonstrative histological specimens were photographed using a Digital Camera for Microscope Science Lab DCM 820 Resolution 8.0 Mp.

Results

Histological examination of the main arteries and veins of the thigh and lower leg showed that the structural organization of their walls corresponds to the generally accepted criteria. Elastic membranes are clearly contoured in the form of a homogeneous eosinophilic strip. Arteria of the tibia and femur segments differ only in diameter (Fig. 1).

After 1 hour of reperfusion changes became systemic and appeared at all levels of structural organization of blood vessels. Rounded, due to the swelling of the cytoplasm, endothelial cells protruded into the lumen of blood vessels,

Fig. 1. Clearly contoured inner and outer elastic membranes of the femoral arteria of the rat of the control group. 1 - inner elastic membrane; 2 - outer elastic membrane. Weigert's elastic stain, x200.

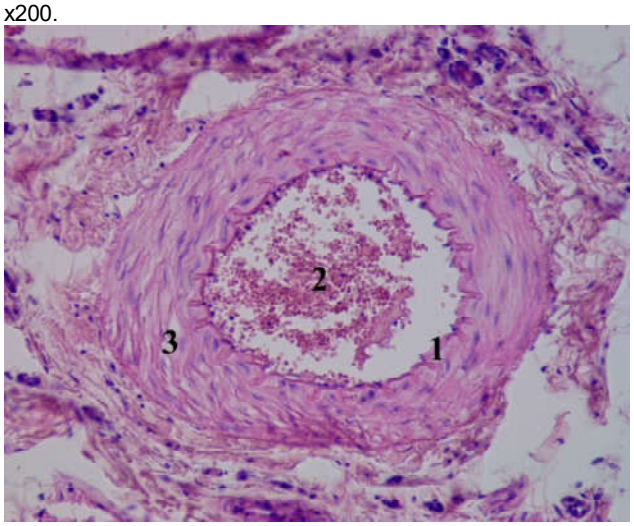

Fig. 2. Endothelial cell exfoliation, aggregation and adhesion of erythrocytes. The edema of the media. Section of the femoral arteria of the rat after 1 hour of reperfusion. 1 - exfoliation of endothelial cells; 2 - aggregation and adhesion of erythrocytes; 3 - edema of the artery wall. Hematoxylin and eosin stain, x200.

and some of them peeled off. The tortuosity of the inner elastic membrane became irregular, split. There have been sticking and adhesion erythrocytes. As a result of the swelling, the subendothelial prosthesis expanded, and smooth myocytes sometimes lost their compact position. Dystrophic changes of myocytes were determined in parallel. Lymphocytes were occasionally detected. Adventitia was disturbed (Fig. 2).

Histologically, after 2 hours of reperfusion, structural changes intensified. Often endothelial cells were exfoliated in layers. The intima thickened, lost its integrity, and sometimes exfoliated along with endothelial cells. Swelling of the subendothelial layer increases. Elastic membranes at this time are split, straightened and often fragmented, which we regarded as a sign of loss of vascular wall tone. Smooth myocytes with signs of vacuolar dystrophy were distinguished by intercellular substance. The swelling of the outer membrane, enriched at this time by cells of hematogenous origin, including lymphocytes, visually thickened the vascular wall (Fig. 3).

After 1 day, structural changes became the most significant. The wall thickness increased. Elastic membranes were partially leveled, thinned and developed, sometimes transforming into chains of fragments of various sizes. Endotheliocytes did not differ structurally from those we had already found in the previous terms of the experiment. The difference was that after 1 day these manifestations became systemic and almost uniformly expressed in all segments of the vascular bed. The clarity of the layered structure of the arteria walls was lost. Dystrophic and degenerative changes of smooth myocytes in the form of their vacuolation, focal and total cytolysis were manifested. Round-cell infiltrates are present in all layers. Defects of the endothelial lining and the appearance of vasculitis created the preconditions for parietal aggregation of erythrocytes and thrombosis. Edema acquired a total character and tended to spread to the paravasal prostheses and skeletal muscles (Fig. 4).

Changes in the main vessels after 7 days were generally identical to the previous reperfusion period. The swelling of the arteria walls decreased due to the restoration of the endothelial covering of the intima. Among myocytes, dystrophically altered cells and low-intensity cellular infiltrates, predominantly lymphocytes with an admixture of proliferating fibroblasts and single histiocytes, were not uncommon. In general, the condition of the elastic membranes improved. In most cases, the integrity of the elastic membranes was preserved. However, straightening and fragmentation of elastic fibrils were also not uncommon (Fig. 5).

In adventitia and perivascular stoma there was a

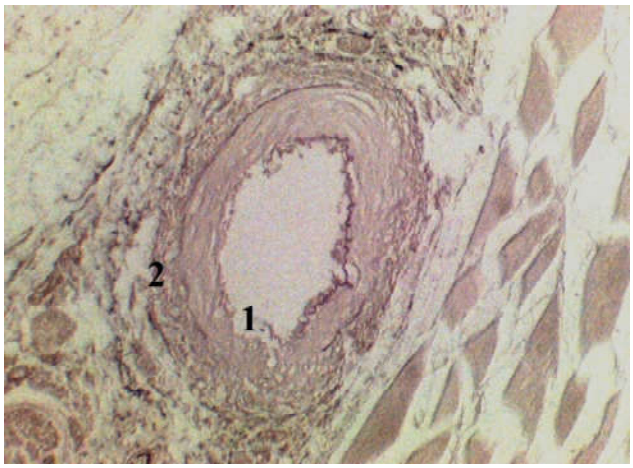

Fig. 3. Thinned, split and partially lysed elastic fibers. Cranial tibial arteria of the rat after 2 hours of reperfusion. 1 - thinned and split inner elastic membrane; 2 - partially lysed outer elastic membrane. Weigert's elastic stain, x100.

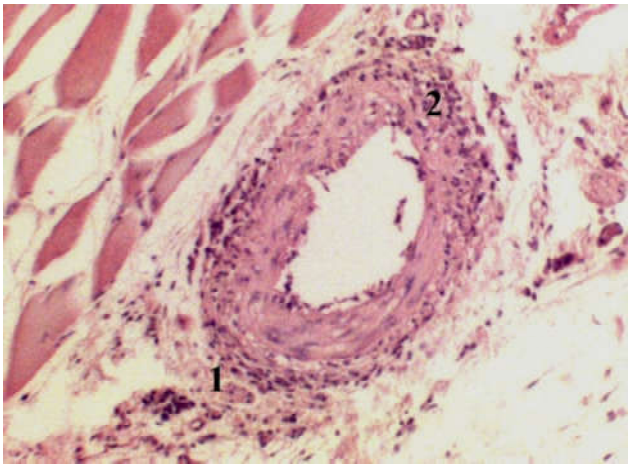

Fig. 4. Destructive changes in the wall of the arteria, combined with an intense inflammatory reaction, expressed in swelling around the vessel with spread to the muscle. Section of the femoral artery of the rat after 1 day of perfusion. 1 - paravasal edema; 2 - wall infiltration. Hematoxylin and eosin stain, x100.

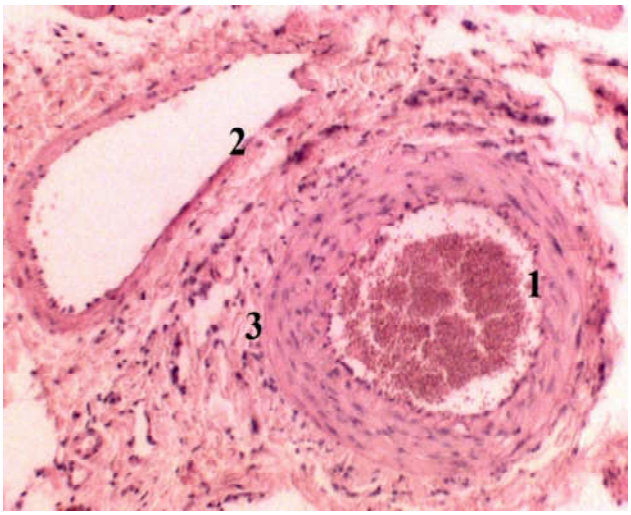

Fig. 5. Multiple foci of desquamation of damaged endothelial cells of the arteria and veins of the tibial segment after 7 days of reperfusion. Low-intensity cellular infiltration of adventitia and media. 1 - desquamation of endothelial cells of the cranial artery of the tibia; 2 - desquamation of endothelial cells of the tibial vein intima; 3 - moderate lymphocytic infiltration of the adventitia. Hematoxylin and eosin stain, x100.

proliferation of collagen fibers, which was an adequate response to long-term ischemic effects.

After 14 days in the arteria of all segments revealed an increase in the number of collagen fibers in the subendothelial space and the outer membrane of the arteria. Leiomyocyte hyperopia and an increased proportion of connective tissue component were detected in the thickened media. The elastic fibers of the inner elastic membrane were unevenly polished, restoring integrity. However, in the media and at the sites of localization of the outer membrane, the elasticity was blurred or absent. Along with this, swelling, desquamation of individual and dystrophic changes of smooth myocytes were preserved. In all wall membranes, the intensity of lymphohistiocytic infiltration was significantly reduced, but the proliferative activity of fibroblasts was preserved (Fig. 6).

The morphological studies of the vascular bed under the conditions of carbacetam correction showed that after 1 hour the systemic hemodynamic disturbances in all segments of the vascular bed did not differ much from the ischemia-reperfusion already detected by us at the same time, without correction and increased in the direction of shin.

After 2 hours, the positive dynamics of structural changes in the arteria became more pronounced. The number of modified and exfoliated endothelial cells decreased. Most of the cells were located on the basement membrane, which reduced the intensity of plasma penetration of arteria walls.

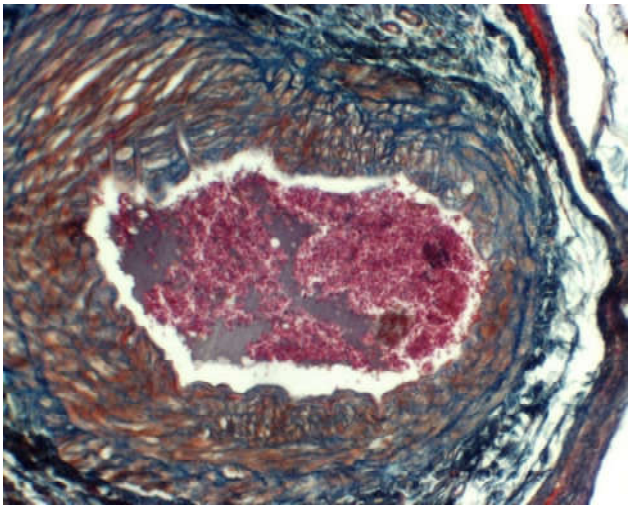

Fig. 6. Proliferation of connective tissue fibers in all membranes of the wall of the femoral arteria of rat after 14 days of reperfusion. Heidenhain's AZAN trichrome stain, x100.

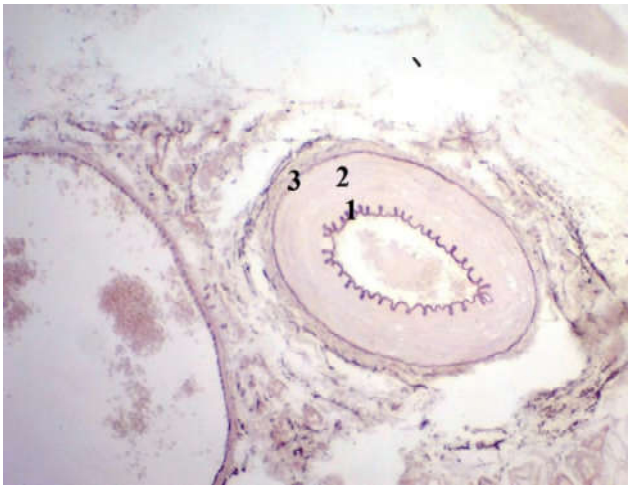

Fig. 7. The inner elastic membrane of the arteria is preserved, the elastic of the middle membrane is absent, in the vein wall it is partially fragmented. Knee arteria and vein of the rat after 2 hours of reperfusion with correction. 1 - clear inner elastic membrane; 2 - lack of elastic fibers in the media; 3 - outer elastic membrane. Weigert's elastic stain, x100.

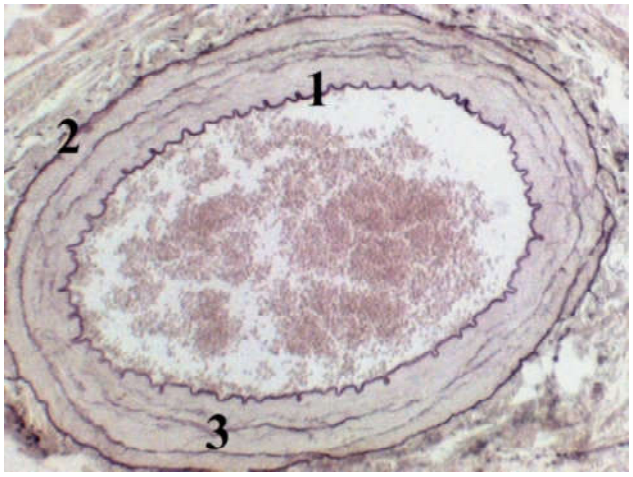

Fig. 8. Clear inner and outer elastic membranes of arteria and fragmentation of elastic fibers of media. Femoral arteria of the rat after 14 days of reperfusion with correction. 1 - clear inner elastic membrane; 2 - outer elastic membrane; 3 - fragmentation of elastic fibers of the media. Weigert's elastic stain, x200.

The reduction of ischemic effects contributed to the deterioration of smooth myocytes - the number of cells with vacuolated sarcoplasm decreased. The intercellular amorphous substance was poorly differentiated. Single lymphocytes, macrophages, and fibroblasts were present in all wall membranes (Fig. 7).

Destructive changes in elastic fibers lost their systemicity and were rather sporadic. In the large and middle veins, plethora prevailed. The endothelial lining largely preserved integrity.

After 1 day, the positive dynamics increased and reached its maximum after 7 days of the study, slowing down and stabilizing after 14 days of the experiment.

During these periods, we found a gradual restoration of endothelial coverage of the intima. Most cells had normal outlines, but among them there were cells with cytoplasmic swelling. Elastic membranes had a characteristic configuration. Closer to the end of the experiment, we did not notice their splitting or fragmentation (Fig. 8).

Despite the fact that under the condition of correction a significant share of structural disturbances has consistently returned to its initial state, starting from the early perfusion period, at the final stage we detected residual phenomena. Thus, hypertrophy of a part of smooth myocytes of arteria (together with atrophic ones) and an increase in the number of thin collagen fibers in the extracellular matrix, mainly on the border with the outer shell, were detected. In adventitia, the proportion of collagen fibers also increased.

Discussion

It is known that ischemia and reperfusion is a complex multifactorial process with changes in cellular metabolism, disruption of ion transport and activation of proteinases, processes of lipid peroxidation, which leads to cell death in cells and and release of cytotoxic intracellular components and is a consequence not only of ischemia but also of reoxygenation, which often significantly activates pathological processes and causes local and systemic disorders [2]. Their morphological manifestations are: remodeling of vessels of both large caliber and microvessels of the hemomicrocirculatory tract, soft tissues with the development of edema, necrotic-destructive changes and violation of the rheological properties of blood [3].

The mechanism of perfusion damage is associated with impaired microcirculation, with pronounced endothelial swelling, leukocyte-endothelial adhesion, albumin extravasation and impaired arteriole relaxation [16]. Thus, the processes that occur during ischemia are the result not only of ischemia, but also of reoxygenation, which not only does not stop their development, but also often significantly activates pathological processes [21].

At long ischemia of extremity tissue there is a desolation of a microcirculatory channel with the subsequent reduction of microvessels that is shown by decrease in their quantity and decrease in a tissue blood flow. Against the background of restoration of arterial hemodynamics in the limb, the volume of blood entering the microcirculatory tract approaches normal, and the volume of the microcirculatory tract does not increase, which leads to a simultaneous increase in blood flow velocity in all microvessels of basal blood flow [8, 14, 18]. At the same time, these capillaries are not enough to provide adequate blood volume through the arterial bed, which leads to increased arteriovenous shunting [12]. Direct revascularization is accompanied by progression of regional venous hypertension and profound disruption of tissue circulation.

In studies of vascular reorganization during 6-hour ischemia and 6-hour perfusion, it is noted that in morphological examination - there are signs of moderately expressed perivascular edema, as well as a significant number of petechial hemorrhages [2, 6]. In certain fields, hemorrhages merge and resemble hemorrhagic infiltration [20]. Signs of sludge, as well as a significant number of fibrin clots are expressed in the lumen of some vessels, and inflammatory cells are located along the vessels [1].

As a result of our research, it was found that ischemia and perfusion cause remodeling of vessels of both large and small diameters. In the early perfusion period, structural changes included edematous syndrome, dystrophic-degenerative, and destructive changes in vessels with an inflammatory response to injury; the initiating factor can be considered ischemic endothelial damage.

In the late perfusion period, the remodeling of structural components was characterized by a slowing down of acute manifestations with a partial return to the initial state and the onset of fibroblastic diferon activity and the synthesis of connective tissue matrix in the walls of vessels and near them.

Changes in the histoarchitectonics of the vascular walls intensified in the distal direction, and after 14 days of reperfusion most of the signs returned to the control group.

In the stages of post-ischemic reperfusion under the conditions of carbacetam correction, soft tissue remodeling is sequential with stabilization of the process and structural recovery after 7 days of the experiment, while in animals without correction morphological signs of recovery were detected after 14 days.

Conclusions

Ischemia and reperfusion cause vascular remodeling after 1 hour with a peak of manifestations after 1 day of reperfusion, which includes edematous syndrome, dystrophic-degenerative changes with an inflammatory response to damage, and in the late reperfusion period increase in the activity of fibroblastic diferon. Gradual return of morphological changes occurs after 14 days of the experiment. Under the conditions of correction, there was an increase in remodeling with stabilization of the process and the most possible structural restoration after 7 days of the study.

References

[1] Ballestin, A., Casado, J. G., Abellan, E., Vela, F. J., Alvarez, V., Uson, A., ... Sanchez-Margallo, F. M. (2018). Ischemia-reperfusion injury in a rat microvascular skin free flap model: a histological, genetic, and blood flow study. *Plos One*, 13(12), e0209624. doi: 10.1371/journal.pone.0209624

[2] Blaisdell, F. W. (2002). The pathophysiology of skeletal muscle ischemia and the reperfusion syndrome: a review. *Cardiovascular Surgery,* 10(6), 620-630. doi: 10.1016/s0967-2109(02)00070-4

[3] DeAnda Jr., A., & Spiess, B. D. (2012). Aprotinin revisited. The *Journal of Thoracic and Cardiovascular Surgery,* 144(5), 998-1002. doi: 10.1016/j.jtcvs.2012.06.035

[4] Dunn, J. C., Kusnezov, N., Schoenfeld, A. J., Orr, J. D., Cook, P. J., & Belmont Jr, P. J. (2016). Vascular injuries in combat-specific soldiers during operation Iraqi freedom and operation enduring freedom. *Annals of Vascular Surgery,* 35, 30-37. doi: 10.1016/j.avsg.2016.01.040

[5] Elsharawy, M. A., Elsaid, A., & Elsharawi, I. (2014). Reperfusion of Delayed Acute Occlusive Limb Ischemia: Is It Worthwhile? *World Journal of Cardiovascular Diseases,* 4(12), 580-585. doi: 10.4236/wjcd.2014.412070

[6] Frias Neto, C. A. D. S., Koike, M. K., Saad, K. R., Saad, P. F., & Montero, E. F. D. S. (2014). Effects of ischemic preconditioning and cilostazol on muscle ischemia-reperfusion injury in rats. *Acta Cirurgica Brasileira*, 29, 17-21. doi: 10.1590/s0102-86502014001700004

[7] Gamzin, S. S., Alekseeva, L. V., & Lapina, G. P. (2015). Methodological aspects of biochemical and pharmacological analysis of the effect of nootropics on the peptidergic system and metabolism in general. *Bulletin of Tver State University. Series: Biology and Ecology,* (3), 40-52.

[8] Gleissner, C. A., Leitinger, N., & Ley, K. (2007). Effects of native and modified low-density lipoproteins on monocyte recruitment in atherosclerosis. *Hypertension*, 50(2), 276-283. doi: 10.1161/HYPERTENSIONAHA.107.089854

[9] Henyk, S. M., & Symchych, A. V. (2016). Reperfusion syndrome after revascularization of lower extremity ischemia. *Heart and Blood Vessels*, (3), 104-108.

[10] Hubka, V. O., Konovalenko, I. A., & Suzdalenko, O. V. (2015). The results of treatment of patients with acute arterial ischemia of the extremities. *Pathology*, 2(34), 55-58.

[11] Kabaroudis, A., Gerassimidis, T., Karamanos, D., Papaziogas, B., Antonopoulos, V., & Sakantamis, A. (2003). Metabolic alterations of skeletal muscle tissue after prolonged acute ischemia and reperfusion. *Journal of Investigative Surgery*, 16(4), 219-228. PMID: 12893498

[12] Klijn, E., Groeneveld, A. J., van Genderen, M. E., Betjes, M., Bakker, J., & van Bommel, J. (2015). Peripheral perfusion index predicts hypotension during fluid withdrawal by continuous veno-venous hemofiltration in critically ill patients. *Blood Purification*, 40(1), 92-98. doi: 10.1159/000381939

[13] Malchenko, O. A. (2016). *Pathogenetic substantiation of approaches to the correction of limb tissue damage in experimental perfusion syndrome*. (Dis. Ph. D.). Kyiv.

[14] Rossi, M., & Carpi, A. (2004). Skin microcirculation in peripheral arterial obliterative disease. *Biomedicine & Pharmacotherapy,* 58(8), 427-431. doi: 10.1016/j.biopha.2004.08.004

[15] Rudolf, R. (2017). Avoiding long-term muscle damage upon ischaemia-reperfusion. *Acta Physiologica,* 219(2), 343-345. doi: 10.1111/apha.12769

[16] Sabido, F., Milazzo, V. J., Hobson, R. W., & Duran, W. N. (1994). Skeletal muscle ischemia-reperfusion injury: a review of endothelial cell-leukocyte interactions. *Journal of Investigative Surgery,* 7(1), 39-47. doi: 10.3109/08941939409018281

[17] Sapozhnikov, A. G., & Doposevich, A. E. (2000). *Histological and Microscopic Technique: A Guide*. Smolensk: SPG.

[18] Van Genderen, M. E., Bartels, S. A., Lima, A., Bezemer, R., Ince, C., Bakker, J., & van Bommel, J. (2013). Peripheral perfusion index as an early predictor for central hypovolemia in awake healthy volunteers. *Anesthesia & Analgesia,* 116(2), 351-356. doi: 10.1213/ANE.0b013e318274e151

[19] Venher, I. K., Kolotilo, O.B., Kostiv, S. Y., Shkrobot, L. V., Husak, M. O., & Zvarich, R. V. (2017). Revascularization in patients at high risk of developing reperfusion syndrome. Hospital surgery. *Magazine named after L. Y. Kovalchuk*, (2), 26-29.

[20] Widgerow, A. D. (2014). Ischemia-reperfusion injury: influencing the microcirculatory and cellular environment. *Annals of Plastic Surgery,* 72(2), 253-260. doi: 10.1097/SAP.0b013e31825c089c

[21] Wu, Z. K., Iivainen, T., Pehkonen, E., Laurikka, J., & Tarkka, M. R. (2002). Ischemic preconditioning suppresses ventricular tachyarrhythmias after myocardial revascularization. *Circulation,* 106(24), 3091-3096. doi: 10.1161/01.cir.0000041430.32233.5b

[22] Zasimovich, V. N., & Ioskevich, N. N. (2017). Reperfusion-reoxygenation syndrome as a problem of reconstructive surgery of arteries in chronic ischemia of the lower extremities of atherosclerotic genesis. *Surgery News*, 25(6), 632-642.

[23] Ziablitsev, S. V., Starodubska, O. O., Bohza, S. L. (2017). Pharmacological correction of cognitive disorders in traumatic brain injury. Actual Problems of Modern Medicine. *Bulletin of VSEIU "Ukrainian Medical Dental Academy",* 17(3(59)), 25-29.

ГІСТОЛОГІЧНІ ЗМІНИ СУДИННОГО РУСЛА ЗАДНІХ КІНЦІВОК ЩУРІВ ЗА УМОВ ГОСТРОЇ ІШЕМІЇ-РЕПЕРФУЗІЇ ТА ПРИ КОРЕКЦІЇ КАРБАЦЕТАМОМ

Вересюк Т.О., Сельський П.Р.

Ішемічно-реперфузійне ураження - це складне мультифакторне пошкодження первинно ішемізованих тканин у результаті

відновлення в них артеріального кровообігу, яке супроводжується локальною морфофункціональною реорганізацією судинного русла задніх кінцівок щурів. Одним із перспективних засобів у лікуванні і профілактиці реперфузійних порушень є карбацетам, котрий згладжує феномени гіпо- та гіперпефузії в постішемічному періоді. Мета дослідження - встановити прояви морфофункціонального ремоделювання судинного русла задніх кінцівок щурів при ішемії-реперфузії та за умов корекції карбацетамом. Проведено гістологічне дослідження судинного русла задніх кінцівок 30 щурів за умов ішемії-реперфузії (I група) та 30 щурів при моделюванні ішемії-реперфузії, котрим у постішемічному періоді вводили карбацетам 1 раз на добу (5 мг/кг) протягом 14 діб (II група). У контрольній групі було 6 інтактних тварин. Моделювання ішемії проводили шляхом накладення гумових джгутів SWAT на задні кінцівки впродовж 2 годин, а реперфузії - шляхом зняття турнікету. Тварини експериментальних груп були розподілені на 5 підгруп з реперфузійними термінами через 1, 2 години, 1 добу, а також через 7 та 14 діб. Гістологічне дослідження проводили за загальноприйнятими методиками. Досліджували судинне русло в середній третині стегна та гомілки нижче ділянки накладання турнікету за допомогою мікроскопа Bresser Trino Researcher 40x-1000x. Аналізуючи отримані результати встановили, що через 1 годину реперфузії гістологічні зміни набували системності, а через 1 добу були найбільш вираженими. Необхідно відмітити, що товщина стінок судин збільшувалася, а еластичні мембрани частково вирівнювались, витончувались та розривались. Нерідко втрачалась чіткість пошарової структури стінок артерій. Набряк набував тотального характеру. При гістологічному дослідженні судин через 7 діб виявили, що набряк стінок зменшувався, а стан еластичного каркасу покращувався. В адвентиції мала місце проліферація колагенових волокон, що було відповіддю на ішемічні впливи. Відмічено, що через 14 діб у всіх оболонках стінки зберігалася проліферативна активність фібробластів. За умов корекції карбацетамом через 2 години структурна позитивна динаміка ставала більш виразною та сягала максимуму через 7 діб експерименту. Зменшувалася кількість видозмінених та злущених ендотеліоцитів, а стан гладких міоцитів покращувався. Гістологічно встановлено поступове відновлення ендотеліального покриття інтими. Таким чином, ішемія та реперфузія зумовлює ремоделювання судин вже через 1 годину із піком проявів через 1 добу реперфузії, що включає в себе набряковий синдром, дистрофічно-дегенеративні зміни із запальною відповіддю на пошкодження, а у пізньому реперфузійному періоді наростання активності фібробластичного дифферону. Поступове повернення морфологічних змін відбувається через 14 діб експерименту. За умов корекції відмічено прискорення ремоделювання зі стабілізацією процесу та найбільш можливим структурним відновленням уже через 7 діб дослідження.
Ключові слова: *артерія, ремоделювання, ішемія-реперфузія, еластичні мембрани, карбацетам.*

ГИСТОЛОГИЧЕСКИЕ ИЗМЕНЕНИЯ СОСУДИСТОГО РУСЛА ЗАДНИХ КОНЕЧНОСТЕЙ КРЫС ПРИ ОСТРОЙ ИШЕМИИ-РЕПЕРФУЗИИ И ПРИ КОРРЕКЦИИ КАРБАЦЕТАМОМ

Вересюк Т.О., Сельский П.Р.

Ишемически-реперфузионное повреждение - это сложное мультифакторное повреждение первично ишемизированных тканей в результате восстановления в них артериального кровообращения, которое сопровождается локальной морфофункциональной реорганизацией сосудистого русла задних конечностей крыс. Одним из перспективных средств в лечении и профилактике реперфузионных повреждений является карбацетам, который сглаживает феномены гипо- и гиперперфузии в постишемическом периоде. Цель исследования - установить проявления морфофункционального ремоделирования сосудистого русла задних конечностей крыс при ишемии-реперфузии и в условиях коррекции карбацетамом. Проведено гистологическое исследование сосудистого русла задних конечностей 30 крыс в условиях ишемии-реперфузии (I группа) и 30 крыс при моделировании ишемии-реперфузии, которым в постишемическом периоде вводили карбацетам 1 раз в сутки (5 мг/кг) в течение 14 суток (II группа). В контрольной группе было 6 интактных животных. Моделирование ишемии проводили путем наложения резиновых жгутов SWAT на задние конечности в течении 2 часов, а реперфузии - путем снятия турникета. Животные экспериментальных групп были разделены на 5 подгрупп с реперфузионными сроками через 1, 2 часа, 1 сутки, а также через 7 и 14 суток. Гистологическое исследование проводили по общепринятым методикам. Исследовали сосудистое русло в средней трети бедра и голени ниже участка наложения турникета с помощью микроскопа Bresser Trino Researcher 40x-1000x. Анализируя полученные результаты установили, что через 1 час реперфузии гистологические изменения становились системными, а через 1 сутки были наиболее выраженными. Необходимо отметить, что толщина стенок сосудов увеличивалась, а эластичные мембраны частично выравнивались, истончались и разрывались. Терялась четкость послойной структуры стенок артерий. Отек приобретал тотальный характер. При гистологическом исследовании сосудов через 7 дней обнаружили, что отек стенок уменьшался, а состояние эластичного каркаса улучшалось. В адвентиции имела место пролиферация коллагеновых волокон, что было ответом на ишемические воздействия. Отмечено, что через 14 дней во всех оболочках стенки сохранялась пролиферативная активность фибробластов. В условиях коррекции карбацетамом через 2 часа структурная положительная динамика становилась более выразительной, достигая максимума через 7 дней эксперимента. Уменьшалось количество видоизмененных и слущенных эндотелиоцитов, а состояние гладких миоцитов улучшилось. Гистологически установлено постепенное восстановление эндотелиального покрытия интимы. Таким образом, ишемия и реперфузия предопределяет ремоделирование сосудов уже через 1 час с пиком проявлений через 1 сутки реперфузии, что включает в себя отечный синдром, дистрофически-дегенеративные изменения с воспалительным ответом на повреждение, а в позднем реперфузионном периоде - нарастание активности фибробластического дифферона. Постепенное возвращение морфологических изменений происходит через 14 дней эксперимента. В условиях коррекции отмечено ускоренное ремоделирование со стабилизацией процесса и наиболее возможным структурным восстановлением уже через 7 суток исследования.
Ключевые слова: *артерия, ремоделирование, ишемия-реперфузия, эластические мембраны, карбацетам.*

DOI: 10.31393/morphology-journal-2020-26(2)-02 Reports of Morphology, Vol. 26, №2, Pages 12-18

ISSN 1818-1295 eISSN 2616-6194

REPORTS OF MORPHOLOGY

Official Journal of the Scientific Society of Anatomists, Histologists, Embryologists and Topographic Anatomists of Ukraine

journal homepage: https://morphology-journal.com

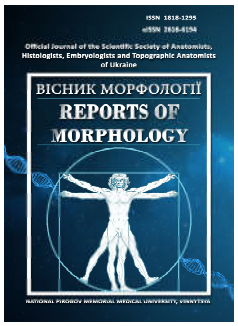

Features of translation of some rarely used anthropometric terms from Ukrainian into English

Cherepakha O.L., Gadzhula N.G., Hnenna V.O., Hrytsenko A.S.
National Pirogov Memorial Medical University, Vinnytsia, Ukraine

ARTICLE INFO
Received: 15 June, 2020
Accepted: 20 July, 2020

UDC: 811.161.2/.111:572

CORRESPONDING AUTHOR
e-mail: cherepakha79@gmail.com
Cherepakha O.L.

Nowadays, anthropometric researches have confidently taken its place in medicine. They are useful not only for health assessment, but also are used in many fields: forensic medicine (to estimate the age of the subject), forensic dentistry (it is an interdiscipline of forensic medicine and dentistry) for the identification of individual and age estimation, dentistry (anthropometric diagnostic methods of dentognathic anomalies and deformations, and there is a potential correlation among number of teeth, chewing ability and anthropometric profile), pediatrics, obstetrics and gynecology, as well as for the diagnosis of overweight (important indicators of nutritional status in the children and adults), for sports control and for the standardization purpose. The symptoms of many diseases are expressed in anthropometric changes. Unfortunately, in Ukraine there is still no generally accepted translation of anthropometric terms from Ukrainian into English. Often for the same medical anthropological term, different names and definitions are used in foreign scientific works. Therefore, the aim of the work was to unify and standardize the translation of rarely used anthropometric terms from Ukrainian into English, as well as determination of the place of the anthropometric point measurement and its schematic representation. We have used the standardized techniques proposed by Shaparenko P.P. and Burikh, M.P. (2000), set out in the "Anthropometric data analysis sets manual" (1994), in the works of Hobbs P.C. (1975) and Brinkley, J.F with co-authors (2016), where some anthropometric terms were described that are used when measuring the head, determining the height above the floor of some points of the trunk and upper limb of a person, and anthropometric parameters of the hand. The conclusion is made about the correctness of the proposed translation from Ukrainian into English, considering the specialized terminology. We hope that in the future this list will be supplemented with the new terms related to measurements of the auricle, upper and lower extremities.

Key words: *anthropometric terminology, anthropometric measurements, translation, English language.*

Introduction

Anthropometry is directly or indirectly related to all branches of medical science. Nowadays, anthropometric researches have confidently taken its place in medicine. So they are useful not only for health assessment, but also are used in many fields: forensic medicine (to estimate the age of the subject) [13], forensic dentistry (it is an interdiscipline of forensic medicine and stomatology) for the identification of individual and age estimation [24], dentistry (anthropometric diagnostic methods of dentognathic anomaly, and there is potential correlation among number of teeth, chewing ability and anthropometric profile) [7, 9, 29], pediatrics, obstetrics and gynecology [17, 21, 27], as well as for the diagnosis of overweight (important indicators of nutritional status in the children and adults) [11, 16, 20], for sports control [22] and for the standardization purpose [3, 15, 23, 26, 30]. The symptoms of many diseases are expressed in anthropometric changes [12].

So on the basis of the research center of the National Pirogov Memorial Medical University, Vinnytsya, as a part of the general university scientific project "Development of normative health criteria of the various age and sex groups of the population based on the study of anthropogenetic and physiological characteristics of the body in order to determine markers of multifactorial diseases", for many years, scientists and employees working in different departments of the university have been performing

scientific work and using anthropometric terminology.

Today, scholars often have problems working with anthropometric articles and textbooks in English. To date, we have published 2 methodological articles [5, 6] which include the translation from Ukrainian into English of the most commonly used anthropometric terms with a description of the place and methods of determining the corresponding anthropometric points or sizes and also figures that schematically show determination of human head parameters.

Unfortunately, there is still no generally accepted unified use of the translation of anthropometric terms from Ukrainian into English on the territory of Ukraine.

Therefore, *the aim* of the work was to standardize and unify the translation from Ukrainian into English of some anthropometric terms that are rarely used.

Materials and methods

Thus, to determine some anthropometric points and parameters of the human head measure the following:

bitragion - coronal arc: the surface distance between the right and left tragion landmarks across the top of the head is measured with a tape (tape tension sufficient to flatten hair). The head is in the Frankfort plane (Fig. 1) [2, 25];

bitragion breadth: as a result of this measurement, we obtain the digital value of the breadth of the head which is determined by measuring the distance from the right to the left tragion with a head caliper (Fig. 2) [2, 25];

tragion to top of head (vertex): measure the distance from the tragion to the vertex [2, 25];

palpebral fissure length: measure the horizontal length of the eye fissure, from corner to corner. (i.e., as a result, we receive the digital value of the horizontal dimension, or width, of the palpebral fissure) (Fig. 3), [4, 25];

interocular distance: carry out a horizontal measurement between the inner corners of the eyes, as a result of which a digital value of the inner distance between the eyes is obtained [2, 25];

menton-crinion length: measure the distance from the bottom surface of the chin to the midpoint of the hairline. Not measured on bald and balding [2, 25];

minimum frontal arc these measurements are performed using a tape - measure the arc across forehead between points of the greatest indentation of temporal crests (Fig. 4), [14, 25];

maximum nose breadth: researcher is placing recording parts of the caliper on broadest part of nose then moving horizontally across to other side of nose, measurement of maximum nose breadth without applying a pressure (Fig. 5), [14, 25];

upper facial height: this measurement is designed to principally capture the vertical length or height of the upper portion of the face or viscerocranium. Despite its name, this measurement contains segments of the classically defined middle and lower facial thirds which are determined by measuring the straight distance between nasion and stomion. (Fig. 6), [4, 25];

lower facial height: this measurement is designed to principally capture the vertical length or height of the lower portion of the face or viscerocranium. Straight distance between subnasale and gnathion is measured. (Fig. 7), [4, 25];

upper lip height: vertical measurement designed to capture the length or height of the entire upper lip including the skin and vermillion segments. Other common names for this measurement include: total upper lip height or length. The upper lip height is determined by measuring the distance between subnasale and stomion [4, 25];

lower lip height: vertical measurement designed to capture the length or height of the entire lower lip including the skin and vermillion segments. Other common names for this measurement include: total lower lip height or length. The lower lip height is determined by measuring the distance between stomion and sublabiale [4, 25];

ear length: measure the distance from the highest to the lowest points on a line parallel to the long axis of the ear [2, 25];

ear breadth: measure the maximum breadth of the right ear, which is perpendicular to its long axis [2, 25];

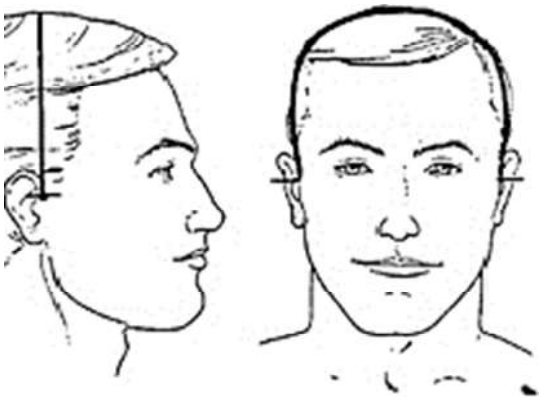

Fig. 1. Поперечна дуга. Bitragion - Coronal Arc.

Fig. 2. Вушний діаметр. Bitragion Breadth.

Fig. 3. Ширина очної щілини. Palpebral fissure length.

Fig. 4. Мінімальна фронтальна ширина. Minimum Frontal Arc.

Fig. 5. Максимальна ширина носа. Maximum Nose Breadth.

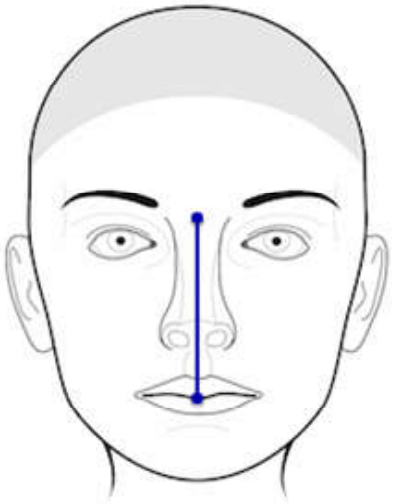

Fig. 6. Висота верхньої частини обличчя. Upper Facial Height.

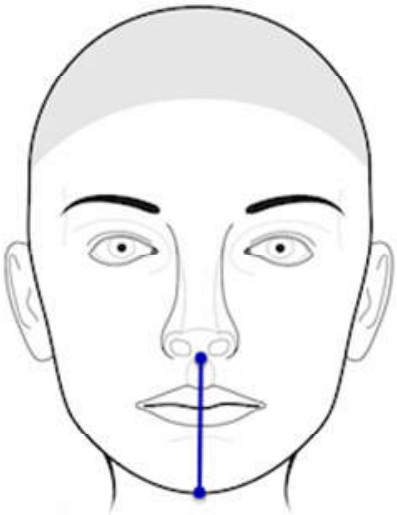

Fig. 7. Висота нижньої частини обличчя. Lower Facial Height.

It should be noted that *ear length* and *ear breadth* are measured with a sliding caliper. During research, the subject should sit erect looking straight ahead. The head is in the Frankfort plane (the Frankfurt plane is a plane formed by drawing a straight horizontal line from the top of the ear canal to the inferior margin of the eye along either side of the human skull provided that the median plane of the head is vertical). The researcher carries out measurements with a caliper without applying a pressure. All measurements are performed with a caliper or a tape according to the method described by Hobbs in 1975 [14], set out in the "Anthropometric data analysis sets manual" 1994 [2], in the work of Shaparenko P.P. and Burikh, M.P. in 2000 [25], as well as by Brinkley, J. F et al., who provided the appropriate methodology in their work in 2016 [4].

To determine the height of the torso point's locations above a standing surface measure the following:

substernale height: established by measuring the height of the midpoint of the lower edge of the breast bone from the floor [2, 25];

tenth rib height: established by measuring the vertical distance between a standing surface and the tenth rib landmark at the bottom of the right side of the rib cage [2, 25];

iliospinale height: established by measuring the vertical distance from the floor to the left iliospinale [2, 25];

Iliocristale height: established by measuring the vertical distance between a standing surface and the iliocristale landmark on the top of the right side of the pelvis [2, 25];

cervicale height: established by measuring the vertical distance between a standing surface and the cervicale landmark on the spine at the base of the neck [2, 25];

It should be noted that in the study, the subject should stand erect, looking straight ahead, his head should be in the Frankfort plane, shoulders and upper extremities should be relaxed. All measurements are performed with an anthropometer according to the method described by Shaparenko P.P. and Burikh, M.P. in 2000 [25] and by "Anthropometric data analysis sets manual" (1994) [2].

To determine the height of the anthropometric points of the upper limb above a standing surface and the anthropological parameters of the human hand measure the following:

acromion height: established by measuring the vertical distance between a standing surface and the acromion landmark on the tip of the right. The subject should stand upright looking straight ahead. The measurement is performed with an anthropometer [2, 25];

radial-stylion length: established by measuring the distance between the radiale landmark on the right elbow and the stylion landmark on the right wrist. It is measured with a beam caliper held parallel to the long axis of the forearm. Subject stands with the arms relaxed at the sides. The hand and fingers are held straight in line with the long axis of the forearm [2, 25];

hand length: established by measuring the length of the right hand between the stylion landmark on the wrist and the tip of the middle finger. The subject places the palm on a table with the fingers together, and the thumb

abducted. The middle finger is parallel to the long axis of the forearm. The measurement is carried out with a Poech sliding caliper [2, 25];

palm length: established by measuring the distance from the base of the hand to the furrow where the middle finger folds upon the palm [2, 25];

hand breadth at metacarpale: established by measuring the breadth of the right hand between the landmarks at metacarpale II and metacarpale V The subject places the palm on a table, the fingers together and the thumb abducted. The middle finger is parallel to the long axis of the forearm. The measurement is carried out with a sliding caliper [2, 25];

Currently, we have proposed a number of unified anthropometric terms in Ukrainian, which are rarely used with their translation into English, as well as the places of the anthropometric point determination and its schematic representation.

This list was developed by us based on the following scientific sources: Anthropometry and systems of topographic and anatomical coordinates of the human body [25], Anthropometric data analysis sets manual [2], The Face Base Consortium: a comprehensive resource for craniofacial researchers [4], An anthropometric survey of 500 Royal air force aircrew heads [14].

Results

The obtained measurements of some anthropometric parameters of the head and upper limb, as well as the determination of the location of the head and torso points of a person, make it possible to use the following scientific terms in the process of translation from Ukrainian into English:

Anthropometric points of the head

Поперечна дуга - Bitragion - coronal arc (landmarks involved - tragion: the point located at the notch just above the tragus of the ear. This point corresponds approximately to the upper edge of the ear hole. Vertex: highest point on the convexity of the calvarium measured from the Frankfurt plane (auriculo-orbital plane) (Fig. 1).

Вушний діаметр - Bitragion breadth (landmarks involved - tragion (Fig. 2)).

Висота голови - Tragion to top of head (vertex) (landmarks involved - vertex and tragion (Fig. 3)).

Ширина очної щілини - Palpebral fissure length (landmarks involved - endocanthion: apex of the angle formed at the inner corner of the palpebral fissure where the upper and lower eyelids meet. Exocanthion: apex of the angle formed at the outer corner of the palpebral fissure where the upper and lower eyelids meet.)

Міжочноямкова ширина - Interocular distance (landmarks involved - endocanthion: the point of the medial angle of the eye which is located medially from caruncula lacrimalis.).

Фізіологічна довжина обличчя - Menton-crinion length.

Мінімальна лобова ширина - Minimum frontal arc (Fig. 4).

Максимальна ширина носа - Maximum nose breadth (landmarks involved - alare: most lateral point on the nasal ala (Fig. 5)).

Висота верхньої частини обличчя - Upper facial height (landmarks involved - nasion: midline point where the frontal and nasal bones contact (nasofrontal suture). Soft tissue nasion corresponds to the underlying bony landmark. Stomion: the point of contact in the midsagittal plane between the upper and lower lips. (Fig. 6)).

Висота нижньої частини обличчя - Lower facial height (landmarks involved - subnasale: midline point marking the junction between the inferior border of the nasal septum and the cutaneous upper lip. It is the apex of the nasolabial angle. Gnathion: Midline point on the inferior border of the mandible. It corresponds to the underlying bony landmark (Fig. 7)).

Висота верхньої губи - Upper lip height (landmarks involved - subnasale and stomion).

Висота нижньої губи - Lower lip height (landmarks involved - sublabiale: it is midpoint along the inferior margin of the cutaneous lower lip (labiomental sulcus) and stomion).

Фізіономічна довжина вуха - Ear length.

Фізіономічна ширина вуха - Ear breadth.

The following terms should be used to define the height of torso points when translated into English:

Нижньогрудинна - Substernale height.

Нижньореберна передня - Tenth rib height.

Клубово-остиста передня - Iliospinale height.

Клубово-гребнева найвища - Iliocristale height.

Висота шийної точки - Cervicale height.

To determine the name of the height of the anthropometric point's location of the upper limb and anthropological measurements of the hand, when translated into English, the following terms should be used:

Висота плечової точки - Acromion height.

Шилоподібна променева - Radiale-stylion length.

Довжина кисті - Hand length.

Довжина долоні - Palm length.

Ширина кисті або поперечний діаметр - Hand breadth at metacarpale.

Discussion

Often, different terminology is used for the scientific definition of the same point, even in English scientific medical articles. So S. Tripathi with co-authors [28] and A. Dwivedi with co-authors [8] have used in their articles next terms: "interalar width" instead of "maximum nose breadth" and "intercanthal width/distance" instead of "interocular distance". Annelyse Cristine Ballin and co-authors [3] when evaluating the anthropometric measures of Caucasian noses of people living in the city of Curitiba have used the term "intercanthal distance" instead of "interocular distance" and the term "alar distance" instead

of "maximum nose breadth". In Ukrainian, this term sounds like "міжочноямкова ширина", reflecting the correctness of the meaningful use of the term in English "interocular distance" and also term "максимальна ширина носа" will be translated into English "maximum nose breadth".

Ma Huan and co-authors [18] when evaluating effect of aging in periocular appearances in Chinese Han population have used in their article the term "intercanthal width" instead of "interocular distance" and "outercanthal width" instead of "biocular breadth" (unified term used in our previous article [6]). In Ukrainian, this term sounds like "зовнішньо очна ширина", reflecting the correctness of the meaningful use of the term in English "biocular breadth".

S.M. Weinberg and co-authors [31] when describing hypertelorism and orofacial clefting have used in their article the term "intercanthal width" instead of "interocular distance".

Kamlesh B. Patel and co-authors [19] when describing fronto-orbital advancement for metopic synostosis have used in their article the term "intercanthal distance", instead of "interocular distance".

C.L. Fry and co-authors [10] when describing features spanning the morphologic range in the spectrum of the Latino eyelid have used the term "horizontal fissure length" instead of "palpebral fissure length". In Ukrainian, this term sounds like "ширина очної щілини", reflecting the correctness of the meaningful use of the term in English "palpebral fissure length".

Olalekan Agbolade and co-authors [1] when investigating three-dimensional (3D) soft-tissue craniofacial variation, with relation to ethnicity, sex and age variables in British and Irish white Europeans have used in their article the term "intercanthal width" instead of "interocular distance" and "biocular width" instead of "biocular breadth" (unified term used in our previous article [6]).

Gloria Staka and co-authors [26] та Saurab S. Virdi and co-authors [30] have used in their article the term "nasal width" (the straight distance between right and left alare) instead of "maximum nose breadth".

If you are translating from Ukrainian into English without terminology knowledge you will get wrong translation.

As an example, translation of the term "фізіологічна довжина голови" into English you will get "physiologic head length" instead of "menton-crinion length" or translation of the term "вушний діаметр" you will get "ear diameter" instead of "bitragion breadth".

In the future, it is planned to revise and supplement the list of terms with new terms regarding measurements of the auricle, upper and lower extremities of a person.

Conclusions

Thus, the given traditional unified anthropometric terms concerning anthropometric points and measurements of the head, trunk and several points of the upper limb with their translation into Ukrainian, as well as the definition of the place of anthropometric points measurement and their schematic representations, namely bitragion, coronal arc, bitragion breadth, tragion to top of head (vertex), horizontal palpebral aperture, interocular distance, menton-crinion length, minimum frontal arc, maximum nose breadth, upper facial height, lower facial height, upper lip height, lower lip height, ear length, ear breadth, substernale height, tenth rib height, iliospinale height, iliocristale height, acromion height, radiale-stylion length, hand length, palm length and hand breadth at metacarpale.

References

[1] Agbolade, O., Nazri, A., Yaakob, R., Ghani, A. A., & Cheah, Y. K. (2020). Morphometric approach to 3D soft-tissue craniofacial analysis and classification of ethnicity, sex, and age. *PLoS One*, 15(4): e0228402. doi: 10.1371/journal.pone.0228402

[2] Anthropometric data analysis sets manual [Electronic resource] by data of Human Systems Information Analysis Center / the United States Department of Defense - 1994. - http://mreed.umtri.umich.edu/mreed/downloads/anthro/ansur/ADAS-Dimension_Definitions.pdf

[3] Ballin, A. C., Carvalho, B., Dolci, J. E. L., Becker, R., Berger, C., & Mocellin, M. (2018). Anthropometric study of the caucasian nose in the city of Curitiba: relevance of population evaluation. *Brazilian Journal Otorhinolaryngology,* 84(4), 486-493. doi: 10.1016/j.bjorl.2017.06.004

[4] Brinkley, J. F., Fisher, Sh., Harris, M. P., Holmes, G., Hooper, J. E., Jabs, E. W., … Chai, Y. (2016). The Face Base Consortium: a comprehensive resource for craniofacial researchers. *Development,* 143(14), 2677-2688. doi: 10.1242/dev.135434

[5] Cherepakha, O. L. (2014). Особливості перекладу антропометричної термінології з української на англійську мову. *Вісник морфології,* 20(2), 298-303.

[6] Cherepakha, O. L., & Terehovska, O. I. (2015). Уніфіковані традиційні антропометричні терміни та їх еквіваленти англійською мовою з перекладом українською мовою. *Вісник морфології*, 21(2), С.515-518.

[7] Culebras-Atienza E, Silvestre FJ, Silvestre-Rangil J. (2018). Possible association between obesity and periodontitis in patients with Down syndrome. *Med. Oral. Patol. Oral. Cir. Bucal.,* 23(3), 335-343. doi: 10.4317/medoral.22311

[8] Dwivedi, A., Yadav, N. S., & Mishra, S. K. (2017). Inter-Canthal and Inter Alar Distance as a Predictor of Width of Maxillary Central and Lateral Incisor - An In Vivo Study. *Annals of Medical and Health Sciences Research,* 7, 276-279.

[9] Farsi, D. J., Elkhodary, H. M., Merdad, L. A., Farsi, N. M., Alaki, S. M., Alamoudi, N. M., … Alolayyan, M. A. (2016). Prevalence of obesity in elementary school children and its association with dental caries. *Saudi Med. J.,* 37(12), 1387-1394. doi: 10.15537/smj.2016.12.15904

[10] Fry, C. L., Naugle, T. C., Cole, Sh. A., Gelfond, J., Chittoor, G., Mariani, A. F., … Voruganti, V. S. (2017). The Latino eyelid: anthropometric analysis of a spectrum of findings. *Ophthalmic Plastic and Reconstructive Surgery,* 33(6), 440-445. doi: 10.1097/IOP.0000000000000821

[11] Gažarová M, Galšneiderová M, Mečiarová L. (2019). Obesity diagnosis and mortality risk based on a body shape index (ABSI) and other indices and anthropometric parameters in university students. *Rocz. Panstw. Zakl. Hig.*, 70(3), 267-275. doi: 10.32394/rpzh.2019.0077

[12] G?a-Horta, T., Beinner, M. A., Gazzinelli, A., Mendes, M. S. F., & Velasquez-Melendez, G. (2018). Anthropometric changes and their effects on cardiometabolic risk factors in rural populations in Brazil. *Cien. Saude Colet.*, 23(5), 1415-1423. doi: 10.1590/1413-81232018235.19552016

[13] Haghanifar, S., Ghobadi, F., Vahdani, N., & Bijani, A. (2019). Age estimation by pulp/tooth area ratio in anterior teeth using cone-beam computed tomography: comparison of four teeth. *J. Appl. Oral. Sci.*, e20180722. doi: 10.1590/1678-7757-2018-0722

[14] Hobbs, P. C. (1975). An anthropometric survey of 500 Royal Air Force aircrew heads - Farnborough: by the Royal Air Force Institute of Aviation Medicine and the Royal Aircraft Establishment

[15] Japatti, S. R., Engineer, P. J., Reddy, B. M., Tiwari, A. U., Siddegowda, C. Y., & Hammannavar, R. B. (2018). Anthropometric Assessment of the Normal Adult Human Ear. *Ann. Maxillofac. Surg.*, 8(1), 42-50. doi: 10.4103/ams.ams_183_17 (4)

[16] JJaroszynski, A., Dereziński, T., Jaroszyńska, A., Zapolski, T., Wąsikowska, B., Wysokiński, A. … Horoch, A. (2016). Association of anthropometric measures of obesity and chronic kidney disease in elderly women. *Ann. Agric. Environ. Med.*, 23(4), 636-640. doi: 10.5604/12321966.1226859

[17] Kesterke, M. J., Raffensperger, Z. D., Heike, C. L., Cunningham, M. L., Hecht, J. T., Kau, C. H., … Weinberg, S. M. (2016). Using the 3D Facial Norms Database to investigate craniofacial sexual dimorphism in healthy children, adolescents, and adults. *Biol. Sex Differ.* 7:23. doi: 10.1186/s13293-016-0076-8

[18] Ma, H., Chen, Y., Cai, X., Tang, Z., Nie, C., & Lu, R. (2019). Effect of aging in periocular appearances by comparison of anthropometry between early and middle adulthoods in Chinese Han population. *Journal of Plastic, Reconstructive and Aesthetic Surgeons,* 72(12), 2002-2008. doi: 10.1016/j.bjps.2019.07.030

[19] Patel, K. B., Skolnick, G. B., & Mulliken, J. B. (2016). Anthropometric Outcomes following Fronto-Orbital Advancement for Metopic Synostosis. *Plastic and Reconstructive Surgery,* 137(5), 1539-1547. doi: 10.1097/PRS.0000000000002129

[20] Patnaik L, Pattnaik S, Rao EV, Sahu T. (2017) Validating Neck Circumference and Waist Circumference as Anthropometric Measures of Overweight. *Obesity in Adolescents Indian Pediatr.,* 54(5), 377-380. doi: 10.1007/s13312-017-1110-6

[21] Phelan, S., Clifton, R. G., Haire-Joshu, D., Redman, L. M., Van Horn, L., Evans, M. … Pi-Sunyer, X. (2020). One-year postpartum anthropometric outcomes in mothers and children in the LIFE-Moms lifestyle intervention clinical trials. *Int. J. Obes.* (Lond)., 44(1), 57-68. doi: 10.1038/s41366-019-0410-4

[22] Pizzigalli, L., Cremasco, M. M., Torre, A.L.A., Rainoldi, A., & Benis, R. (2017). Hand grip strength and anthropometric characteristics in Italian female national basketball teams. *J. Sports Med. Phys. Fitness.*, 57(5), 521-528. doi: 10.23736/S0022-4707.16.06272-1

[23] Sadacharan, C. M. (2016). Vertical and horizontal facial proportions of Indian American men. *Anatomy & Cell Biology.,* 49(2), 125-131. doi: 10.5115/acb.2016.49.2.125

[24] Schmeling, A., Dettmeyer, R., Rudolf, E., Vieth, V., & Geserick, G. (2016). Forensic Age Estimation. *Dtsch. Arztebl. Int.,* 113(4), 44-50. doi: 10.3238/arztebl.2016.0044

[25] Shaparenko, P. P., & Burikh, M. P. (2000). *Антропометрія та системи топографоанатомічних координат тіла людини.* Вінниця: ВДМУ.

[26] Staka, G., Asllani-Hoxha, F., & Bimbashi V. (2017). Facial anthropometric norms among Kosovo - Albanian adults. *Acta Stomatol. Croat.*, 51(3), 195-206. doi: 10.15644/asc51/3/3

[27] Szczuko M, Skowronek M, Zapalowska-Chwyc M, Starczewski A. (2016) Quantitative assessment of nutrition in patients with polycystic ovary syndrome (PCOS). *Rocz. Panstw. Zakl. Hig.,* 67(4), 419-426. PMID: 27925712

[28] Tripathi, S., Singh, R. D., Chand, P., Kumar, L., & Singh, G. K. (2018). A study to correlate various facial landmarks with intercanine distance. *Indian Journal of Dental Research,* 29(4), 440-444. doi: 10.4103/ijdr.IJDR_80_17

[29] Vazquez-Casas, I., Sans-Capdevila, O., Moncunill-Mira, J., & Rivera-Bar, A. (2020). Prevalence of sleep-related breathing disorders in children with malocclusion. *J. Clin. Exp. Dent.,* 12(6), 555-560. doi: 10.4317/jced.56855

[30] Virdi, S., Saurab, Wertheim, D., & Naini, F. B. (2019). Normative anthropometry and proportions of the Kenyan-African face and comparative anthropometry in relation to African Americans and North American Whites. *Maxillofac. Plast. Reconstr. Surg.,* 41(1), 9. doi: 10.1186/s40902-019-0191-7

[31] Weinberg, S. M., Leslie, E. J., Hecht, J. T., Wehby, G. L., Deleyiannis, F. W. B., Moreno, L. M., … Marazita, M. L. (2017). Hypertelorism and Orofacial Clefting Revisited: An Anthropometric Investigation. *Cleft Palate-Craniofacial Journal,* 54(6), 631-638. doi: 10.1597/15-256

[32] Zhao, K., Hohmann, A., Chang, Y., Zhang, B., Pion, J., & Gao, B. (2019). Physiological, Anthropometric, and Motor Characteristics of Elite Chinese Youth Athletes From Six Different Sports. *Front. Physiol.,* 10, 405. doi: 10.3389/fphys.2019.00405

ОСОБЛИВОСТІ ПЕРЕКЛАДУ З УКРАЇНСЬКОЇ МОВИ НА АНГЛІЙСЬКУ ДЕЯКИХ АНТРОПОМЕТРИЧНИХ ТЕРМІНІВ, ЩО РІДКО ВИКОРИСТОВУЮТЬСЯ

Черепаха О.Л., Гаджула Н.Г., Гненна В.О., Гриценко А.С.

На теперішній час антропометричні дослідження впевнено зайняли свою нішу в медицині. Тож вони корисні не тільки для оцінки стану здоров'я, але й використовуються в багатьох галузях: судова медицина (для оцінки віку особи, що досліджується), судова стоматологія (це дисципліна на стику судової медицини та стоматології) для ідентифікації особистості та оцінки віку, стоматологія (антропометричні методи діагностики зубо-щелепної аномалії, а також існує потенційна кореляція між кількістю зубів, жувальними можливостями та антропометричним профілем), педіатрії, акушерства та гінекології, а також для діагностики зайвої ваги (важливі показники харчового статусу у дітей та дорослих), для спортивного контролю та з метою стандартизації. Симптоми багатьох захворювань знаходять своє відображення в змінах антропометричних показників. На жаль, в Україні досі немає загальноприйнятого перекладу антропометричних термінів з української на англійську мову. Нерідко в зарубіжних наукових роботах для одного і того ж медичного антропологічного терміну використовують різні назви і визначення. Тому метою роботи було уніфікація і стандартизація перекладу з української мови на англійську деяких антропометричних термінів, які рідко використовуються, а також уточнення місця вимірювання антропометричної точки та її схематичне зображення. Використовуючи стандартизовані методики, запропоновані Шапаренко П.П. та Бурих М.П. (2000), викладені у Посібнику аналізу антропометричних даних (1994), Hobbs P.C. (1975), а

також у роботі Brinkley, J.F. зі співавторами (2016) були описані деякі антропометричні терміни, котрі використовують при вимірах голови, визначенні висоти знаходження деяких точок верхньої кінцівки і тулуба людини над підлогою, а також антропометричних параметрів кисті. Зроблено висновок про правильність і коректність запропонованого перекладу з української мови на англійську, з огляду на спеціалізованість термінології. В подальшому цей перелік буде доповнено новими термінами, що стосуються вимірів вушної раковини, верхніх і нижніх кінцівок.
Ключові слова: *антропометрична термінологія, антропометричні вимірювання, переклад, англійська мова.*

ОСОБЕННОСТИ ПЕРЕВОДА С УКРАИНСКОГО ЯЗЫКА НА АНГЛИЙСКИЙ НЕКОТОРЫХ АНТРОПОМЕТРИЧЕСКИХ ТЕРМИНОВ, КОТОРЫЕ РЕДКО ИСПОЛЬЗУЮТСЯ

Черепаха Е.Л., Гаджула Н.Г. Гненна В.О., Гриценко А.С.

В настоящее время антропометрические исследования уверенно заняли свою нишу в медицине. Поэтому они полезны не только для оценки состояния здоровья, но и используются во многих отраслях: судебная медицина (для оценки возраста исследуемого человека), судебная стоматология (это дисциплина на стыке судебной медицины и стоматологии) для идентификации личности и оценки возраста, стоматология (антропометрические методы диагностики зубо-челюстной аномалии, а также существует потенциальная корреляция между количеством зубов, жевательными возможностями и антропометрическим профилем), педиатрии, акушерства и гинекологии, а также для диагностики лишнего веса (важные показатели пищевого статуса у детей и взрослых), для спортивного контроля и с целью стандартизации. Симптомы многих заболеваний выражаются в антропометрических изменениях. К сожалению, в Украине до сих пор нет общепринятого перевода антропометрических терминов с украинского на английский язык. Нередко в зарубежных научных работах для одного и того же медицинского антропологического термина используют разные названия и определения. Поэтому целью работы было унификация и стандартизация перевода с украинского языка на английский некоторых антропометрических терминов, которые редко используются, а также определения места измерения антропометрической точки и ее схематическое изображение. Используя стандартизированные методики, предложенные Шапаренко П.Ф. и Бурых М.П. (2000), изложенные в Пособии для анализа антропометрических данных (1994), Hobbs P.C. (1975), а также в работе Brinkley, J.F. с соавторами (2016) были описаны некоторые антропометрические термины, которые используют при измерениях головы, определении высоты нахождения некоторых точек верхней конечности и туловища человека над полом, а также антропометрических параметров кисти. Сделан вывод о правильности и корректности предложенного перевода с украинского языка на английский, учитывая специализированность терминологии. В будущем это перечень будет дополнен новыми терминами, касающимися измерений ушной раковины, верхних и нижних конечностей.
Ключевые слова: *антропометрическая терминология, антропометрические измерения, перевод, английский язык.*

DOI: 10.31393/morphology-journal-2020-26(2)-03 Reports of Morphology, Vol. 26, №2, Pages 19-25

ISSN 1818-1295 eISSN 2616-6194

REPORTS OF MORPHOLOGY

Official Journal of the Scientific Society of Anatomists, Histologists, Embryologists and Topographic Anatomists of Ukraine

journal homepage: https://morphology-journal.com

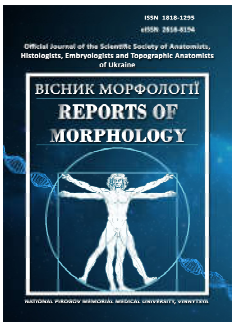

Morphological changes of the liver under conditions of hyperhomocysteinemia in the background of hypo- and hyperthyroidism

Nechyporuk V.M.[1], Korda M.M.[2], Kovalchuk O.V.[1]

[1]National Pirogov Memorial Medical University, Vinnytsya, Ukraine

[2]I. Horbachevsky Ternopil National Medical University, Ternopil, Ukraine

ARTICLE INFO

Received: 08 June, 2020

Accepted: 10 July, 2020

UDC: 577.1:661.29:577.112.3:599.323.4

CORRESPONDING AUTHOR

e-mail: nechiporuk@vnmu.edu.ua

Nechyporuk V.M.

Thyroxine and Triiodothyronine are very important for normal growth, development and organ function. These hormones regulate the basal rate of metabolism of all cells, including hepatocytes, and thus modulate liver function. There is a close connection between hyperhomocysteinemia (HHCy) and the induction of oxidative processes, disruption of nitric oxide production of NO synthase, damage to the endoplasmic reticulum and activation of inflammatory processes in the liver. Disorders of homocysteine metabolism (HC) in thyroid dysfunction are also known. Therefore, it can be assumed that the violation of the structure and functions of the liver will be an important manifestation of the negative impact of HHCy on organs and tissues in hyper- and hypothyroidism. The aim of the study was to establish the reorganization of the structural components of the liver in the conditions of modelized HHCy, hyper- and hypothyroidism and their joint effects. Thiolactone HHCy was modelized by administering to animals an exogenous HC in the form of thiolactone at a dose of 100 mg/kg body weight once a day for 28 days. Hyperthyroidism was modelized by daily administration of L-thyroxine at a dose of 200 μg/kg for the 21days, hypothyroidism - daily administration of thiamazole at a dose of 10 mg/kg for the 21 days. Individual groups of animals were administered L-thyroxine and thiamazole in parallel with HC. It was found that in the conditions of simulated HHCy, hypo- and hyperthyroidism in the liver of experimental animals there is an incompleteness of hepatocyte beams, changes in hepatocytes of destructive, dystrophic and necrotic nature with signs of steatosis, vascular disorders. Conclusions: both HHCy and hypo- or hyperthyroidism lead to a violation of the structural organization of liver tissue. With the development of thyroid dysfunction on the background of HHCy, the disturbances of the histological structure of hepatocytes significantly increased.

Key words: *hyperthyroidism, hypothyroidism, hyperhomocysteinemia, homocysteine, liver.*

Introduction

Thyroxine and triiodothyronine are necessary for normal growth, development and functioning of organs. These hormones regulate the rate of basic metabolism of all cells, including hepatocytes, and thus modulate liver function; the liver in turn metabolizes thyroid hormones and regulates their systemic endocrine effect. Graves' disease has been shown to cause asymptomatic elevations in liver enzymes, jaundice, and, less commonly, acute liver failure, but the relationship between thyroid hormone levels and liver tissue status remains unclear [18].

Mechanisms associated with disorders of sulfur-containing amino acid metabolism are known to play a significant role in the development of liver pathology. A special role belongs to homocysteine (HC), an intermediate product of methionine metabolism [8]. The accumulation of HC in the blood is a consequence of an imbalance between the level of its synthesis and elimination. A special role in the synthesis and metabolism of the latter is assigned to the liver, in which a significant part of transmethylation reactions occurs [17]. Obviously, elevated levels of HC in the blood can cause liver damage and, conversely, liver damage often leads to disorders of HC metabolism. Cirrhosis of the liver in humans is known to be associated with HC metabolism, in particular the expression of methionine synthase, betaine-

homocysteine-S-methyltransferase, cystathionine-β-synthase genes is reduced [11, 12].

In previous studies, we have shown that the experimental reproduction of hyperthyroidism leads to a decrease in the level of HC, and hypothyroidism, in contrast, causes an increase in the content of HC in the blood, which is associated with changes in the activity of methionine and cysteine [15].

The aim of this study was to establish changes in the structure of the liver under the conditions of HHCy, hyper- and hypothyroidism and their combined effects.

Materials and methods

The experiments were performed on 50 outbred white male rats weighing 180-200 g. Rats were kept at standard daylight on a normal diet. All studies were conducted in compliance with the requirements of humane treatment of experimental animals, regulated by the Law of Ukraine "On protection of animals from cruel treatment" (№ 3447-IV of 21.02.2006) and the European Convention for the protection of vertebrate animals used for experimental and other scientific purposes (Strasbourg, March 18, 1986).

All animals were divided into 5 groups: 1 - intact rats. This group of animals was injected intragastrically with 1% starch solution; 2 - animals with thiolactone HHCy, which was caused by intragastric administration of HC in the form of thiolactone at a dose of 100 mg/kg body weight in 1% starch solution once a day for 28 days. The dose, routes and duration of administration of thiolactone HC are borrowed from the literature and did not cause death of animals [19]; 3 - animals with hyperthyroidism, which were administered intragastrically daily for 21 days L-thyroxine at a dose of 200 μg/kg in 1% starch solution [14]; 4 - animals with thiolactone HHCy, which were daily administered intragastrically for 21 days L-thyroxine at a dose of 200 μg/kg in 1% starch solution; 5 - animals with hypothyroidism, which were daily administered intragastrically for 21 days Mercazolil in 1% starch solution at a dose of 10 mg/kg body weight [14]; 6 - animals with thiolactone HHCy, which were daily administered intragastrically Mercazolil at a dose of 10 mg/kg in 1% starch solution.

Animals were removed from the experiment 24 hours after the last administration of the selected substances. Collection of material for microscopic examinations and its processing was performed according to the generally accepted method [7]. Pieces of liver were fixed in 10% neutral formalin solution, dehydrated in alcohols of increasing concentration, poured into paraffin blocks. The sections made, 4-5 μm thick, were stained with hematoxylin-eosin [7]. Histological specimens were examined using a MIKROmed SEO SCAN light microscope and photo-documented using a Vision CCD Camera with an image output system from histological specimens.

Results

Microscopic examination of the liver of white rats of the intact group revealed that the organ has a typical, lobular organization. Stromal loose connective tissue is poorly developed, clearly manifested in the area of triads or portal tracts of the hepatic artery, vein, bile duct, lymphatic vessel and nerves. The lobule is formed by anastomotic hepatic canaliculi consisting of hepatocytes (Fig. 1). Sinusoidal capillaries that flow into the central vein and bile capillaries are located between the canaliculi.

Hepatocytes - the main cells of the organ of irregular polygonal shape have one, sometimes two, weakly basophilic nuclei. The cytoplasm of the cells is little oxyphilic, containing basophilic nodules. The wall of sinusoids is formed by elongated endothelial cells, between which macrophages of the liver, Kupffer cells, are found.

Conducted histological examinations of the liver of animals under the conditions of the simulated HHCy established dyscirculatory disorders with venous plethora, stasis, thrombosis. There is an expansion of lumens and plethora of the central, hepatic and portal veins, and to a lesser extent to the hepatic veins. Large areas of leukocyte infiltrations were identified in the zones of the portal tracts.

Damage to the canaliculi-lobule organization of the organ was revealed. The sinusoidal capillaries are widened, full-blooded, the wall of the capillaries is indistinct. Hepatocytes with swollen cytoplasm and manifestations of vaculo-hydropic and fatty dystrophy were mainly defined in the centripulobular zones. Cells with small-droplet fatty dystrophy were found in certain zones. The nuclei of hepatocytes are hyperchromic, pyknotically altered (Fig. 2). The figures of mitosis in hepatocytes were practically not revealed. The number of Kupffer cells in the wall of sinusoids increased.

In the group of animals with experimental hyperthyroidism, histological changes of the liver are also destructive and manifested by discomplexation of liver canaliculi, expansion and blood supply of sinusoidal hemocapillaries, in their lumens are numerous erythrocytes, leukocytes, and in the wall - activated

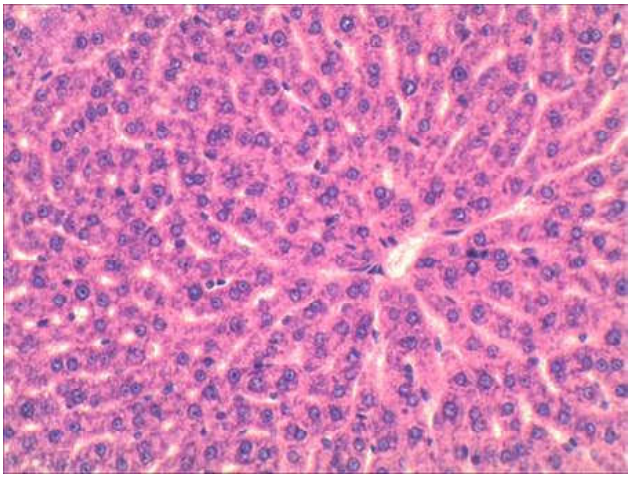

Fig. 1. Histological organization of the liver of intact group animals. Lobule-canaliculi placement of hepatocytes, central vein, sinusoidal hemocapillary. Hematoxylin-eosin. x200.

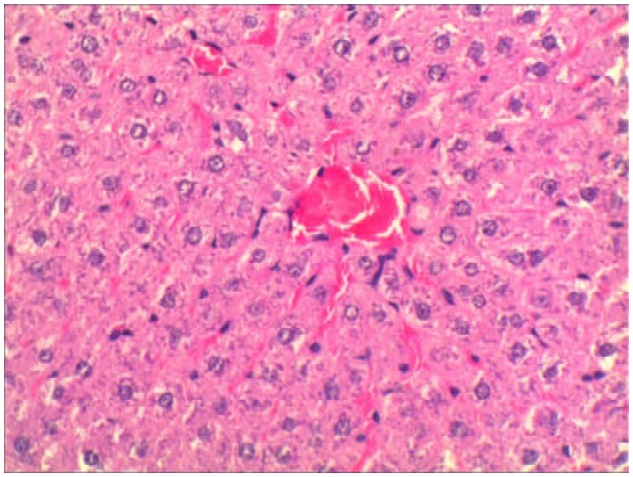

Fig. 2. Histological changes of the animal liver under conditions of hyperhomocysteinemia. Discomplexation of hepatic canaliculi, dystrophic changes of hepatocytes, destruction of hepatocytes. Hematoxylin-eosin. x200.

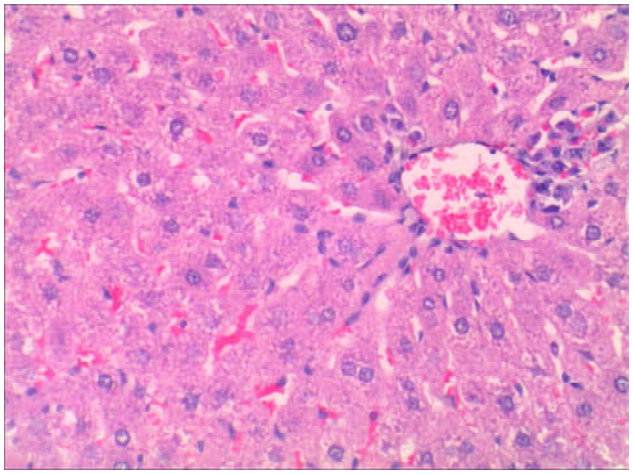

Fig. 3. Microscopic changes of the animal liver under the conditions of modeled hyperthyroidism. Altered lobule-canaliculi organization of the organ, dilated, blood-filled central vein with paravasal histoleukocyte infiltration, alternative changes in hepatocytes. Hematoxylin-eosin. x200.

macrophage cells. Vascular disorders are significant, especially plethora is characteristic for central veins, and hepatic portal veins have moderate lumens, but indistinct wall, arteries often have spasmodic lumen, edema and wall thickening, there is significant perivascular edema, histoleukocyte infiltrates (Fig. 3). The number of activated fibroblasts is growing. Hepatocytes are moderately oxyphilic, with signs of cytoplasmic onset, dystrophically altered, containing dark, compacted basophilic nuclei.

Microscopic studies of the liver of experimental animals in the simulated hyperthyroidism and HHCy established a more significant degree of damage to the liver compared to the previous group of observations. The reorganization of the vessels of the organ is manifested by a sharp enlargement, plethora, especially of the central and portal veins, their walls are swollen or vaguely expressed, thinned, which determines the formation of local hemorrhages. The veins in the composition of the triads are also blood-filled, there is a thickening of the wall of the portal arteries. Leukocyte infiltration is defined both in the areas of the potent tracts and along the course of sinusoids (Fig. 4A). Alterative changes in the parenchyma of the organ are manifested by discomplexation of hepatocyte canaliculi. Altered cells with weakly oxyphilic cytoplasm, hyperchromia and pyknosis of the nucleus are mainly observed in the central zones of the lobes. There are signs of hydropic, small- and large-droplet hepatocyte dystrophy, formation of centrilobular necrosis and foci of the lysis (Fig. 4B). Sinusoidal hemocapillaries were mainly determined only in the peripheral areas of the lobules and were filled with blood.

Microscopic studies of the liver under the conditions of a simulated experimental hypothyroidism have established disturbances of the histoarchitectonics of the organ and

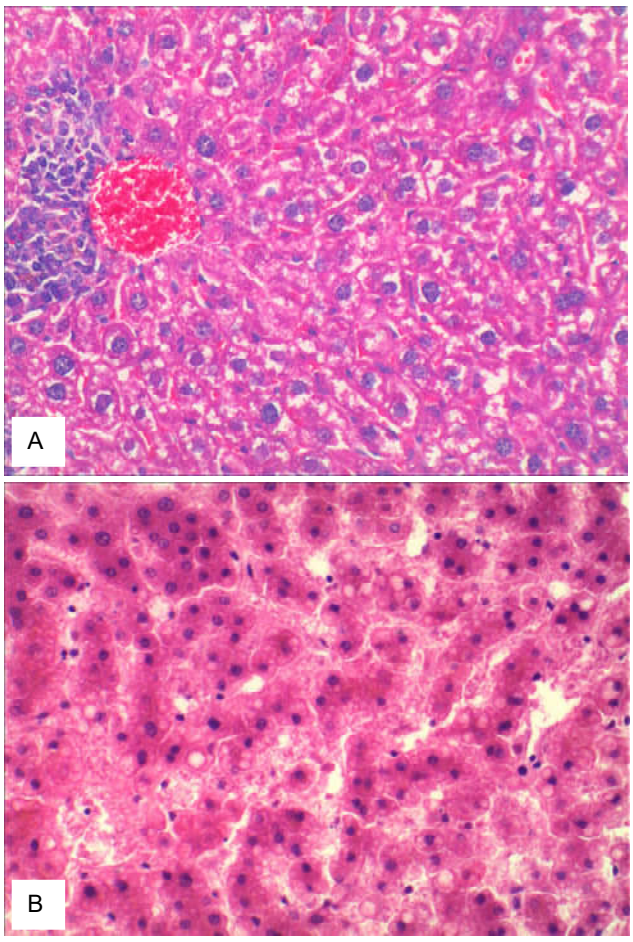

Fig. 4. Microscopic changes of the animal liver under the conditions of modeled hyperthyroidism and hyperhomocysteinemia. A - Enlarged, blood-filled lumen of the central vein with paravasal leukocyte infiltration, dystrophically altered hepatocytes. Hematoxylin-eosin. x200. B - Destructively and necrobiotically altered hepatocytes with signs of fatty degeneration. Hematoxylin-eosin. x200.

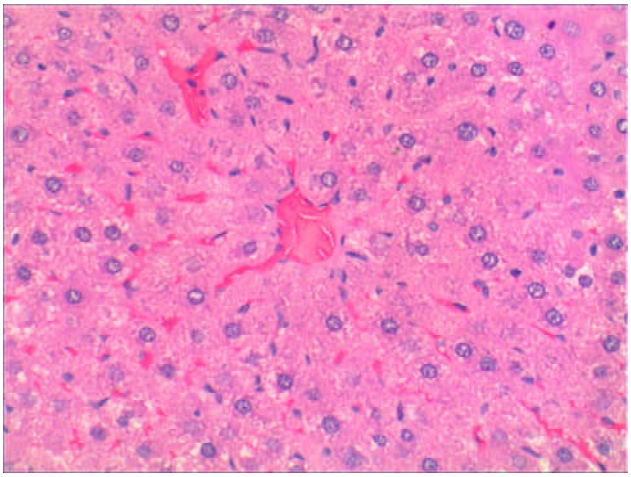

Fig. 5. Histological changes of the animal liver under the conditions of experimental hypothyroidism. Blood-filled central vein, destructively altered hepatocytes, full-blooded sinusoidal capillaries. Hematoxylin-eosin. x200.

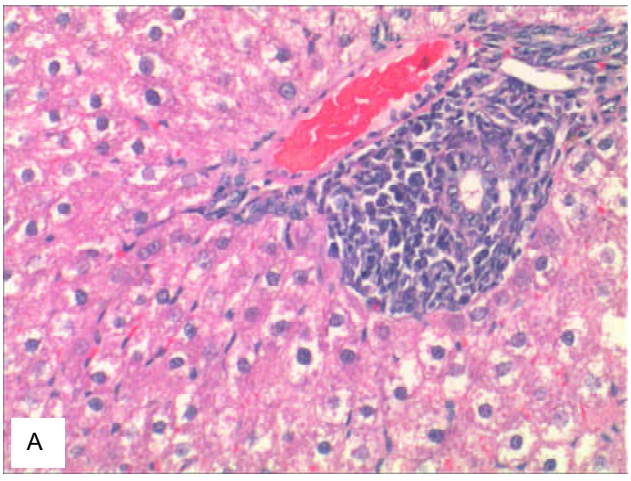

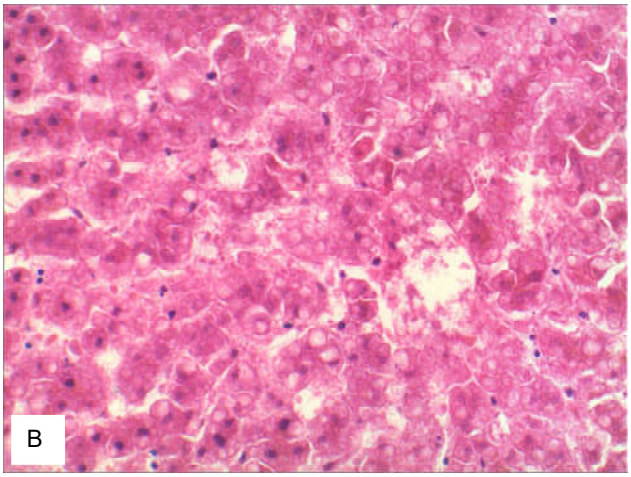

Fig. 6. Histological changes of the animal liver in modeled hypothyroidism and hyperhomocysteinemia. A - Vessels of the portal tract with paravasal and periductal leukocyte infiltration, dystrophically altered hepatocytes. Hematoxylin-eosin. x200. B - Hepatocytes with small and large droplet fatty dystrophy, areas of cell lysis. Hematoxylin-eosin. x200.

alteration of hepatocytes. Predominantly in the centrilobular zones, the cells were swollen with signs of destruction, vacuolar, small- and large-droplet fatty dystrophy. Most of the nuclei were hyperchromic, pyknotic, but mainly in the peripheral parts of the particle there were normochromic, moderately basophilic nuclei with enlightened weakly basophilic cytoplasm. Most of the vessels are plethora, with large lumens, especially central and portal veins (Fig. 5). There was an uneven blood supply to the sinusoidal hemocapillaries, the full-blown lumens of the microvessels were present mainly on the periphery of the lobules, they were full by erythrocytes, neutrophilic granulocytes, and thrombocytes. Periductal areas are infiltrated by leukocytes, activated fibroblasts.

A microscopic study of the liver of animals under the combined effects of hypothyroidism and HHCy revealed the most pronounced changes in the necrotic and degenerative nature of the structural components of the lobes of the organ on the background of significant vascular disorders. The remodeling of hepatocytes is characterized by small- and large-scale fat dystrophy, and to a lesser extent by protein-vacuolar, as well as step necrosis was also found in the lobes of the liver (Fig. 6B). The heteromorphism of the cells in the composition of the cell is observed, they were present as "light" and "dark" hepatocytes, which were in a state of functional tension. Inflammatory changes in the organ were manifested by large leukocyte infiltrates, both in the zone of the portal tracts and around the central veins and bright areas of the lysis in the areas of destroyed hepatocytes (Fig. 6A).

Discussion

The results of microscopic examination of the liver at HHCy are consistent with the available data from the literature. High levels of HC in plasma are associated with the development of hydropic fatty liver disease. In the work of D.O. Nekrut et al., 2017 found that HHCy causes disorders of biosynthetic processes in hepatocytes and is characterized by the development of small droplet fat dystrophy [16]. It was also established that HHCy causes an increase in the number of Kupffer cells in the sinusoid wall. In addition, there is damage to the microcirculation of the liver and the development of fibrogenesis [3]. It is known that one of the reasons for the development and progression of non-alcoholic fatty liver disease may be high levels of HC in the blood. HHCy is one of the important causes of steatohepatitis, changes in the lipid spectrum of the blood, and subsequently - the development of the process into fibrosis and cirrhosis of the liver [5]. HHCy also has a toxic effect on the endothelium of hepatic vessels due to the formation of significant amounts of free radicals and the development of endoplasmic reticulum stress [9]. We found a negative effect of HC on protein, carbohydrate and fat metabolism in liver cells, which at the optical level is manifested in the form of steatosis, multilobule fibrosis with signs of parenchymal and stromal reactions [1].

Hyperthyreosis had a destructive effect on liver tissues, namely, we found discomplexation of hepatic canaliculi, enlargement and plethora of sinusoidal hemocapillary cells (numerous erythrocytes, leukocytes in the lumen, Kupffer cells activated in the wall). In study [4], the relationship between hyperkinetic circulation, hypermetabolism and hyperactivity of the sympathetic nervous system in hyperthyroidism and liver damage in cirrhosis was also noted. The authors found disorders of the vascular system (plethora of the central veins), spasmodic lumen of the arteria, swelling and thickening of the vascular wall, significant histoleukocyte infiltrates. The number of activated fibroblasts increased, hepatocytes were moderately oxyphilic (there was an edema of cytoplasm, dystrophically altered, contained compacted dark basophilic nuclei). Recent studies have shown that liver dysfunction can occur in hyperthyroidism as a result of the use of antithyroid drugs. The authors found that patients with Graves' disease are prone to acute hepatitis, which complicates treatment with antithyroid drugs [2].

We found that in hyperthyroidism and HHCy there is a greater degree of damage to the structural components of the liver in comparison with animals with hyperthyroidism. In this case, the vessels of the liver were with a sharp dilation, plethora, especially the central and hepatic portal veins, the walls of the vessels were thinned, swollen, which caused the formation of local bleedings. Blood-filled veins were found in the composition of the triad and thickening of the wall of hepatic arteria, leukocyte infiltration both in the areas of the portal tracts and along the way of sinusoids. Against the background of hyperthyroidism, alternative changes are observed in the liver parenchyma, which was manifested by discomplexation of hepatocyte canaliculi. Altered cells with weakly oxyphilic cytoplasm, hyperchromia and pyknosis of the nucleus are mainly observed in the central zones of the lobes. Signs of hydropic, small- and large-droplet hepatocyte dystrophy, formation of centrilobular necrosis and loci of the lysis are determined. It is possible that high levels of thyroxine, increasing oxygen consumption, increases the amount of free radicals in the liver and, thus, causes damage to liver cells [13]. In another study, it was found that hyperthyroidism activates both the oxidative and antioxidant systems in brain, liver and heart tissues [6]. The authors of this study in rats suggested that the treatment of hyperthyroidism may inhibit the development of cirrhosis, which reflects the direct effect of hyperproduction of thyroid hormones on the liver.

We found that experimental hypothyroidism caused destructive histological changes of the liver, which was manifested by discomplexation of liver canaliculi, expansion and full-blood of sinusoidal hemocapillaries with numerous erythrocytes, leukocytes in the lumens, and in the wall were found Kupffer cells. There were significant vascular disorders, blood supply disorders, especially characteristic for central veins, and hepatic portal veins had moderate lumens, arteries often had spasmodic lumen, edema and wall thickening, there is significant perivascular edema, histoleukocyte infiltrates. A significant number of activated fibroblasts and moderately oxyphilic dystrophically altered hepatocytes with signs of cytoplasmic edema containing dark, compacted basophils nuclei were found. Similar results were also obtained by Makarova N. G. and etc. [10], who observed centroglobular foci of necrosis in hepatocytes in hypothyroidism. The authors did not detect dystrophically altered hepatocytes, which can probably be explained by the rapid transition from dystrophic to necrotic. The authors concluded that the increase in the mass of Kupffer cells is associated with high acid phosphatase activity, as evidenced by the strengthening of the phagocytic function of the liver macrophages, the elimination of necrotic mass. Despite the destructive processes, the content of glycogen in hepatocytes did not change, and the content of total protein increased. The authors explain such changes by compensatory activation of intralobular blood flow, as evidenced by the expansion of sinusoidal capillaries and an increase in their mass by 1.5 times.

The combined effect of hypothyroidism and HHCy causes the most pronounced changes in the necrotic and degenerative characteristics of the structural components of the liver lobes against the background of significant vascular violations. Small and large-scale fatty dystrophy and, to a lesser extent, protein-vacuolar and liquid necrosis in the lobes of the liver were detected. It is obvious that HHCy causes toxic effects on the endothelium of hepatic vessels due to the production of significant amounts of free radicals and stress of the endoplasmic reticulum. The heteropomorphism of cells and inflammatory changes in the organ, which appeared by large leukocyte infiltrates, both in the zone of the portal tracts and around the central vein, were established.

Conclusions

Under the conditions of simulated HHCy, hypo- and hyperthyroidism and especially with their combined effect in the liver, significant alternative and dystrophic changes of structural components are observed, characterized by the development of steatosis, vascular disorders, discomplexation of liver canaliculi in the lobules, necrotic changes in hepatocytes.

References

[1] Ai, Y., Sun, Z., Peng, C., Liu, L., Xiao, X., & Li, J. (2017). Homocysteine Induces Hepatic Steatosis Involving ER Stress Response in High Methionine Diet-Fed Mice. *Nutrients,* 9(4), E346. https://doi:10.3390/nu9040346

[2] Campbell, N., Agarwal, K., Alidoost, M., Miskoff, J.A., & Hossain M. (2020). Acute Fulminant Hepatic Failure and Renal Failure Induced by Oral Amiodarone: A Case Report and Literature Review. *Cureus,* 12(5), e8311. https://doi:10.7759/cureus.8311

[3] Dai, Y., Zhu, J., Meng, D., Yu, C., & Li, Y. (2016). Association of

homocysteine level with biopsy-proven non-alcoholic fatty liver disease: a meta-analysis. *J. Clin. Biochem. Nutr.*, 58(1), 76-83. https://doi.org:10.3164/jcbn.15-54

[4] De Leo, S., Lee, S.Y., & Braverman, L.E. (2016). Hyperthyroidism. *Lancet* (London, England), 388(10047), 906-918. https://doi.org/10.1016/S0140-6736(16)00278-6

[5] Glushchenko, S. V. (2014). Hyperhomocysteinemia as a predictor of the development and progression of fatty liver disease. *Problems of Continuing Medical Education and Science,* 2, 89-92.

[6] Gomez-Peralta, F., Velasco-Martinez, P., Abreu, C., Cepeda, M., & Fernandez-Puente, M. (2018). Hepatotoxicity in hyperthyroid patient after consecutive methimazole and propylthiouracil therapies. *Endocrinology, diabetes & metabolism case reports,* 2018, 17-0173. https://doi.org/10.1530/EDM-17-0173

[7] Goralskiy, L. P., Homich, V. T., & Kononskiy, O. I. (2011). *Fundamentals of histological technique and morphofunctional methods of research in norm and in pathology.* Zhitomir: Polissya.

[8] Hu, Y., Liu, J., Dong, X., Xu, Y., Leng, S., & Wang, G. (2016). Clinical Study of Serum Homocysteine and Non-Alcoholic Fatty Liver Disease in Euglycemic Patients. *Medical science monitor : international medical journal of experimental and clinical research,* 22, 4146-4151. https://doi.org/10.12659/msm.897924

[9] Lai, W. K., & Kan, M. Y. (2015). Homocysteine-induced endothelial dysfunction. *Ann. Nutr. Metab*., 67(1), 1-12. https://doi:10.1159/000437098

[10] Makarova, N. G., Vasilyeva, L. S., & Garmaeva, D. V. (2010). Structure of liver in experimental hypothyreos. *Siberian Medical Journal*, 94(3), 70-73.

[11] Martinez, Y., Li, X., Liu, G., Bin, P., Yan, W., Mas, D., … & Yin Y. (2017). The role of methionine on metabolism, oxidative stress, and diseases. *Amino Acids,* 49(12), 2091-2098. doi: 10.1007/s00726-017-2494-2. PMID: 28929442

[12] Mato, J. M., Alonso, C., Noureddin, M., & Lu, S. C. (2019). Biomarkers and subtypes of deranged lipid metabolism in non-alcoholic fatty liver disease. *World J. Gastroenterol.,* 25(24), 3009-3020. https://doi:10.3748/wjg.v25.i24.3009 PMID: 31293337

[13] Nadkharni, N., Masoodi, I., Ahmari, A., Sirwal, T., & Malik, N. (2018). Hyperthyroidism induced reversible hepatotoxicity a case report and brief review. International. *Journal of Medical Science and Public Health*, 7, 1. https://doi:10.5455/ijmsph.2018.0823817082018

[14] Nechiporuk, V., & Korda, M. (2017). Metabolism of cysteine in experimental hyper- and hypothyroidism in rats. *Medical and Clinical Chemistry,* 19(4), 32-40. https://doi:10.11603/mcch.2410-681X.2017.v0.i4.8433

[15] Nechiporuk, V., Zaichko, N., Korda, M., Melnyk, A., & Koloshko, O. (2017). Sulphur-containing amino acids metabolism in experimental hyper- and hypothyroidism in rats. *Georgian medical news*. 96-102.

[16] Nekrut, D. O., Zaichko, N. V., & Korol, A. P. (2017). Effect of hypolipidemic agents on morphological changes in rat liver in nonalcoholic fatty liver disease associated with hyperhomocysteinemia. *Biomedical and Biosocial Anthropology*, 28, 66-71.

[17] Peria-Kajan, J., & Jakubowski, H. (2019). Dysregulation of Epigenetic Mechanisms of Gene Expression in the Pathologies of Hyperhomocysteinemia. *International journal of molecular sciences,* 20(13), 3140. https://doi.org/10.3390/ijms20133140

[18] Shetty, S., Rajasekaran, S., & Venkatakrishnan, L. (2014). Grave's Disease and Primary Biliary Cirrhosis-An Unusual and Challenging Association. *Journal of clinical and experimental hepatology*, 4(1), 66-67. https://doi.org/10.1016/j.jceh.2013.08.001

[19] Stangl, G. I. (2007). Homocysteine thiolactone-induced hyperhomocysteinemia does not alter concentrations of cholesterol and SREBP-2 target gene mRNAS in rats. *Exp. Biol. Med.,* 232(1), 81-87.

МОРФОЛОГІЧНІ ЗМІНИ ПЕЧІНКИ ЗА УМОВ ГІПЕРГОМОЦИСТЕЇНЕМІЇ НА ФОНІ ГІПО- ТА ГІПЕРТИРЕОЗУ

Нечипорук В.М., Корда М.М., Ковальчук О.В.

Тироксин і трийодтиронін надзвичайно важливі для нормального росту, розвитку і функцій органів. Ці гормони регулюють базальну швидкість метаболізму всіх клітин, включаючи гепатоцити, і тим самим модулюють печінкові функції. Існує тісний зв'язок гіпергомоцистеїнемії (ГГЦ) з індукцією оксидативних процесів, порушенням продукції оксиду азоту NO-синтазою, пошкодженням ендоплазматичного ретикулуму і активацією запальних процесів у печінці. Відомо також про розлади метаболізму гомоцистеїну (ГЦ) при дисфункції щитоподібної залози. Тому, можна передбачити, що порушення структури та функцій печінки буде важливим проявом негативного впливу ГГЦ на органи та тканини при гіпер- та гіпотиреозі. Метою роботи було встановлення реорганізації структурних компонентів печінки за умов змодельованої ГГЦ, гіпер- та гіпортиреозу та їх сумісному впливі. Тіолактонову ГГЦ моделювали введенням тваринам екзогенного ГЦ у вигляді тіолактону в дозі 100 мг/кг маси тіла один раз на добу протягом 28 діб. Гіпертиреоз моделювали шляхом щоденного введення L-тироксину в дозі 200 мкг/кг протягом 21-го дня, гіпотиреоз - щоденного введення мерказолілу в дозі 10 мг/кг протягом 21-го дня. Окремим групам тварин вводили L-тироксин і мерказоліл паралельно з ГЦ. Встановлено, що за умов змодельованої ГГЦ, гіпо- та гіпертиреозу в печінці дослідних тварин спостерігаються дискомплектація балок гепатоцитів, зміни гепатоцитів деструктивного, дистрофічного та некротичного характеру з ознаками розвитку стеатозу, судинні розлади, що проявляються нерівномірним кровонаповненням, стазами, паравазальними лейкоцитарними інфільтратами, дрібними крововиливами. Таким чином, як ГГЦ, так і гіпо- чи гіпертиреоз призводять до порушення структурної організації тканини печінки. При розвитку дисфункції щитоподібної залози на тлі ГГЦ порушення гістологічної структури гепатоцитів суттєво посилювалися.

Ключові слова: *гіпертиреоз, гіпотиреоз, гіпергомоцистеїнемія, гомоцистеїн, печінка.*

МОРФОЛОГИЧЕСКИЕ ИЗМЕНЕНИЯ ПЕЧЕНИ В УСЛОВИЯХ ГИПЕРГОМОЦИСТЕИНЕМИИ НА ФОНЕ ГИПО- И ГИПЕРТИРЕОЗА

Нечипорук В.М., Корда М.М., Ковальчук О.В.

Тироксин и трийодтиронин очень важны для нормального роста, развития и функций органов. Эти гормоны регулируют базальную скорость метаболизма всех клеток, включая гепатоциты, и тем самым модулируют печеночные функции. Существует тесная связь гипергомоцистеинемии (ГГЦ) с индукцией оксидативных процессов, нарушением продукции

оксида азота NO-синтазой, повреждением эндоплазматического ретикулума и активацией воспалительных процессов в печени. Известно также о расстройствах метаболизма гомоцистеина (ГЦ) при дисфункции щитовидной железы. Поэтому, можно предположить, что нарушение структуры и функций печени будет важным проявлением негативного влияния ГГЦ на органы и ткани при гипер- и гипотиреозе. Целью работы было установление реорганизации структурных компонентов печени в условиях смоделированной ГГЦ, гипер- и гипортиреоза и их совместном влиянии. Тиолактоновую ГГЦ моделировали введением животным экзогенного ГЦ в виде тиолактона в дозе 100 мг/кг массы тела один раз в сутки в течение 28 суток. Гипертиреоз моделировали путем ежедневного введения L-тироксина в дозе 200 мкг/кг в течение 21 дня, гипотиреоз - ежедневного введения мерказолила в дозе 10 мг/кг в течение 21 дня. Отдельным группам животных вводили L-тироксин и мерказолил параллельно с ГЦ. Установлено, что в условиях смоделированной ГГЦ, гипо- и гипертиреоза в печени экспериментальных животных наблюдаются дискомплектация балок гепатоцитов, изменения гепатоцитов деструктивного, дистрофического и некротического характера с признаками развития стеатоза, сосудистые расстройства, проявляющиеся неравномерным кровенаполнением, стазами, паравазальными лейкоцитарными инфильтратами, мелкими кровоизлияниями. Таким образом, как ГГЦ, так и гипо- или гипертиреоз приводят к нарушению структурной организации ткани печени. При развитии дисфункции щитовидной железы на фоне ГГЦ нарушение гистологической структуры гепатоцитов существенно усиливалось.

Ключевые слова: *гипертиреоз, гипотиреоз, гипергомоцистеинемия, гомоцистеин, печень.*

DOI: 10.31393/morphology-journal-2020-26(2)-04 Reports of Morphology, Vol. 26, №2, Pages 26-31

ISSN 1818-1295 eISSN 2616-6194

REPORTS OF MORPHOLOGY

Official Journal of the Scientific Society of Anatomists, Histologists, Embryologists and Topographic Anatomists of Ukraine

journal homepage: https://morphology-journal.com

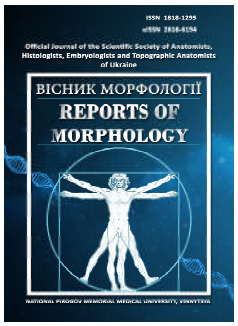

Morphological features of the wall of common bile duct under the conditions of experimental opioid exposure

Mateshuk-Vatseba L.R., Hirniak I.I., Pidvalna U.Y.
Danylo Halytsky Lviv National Medical University, Lviv, Ukraine

ARTICLE INFO
Received: 15 June, 2020
Accepted: 20 July, 2020

UDC: 611.367-018.1:615.212.7]-08

CORRESPONDING AUTHOR
e-mail: lvatseba@gmail.com
Mateshuk-Vatseba L.R.

The morphological condition of the bile ducts remains one of the most important problems of modern medical science. In order to obtain an analgesic effect in patients with acute cholangitis, opioids are often used. However, information on the effectiveness of opioids in the treatment of pathological conditions of the bile ducts is contradictory. The rapidly progressive destruction of the intrahepatic bile ducts associated with the use of narcotic agents has been described. Further study of the effect of opioids on the structural organization of the common bile duct is relevant. In order to establish the morphological state of the common bile duct under conditions of long-term opioid exposure, a study was performed on 24 sexually mature white male rats, aged 3.5-5.0 months and weighing 180-200 g, which were injected intramuscularly with Nalbuphine for 6 weeks. The study material is represented by histological specimens of the common bile duct of white rats. The "Aver Media" computer system was used to photograph microspecimens. The "ImageJ" computer program was used to measure the diameter of the lumen and the wall thickness of the common bile duct. After 2 weeks of Nalbuphine administration to white rats, plethora of wall microvessels and a significant increase in the longitudinal diameter of the lumen of the common bile duct were observed. After 4 weeks of the experiment, the common bile duct was dilated, the transverse and longitudinal diameters of its lumen almost doubled, pathological changes in its wall had all the signs of inflammation. In the later stages of the experiment (introduction of Nalbuphine for 6 weeks), the pathological changes increased and manifested by destructuring the wall of the common bile duct, disorganization of cholangiocytes, thinning of the cell layer due to detachment of cholangiocytes, polymorphism of their nuclei, destruction of intercellular junctions, stratification of its own plate, vacuolar dystrophy of the muscular membrane "varicose" expansion of venules, significant smooth muscle hyperplasia of arterioles, the presence of perivascular lymphocytic infiltrates in the duct wall.

Keywords: *microstructure, bile excretion pathways, white rat, Nalbuphine.*

Introduction

The morphological state of the bile ducts remains one of the most pressing problems of modern medical science [5, 6, 13, 17]. Damage to the bile ducts often poses a serious threat to the patient's life [4, 24, 26]. In 12-30% of patients operated on for cholecystitis or bile duct damage, scars and, accordingly, scar strictures of the common bile duct are formed in the postoperative period [2]. Therefore, especially many works are devoted to the tactics of surgical treatment of bile duct pathology [3, 7, 9, 34].

Studying histological changes in the common bile duct after long placement of a metal stent in animals, inflammation, fibrosis and trauma of the epithelium, an increase in the number of lymphoid follicles, a high degree of neutrophilic infiltration, the presence of ulcers of the mucous membrane were observed [22]. Recent advances in tissue engineering make it possible to create an intrahepatic bile duct tree. It has been proposed to induce the formation of bile ducts using encapsulated immortalized epithelial cells of the mucous membrane of the bile ducts of mice using decelularized hydrogels of the extracellular matrix of the liver [23]. Some works are devoted to the therapeutic treatment of bile duct pathology [11, 14, 35]. Successful treatment of biliary outflow difficulties was achieved by combination therapy, which included the

introduction of drugs into the portal vein and common bile duct [21].

Opioids, in particular morphine, are often used to obtain an analgesic effect in patients with acute cholangitis [12]. However, in the professional literature there are only a few works devoted to the study of the mechanism of action of opioids [8]. Information on the effectiveness of opioids in the treatment of pathological conditions of the bile ducts is often contradictory. The rapidly progressive destruction of the intrahepatic bile ducts associated with the use of narcotic agents has been described [20]. Among the non-obstructive etiologies of bile duct dilation, opioid consumption predominates [10].

The above determined *the purpose* of our study - to establish the features of the morphological state of the common bile duct under conditions of six weeks of opioid exposure in the experiment.

Materials and methods

The studies were performed on 24 adult white male rats weighing 180-200 g and aged 3.5-5.0 months. All experimental animals were divided into 3 series: in the first series (5 rats) studied the structural organization of the common bile duct wall of white rats after 2 weeks of Nalbuphine administration, in 2 series of experiments (5 rats) studied changes in the microstructure of the common bile duct after 4 weeks, and in 3 series of experiments (5 rats) reorganization of the wall of the common bile duct of experimental animals after 6 weeks of Nalbuphine administration. The control group included 9 white rats treated with 0.9% sodium chloride solution.

The study material is represented by histological preparations of the common bile duct of white rats. For histological examination, sections were stained with hematoxylin and eosin. The preparations were studied and photographed under microscope magnifications: x200, x400, x1000. The "Aver Media" computer system was used to photograph the micropreparations. The computer program ImageJ was used to measure the diameter of the lumen and the wall thickness of the common bile duct. For statistical processing of the received digital data the software "Excel" and "STATISTICA" 6.0 were used.

Administration of Nalbuphine was performed intramuscularly according to the following scheme: I week - 8 mg/kg, II week - 15 mg/kg, III week - 20 mg/kg, IV week - 25 mg/kg, V week - 30 mg/kg, week VI - 35 mg/kg.

All animals were kept in the vivarium of Danylo Halytsky Lviv National Medical University. The experiments were carried out in accordance with the provisions of the European Convention for the Protection of Vertebrate Animals Used for Experimental and Other Scientific Purposes (Strasbourg, 1986), Council Directive 86/609/EEC (1986), Law of Ukraine № 3447 - IV "On the protection of animals from cruelty", general ethical principles of animal experiments, approved by the First National Congress of Ukraine on Bioethics (2001).

Results

After 2 weeks of administration of Nalbuphine to white rats, the structural organization of the common bile duct wall of experimental animals, as well as control animals, is mainly preserved and represented by mucous, muscular and adventitial membranes (Fig. 1). The mucous membrane of the wall of the common bile duct is lined with prismatic epithelium, which was adjacent to its own plate, formed by a layer of connective tissue. Epithelial cells - cholangiocytes - had a typical structure, distinct apical, basal and lateral surfaces (the latter in contact with each other), a large oval nucleus with clear contours. In its own plate clearly visible single, but rather large glands with preserved structure. On some histological preparations of this term of experiment we found increase in number of glands in a wall of a common bilious channel, proliferation of their epithelium (Fig. 2). The muscular membrane consisted of smooth myocytes arranged in bundles with a preserved helical arrangement. The adventitial membrane is rich in

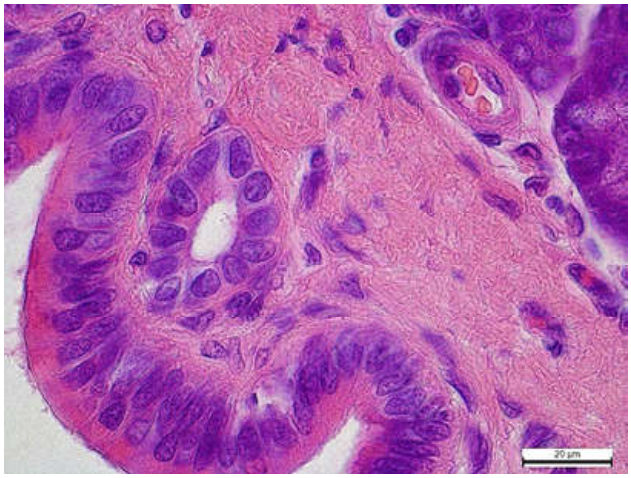

Fig. 1. A fragment of the common bile duct of a white rat after 2 weeks of the experiment. Hematoxylin-eosin. Photomicrograph. x1000.

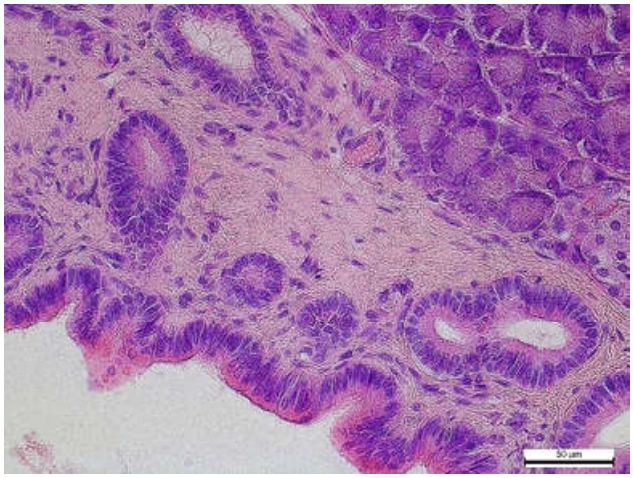

Fig. 2. A fragment of the common bile duct of a white rat after 2 weeks of the experiment. Hematoxylin-eosin. Photomicrograph. x400.

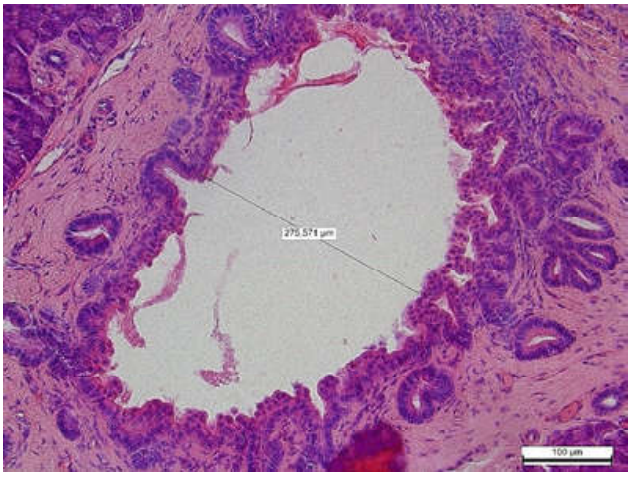

Fig. 3. A fragment of the common bile duct of a white rat after 4 weeks of the experiment. Hematoxylin-eosin. Photomicrograph. x200.

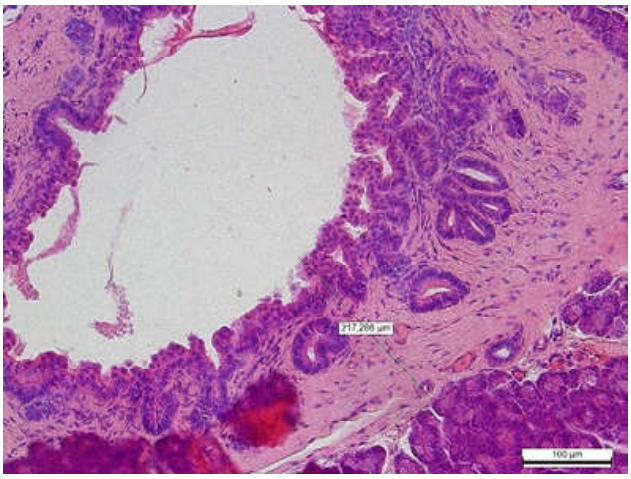

Fig. 4. A fragment of the common bile duct of a white rat after 4 weeks of the experiment. Hematoxylin-eosin. Photomicrograph. x200.

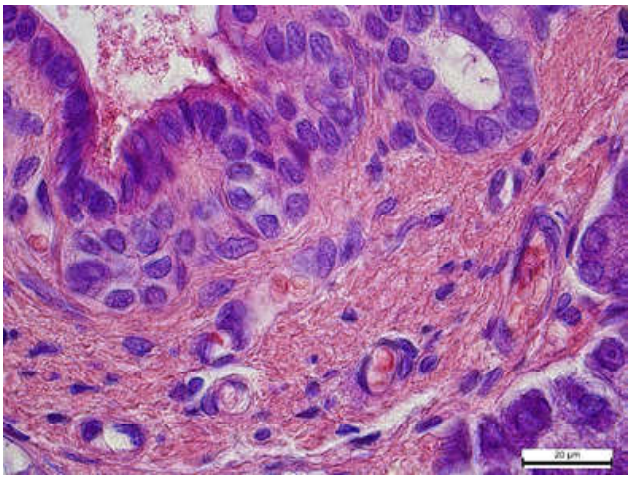

Fig. 5. A fragment of the common bile duct of a white rat after 6 weeks of the experiment. Hematoxylin-eosin. Photomicrograph. x1000.

vessels, which at this time of the experiment are full-blooded (especially arterioles and capillaries, as shown in Fig. 1) and dilated.

Morphometric analysis of histological specimens revealed that the lumen of the common bile duct of white rats in cross section has an oval shape, so we considered it appropriate to measure the longitudinal diameter of the lumen of the common bile duct, which was at this time of the experiment 272.77±15.09 μm (control - 126.97±3.19 μm, $p<0.05$), and the transverse diameter - 97.36±10.86 μm (control - 72.79±13.52 μm, $p>0.05$), wall thickness of common bile duct was 137.85±14.41 μm (control - 144.77±3.91 μm, $p>0.05$).

A significant increase in the longitudinal diameter of the lumen of the common bile duct indicates a change in the shape of its lumen due to two weeks of Nalbuphine introduction. In addition, although the change in the wall thickness of the common bile duct after 2 weeks of the experiment is not significant, but the maximum value of this indicator in experimental animals (152.52 μm) is much larger than its maximum value in control animals (148.69 μm), which indicates about increasing the wall thickness of the common bile duct during this period of the experiment.

After 4 weeks of experimental exposure to Nalbuphine, the shape of the lumen of the common bile duct is incorrect, cholangiocytes are often without clear contours, their nuclei are large, deformed, swollen, observed epithelial protrusions, and in some places - exfoliation of epitheliocytes into the lumen of the common bile duct (Fig. 3).

The own plate is swollen, fluffy, in some places stratified, glands are destructured, shifted in the direction of an epithelial layer, in their gleams - stagnation of secretion. The bundles of smooth muscle myocytes are stratified, partially losing their helical organization. The connective tissue of the adventitial membrane is in a state of edema, the arterioles are dilated, their wall is thickened, parietal thrombi are formed in the lumens, capillaries are hyperemic, often the capillary wall is damaged, diapedetic hemorrhages are found, venules are dilated, the walls of the venules are thinned (Fig. 4). Morphometric analysis showed a pronounced dilatation of the common bile duct, the longitudinal diameter of the lumen of the duct increased to 462.98±24.15 μm ($p<0.05$), the transverse diameter to 275.57±18.34 μm ($p<0.05$), as can be seen from Figure 2. The wall thickness of the common bile duct significantly ($p<0.05$) increased and amounted to 217.29±18.09 μm, as shown in Figure 4.

After 6 weeks of the experiment, the wall of the common bile duct is destructed, it was often difficult to differentiate the boundaries of its membranes, the cholangiocyte layer is disorganized, formed numerous folds, in some places thinning of the epithelial layer due to detachment of cholangiocytes, cholangiocytes acquired a flattened shape, noted the polymorphism of their nuclei, the nuclei lost their location in the center of the cell, shifted to the apical surface of the cell, intercellular contacts are broken, expanded (Fig. 5).The own plate of a wall of a common bilious channel is stratified, gleams of glands are uneven, have lost the

correct form, mainly expanded, filled with contents. The bundles of smooth myocytes are separated by coarse layers of connective tissue, there is a vacuolar dystrophy of the muscular membrane, the adventitial membrane is in a state of edema, sometimes not differentiated.

When performing morphometric analysis, it was often impossible to determine the transverse diameter of the lumen of the common bile duct, because its walls collapsed (glued), the lumen of the duct was deformed, the longitudinal diameter of the lumen ranged from 294.88 μm to 386.46 μm ($p<0.05$), the wall thickness of the common bile duct was 176.44±26.34 μm, which is significantly more than the control animals, but significantly less than the experimental animals in the previous period of the experiment, which confirms the development of dystrophic-degenerative processes in the common bile duct wall after 6 weeks exposure to Nalbuphine. During this period of the experiment, significant changes in the vessels of the hemomicrocirculatory tract of the common bile duct, including dilation of venules, significant smooth muscle hyperplasia of the portal arterioles were also detected. It should be noted that due to plasma infiltration, sclerosis and hyalinosis, the wall of the arterioles was thickened, and perivascular edema and lymphocytic infiltrates were observed.

Discussion

The results of research presented in the professional literature mainly indicate the negative impact of long-term use of opioids on the structural organization of organs and tissues [29]. At the heart of the development of pathological processes due to the action of narcotic drugs is often angiopathy [25, 27], which is confirmed in our studies.

A characteristic feature of the effect of Nalbuphine on the wall structure of the common bile duct is its dilatation. According to the literature, opioids can cause an increase in the basic pressure and frequency of phase contractions of the sphincter of Oddi, which leads to dilation of the common bile duct [10]. The author describes an association between elevated bile duct diameter and opioid dependence even in patients without clinical symptoms, normal bilirubin and alkaline phosphatase, and no obstructive factors. On histological specimens we found nonspecific morphological changes in the components of the common bile duct, as degeneration of the epithelial layer of its mucous membrane, lymphocytic infiltration, microvascular hyperemia is characteristic of cholangitis of various etiologies. Epithelial cells of the bile duct mucosa can serve as antigens to activate the cells of the natural killer T [31]. The bile ducts dilate, cholestasis develops, and lymphocytic infiltrates appear around the bile ducts. Inflammation of the bile duct (cholangitis) is based mainly on bile stasis, which leads to its thickening, sludge and subsequent infection, or, conversely, acute inflammation of the bile ducts (cholangitis) causes impaired bile flow [18, 32].

An important finding of our study is the degenerative changes in the later stages of the experiment of the muscular membrane of the wall of the common bile duct. Experiments have shown that damage to the muscular layer of the bile duct leads to the development of liver cirrhosis [16, 19, 28, 33] and even hepatocellular carcinoma [1, 30]. Significant collagen deposition, portal fibrosis, periductal edema, lymphocytic inflammation, dilatation of all bile ducts, blind end of small bile ducts, cholestasis (bile corks), increased systemic oxidative stress, and fibrosis were observed in rats after ligature was applied to the common bile duct, which eventually leads to liver cirrhosis [15, 32].

In the future, subject to long-term use of opioids, the results of this study can be used in practical medicine for the diagnosis and treatment of pathological conditions of the intrahepatic bile ducts.

Conclusions

Plethora of microvessels of the wall and a significant increase in the longitudinal diameter of the lumen of the common bile duct was observed after 2 weeks of administration of Nalbuphine to white rats.

After 4 weeks of the experiment, the common bile duct was dilated, the transverse and longitudinal diameters of its lumen almost doubled, pathological changes in its wall had all the signs of inflammation.

In the later stages of the experiment (introduction of Nalbuphine for 6 weeks) pathological changes increased and manifested by destructuring of the common bile duct wall, disorganization of cholangiocytes, thinning of the cell layer due to detachment of cholangiocytes, polymorphism of their nuclei, destruction of intercellular contacts, stratification of own plate, vacuolar dystrophy of a muscular cover, "varicose" expansion of venules, expressive smooth muscular hyperplasia of arterioles, existence of perivascular lymphocytic infiltrates in a channel wall.

References

[1] Abshagen, K., Kцnig, M., Hoppe, A., Mьller, I., Ebert, M., Weng, H. … Dooley, S. (2015). Pathobiochemical signatures of cholestatic liver disease in bile duct ligated mice. *BMC Syst. Biology*, 9, 83. doi: 10.1186/s12918-015-0229-0

[2] Burden, N., Kendrick, J., Knight, L., McGregor, V., Murphy, H., Punler, M., & van Wijk, H. (2017). Maximizing the success of bile duct cannulation studies in rats: recommendations for best practice. *Lab. Anim.*, 51(5), 457-464. doi: 10.1177/0023677217698001

[3] Buturovic S. (2014). Iatrogenic Injury to the Common Bile. *Duct. Med. Arch.,* 68(4), 291-293. doi: 10.5455/medarh.2014.68

[4] Carmody, I. C., Romano, J., Bohorquez, H., Bugeaud, E., Bruce, D. S., Cohen, A. J. … Loss, G. E. (2017). Novel Biliary Reconstruction Techniques During Liver Transplantation. *Ochsner J.,* 17(1), 42-45. PMID: 28331447

[5] Cheng, Y., Xiong, X. Z., Zhou, R. X., Deng, Y. L., Jin, Y. W., Lu, J. … Cheng, N. S. (2016). Repair of a common bile duct defect with a decellularized ureteral graft. *World J. Gastroenterol.,*

22(48), 10575-10583. doi: 10.3748/wjg.v22.i48.10575
[6] Cho, H. J., Jwa, H. J., Kim, K. S., Gang, D. Y., & Kim, J. Y. (2013). Urosodeoxycholic Acid Therapy in a Child with Trimethoprim-Sulfamethoxazole-induced Vanishing Bile Duct Syndrome. Pediatr. Gastroenterol. *Hepatol. Nutr.,* 16(4), 273-278. doi: 10.5223/pghn.2013.16.4.273
[7] Chun, K. (2014). Recent classifications of the common bile duct injury. *Korean J. Hepatobiliary Pancreat. Surg.*, 18(3), 69-72. doi: 10.14701/kjhbps.2014.18.3.69
[8] Dai, J., Wu, X. F., Yang, C., Li, H. J., Chen, Y. L., Liu, G.Z. … Li, N. (2015). Study of Relationship Between the Blood Supply of the Extrahepatic Bile Duct and Duct Supply Branches from Gastroduodenal Artery on Imaging and Anatomy. *Chin. Med. J.* (Engl), 128(3), 322-326. doi: 10.4103/0366-6999.150097
[9] Darkahi, B., Liljeholm, H., & Sandblom, G. (2016). Laparoscopic Common Bile Duct Exploration: 9-Years Experience from a Single Center. *Front. Surg.*, 3, 23. doi: 10.3389/fsurg.2016.00023
[10] DeAngelis, C., Marietti, M., Bruno, M., Pellicano, R., & Rizzetto, M. (2015). Endoscopic ultrasound in common bile duct dilatation with normal liver enzymes. *World J. Gastrointest. Endosc.,* 7(8), 799-805. doi: 10.4253/wjge.v7.i8.799
[11] Fahmy, S. R. (2015). Anti-fibrotic effect of Holothuria arenicola extract against bile duct ligation in rats. BMC Complement Altern. *Med.,* 15, 14. doi: 10.1186/s12906-015-0533-7
[12] Farnia, M. R., Babaei, R., Shirani, F., Momeni, M., Hajimaghsoudi, M., Vahidi, E., & Saeedi, M. (2016). Analgesic effect of paracetamol combined with low-dose morphine versus morphine alone on patients with biliary colic:a double blind, randomized controlled trial. *World J. Emerg. Med.*, 7(1), 25-29. doi: 10.5847/wjem.j.1920-8642.2016.01.004
[13] Fazeli Dehkordy, S., Fowler K. J., Wolfson, T., Igarashi, S., Lamas Costantino, C. P., Hooker, J. C. … Sirlin, C. B. (2018). Technical report: gadoxetate-disodium-enhanced 2D R2* mapping: a novel approach for assessing bile ducts in living donors. *Abdom. Radiol.* (NY), 43(7), 1656-1660. doi: 10.1007/s00261-017-1365-3
[14] Fenner, E. K., Boguniewicz, J., Tucker, R. M., Sokol, R. J., & Mack, C. L. (2014). High Dose IgG Therapy Mitigates Bile Duct Targeted Inflammation and Obstruction in a Mouse Model of Biliary. *Atresia Pediatr. Res.*, 76(1), 72-80. doi: 10.1038/pr.2014.46
[15] Garrido, M., Escobar, C., Zamora, C., Rejas, C., Varas, J., P?rraga, M. … Montedonico S. (2017). Bile duct ligature in young rats: A revisited animal model for biliary atresia. *Eur. J. Histochem.*, 61:2803, 249-254. doi: 10.4081/ejh.2017.2803
[16] Giusto, M., Barberi, L., Di Sario, F., Rizzuto, E., Nicoletti, C., Ascenzi, F., Renzi, A. … Merli, M. (2017). Skeletal muscle myopenia in mice model of bile duct ligation and carbon tetrachloride?induced liver cirrhosis. *Physiol. Rep.*, 5(7), 1-13. doi: 10.14814/phy2.13153
[17] Gudnason, H. O., & Bjцrnsson, E. S. (2017). Secondary sclerosing cholangitis in critically ill patients:current perspectives. *Clin. Exp. Gastroenterol.*, 10, 105-111. doi: 10.2147/CEG.S115518
[18] Hatano, R., Akiyama, K., Tamura, A., Hosogi, S., Marunaka, Y., Caplan, M. J. … Asano, S. (2015). Knockdown of Ezrin Causes Intrahepatic Cholestasis by the Dysregulation of Bile Fluidity in the Bile Duct Epithelium in Mice. *Hepatology,* 61(5), 1660-1671. doi: 10.1002/hep.27565
[19] Jiang, J., Wei, J., Wu, J., Gao, W., Li, Q., Jiang, K., & Miao, Y. (2016). Partial Portal Vein Arterialization Attenuates Acute Bile Duct Injury Induced by Hepatic Dearterialization in a Rat Model. *Biomed. Res. Int.,* 2016, 1-14. doi: 10.1155/2016/7427246
[20] Kim, H. Y., Yang, H. K., Kim, S. H., & Park, J. H. (2014). Ibuprofen Associated Acute Vanishing Bile Duct Syndrome and Toxic Epidermal Necrolysis in an Infant. *Yonsei Med. J.*, 55(3), 834-837. doi: 10.3349/ymj.2014.55.3.834
[21] Kubo, N., Harimoto, N., Shibuya, K., Ishii, N., Tsukagoshi, M., Igarashi, T. … Shirabe, K. (2018). Successful treatment of isolated bile leakage after hepatectomy combination therapy with percutaneous transhepatic portal embolization and bile duct ablation with ethanol: a case report. *Surg. Case Rep.*, 4, 1-5. doi: 10.1186/s40792-018-0463-y
[22] Lee, S. S., Song, T. J., Joo, M., Park, D. H., Seo, D. W., Lee, S. K., & Kim, M. H. (2014). Histological Changes in the Bile Duct after Long-Term Placement of a Fully Covered Self- Expandable Metal Stent within a Common Bile Duct: A Canine Study. *Clinical Endoscopy,* 47(1), 84-93. doi: 10.5946/ce.2014.47.1.84
[23] Lewis, P. L., Su, J., Yan, M., Meng, F., Glaser, S. S., Alpini, G. D. … Shah, R. N. (2018). Complex bile duct network formation within liver decellularized extracellular matrix hydrogels. *Sci. Rep.*, 8, 1-14. doi: 10.1038/s41598-018-30433-6
[24] Li, S. Q., Hua, Y. P., Shen, S. L., Hu, W. J., Peng, B. G., & Liang, L. J. (2015). Segmental Bile Duct-Targeted Liver Resection for Right-Sided Intrahepatic Stones. *Medicine* (Baltimore), 94(28), 1-7. doi: 10.1097/MD.0000000000001158
[25] Mateshuk-Vatseba, L., Kost, A., & Pidvalna, U. (2018). Effect of Narcotic Analgesics on the Ultrastructure of the Eyeball (Experimental Study). Journal of Morphological Sciences. *Georg Thieme Verlag KG,* 35(04), 251-254. Available from: http://dx.doi.org/10.1055/s-0038-1676543
[26] Miethke, A. G., Zhang, W., Simmons, J., Taylor, A., Shi, T., Shanmukhappa, S. K. … Setchell, K. D. R. (2016). Pharmacological inhibition of ASBT changes bile composition and blocks progression of sclerosing cholangitis in mdr2 knockout mice. *Hepatology,* 63(2):512-523. doi: 10.1002/hep.27973
[27] Pokotylo, V. U. (2017). Peculiarities of myocardial ultrastructure of rats at the late terms of opioid intoxication. *Deutscher Wissenschaftsherold,* 6, 14-20.
[28] Sheen, J. M., Chen, Y. C., Hsu, M. H., Tain, Y. L., Huang, Y. H., Tiao, M. M. … Huang, Li-T. (2016). Melatonin Alleviates Liver Apoptosis in Bile Duct Ligation Young Rats. *Int. J. Mol. Sci.,* 17(8), 1365. doi: 10.3390/ijms17081365
[29] Soleimanpour, H., Safari, S., Shahsavari, N. K., Sanaie, S., & Alavian, S. M. (2016). Opioid Drugs in Patients With Liver Disease: A Systematic Review. *Hepat. Mon.*, 16(4), e32636. doi: 10.5812/hepatmon.32636
[30] Tag, C. G., Sauer-Lehnen, S., Weiskirchen, S., Borkham-Kamphorst, E., Tolba, R. H., Tacke, F., Weiskirchen, R. … (2015). Bile Duct Ligation in Mice:Induction of Inflammatory Liver Injury and Fibrosis by Obstructive Cholestasis. *J. Vis. Exp.*, 96, 52438. doi: 10.3791/52438
[31] Tomizawa, M., Shinozaki, F., Hasegawa, R., Shirai, Y., Motoyoshi, Y., Sugiyama, T. … Ishige, N. (2017). Comparison of acute cholangitis with or without common bile duct dilatation. *Exp. Ther. Med.,* 13(6), 3497-3502. doi: 10.3892/etm.2017.4401
[32] Van Thuy, T. T., Thuy, L. T., Yoshizato, K., & Kawada, N. (2017). Possible Involvement of Nitric Oxide in Enhanced Liver Injury and Fibrogenesis during Cholestasis in Cytoglobin-deficient Mice. *Scientific Reports,* 7(1), 41888, 1-14. doi: 10.1038/srep41888
[33] Xuan, R., Zhao, X., Hu, D., Jian, J., Wang, T., & Hu, C. (2015). Three-dimensional visualization of the microvasculature of bile duct ligation-induced liver fibrosis in rats by x-ray phase-

contrast imaging computed tomography. *Scientific Repots,* 5(1), 11500. doi: 10.1038/srep11500
[34] Yang, Y. L, Zhang, C., Zhang, H. W., Wu, P., Ma, Y. F., Lin, M. J. … Zhao, M. (2015). Common bile duct injury by fibrin glue: Report of a rare complication. *World J. Gastroenterol.*, 21(9), 2854-2857. doi: 10.3748/wjg.v21.i9.2854
[35] Zhen, Y. Z., Li, N. R., He, H. W., Zhao, S. S., Zhang, G. L., Hao, X. F., & Shao, R. G. (2015). Protective effect of bicyclol against bile duct ligation-induced hepatic fibrosis in rats. *World J. Gastroenterol.,* 21(23), 7155-7164. doi: 10.3748/wjg.v21.i23.

МОРФОЛОГІЧНІ ОСОБЛИВОСТІ СТІНКИ СПІЛЬНОЇ ЖОВЧНОЇ ПРОТОКИ ЗА УМОВ ЕКСПЕРИМЕНТАЛЬНОГО ВПЛИВУ ОПІОЇДУ

Матешук-Вацеба Л.Р., Гірняк І.І., Підвальна У.Є.

Морфологічний стан шляхів виведення жовчі залишається однією з найважливіших проблем сучасної медичної науки. З метою отримання анельгезуючого ефекту у пацієнтів із гострим холангітом часто застосовують опіоїди. Проте відомості щодо ефективності застосування опіоїдів для лікування патологічних станів жовчних проток суперечливі. Актуальним є подальше дослідження дії опіоїдів на структурну організацію спільної жовчної протоки. З метою встановлення морфологічного стану спільної жовчної протоки за умов тривалого впливу опіоїду проведено дослідження на 24 статевозрілих білих щурах-самцях, віком 3,5-5,0 місяців і масою тіла 180-200 г, котрим впродовж 6 тижнів внутрішньом'язово вводили налбуфін. Матеріал дослідження представлений гістологічними препаратами спільної жовчної протоки білих щурів. Для фотодокументування отриманих нами мікропрепаратів була використана комп'ютерна система "Aver Media". Для виміру діаметра просвіту та товщини стінки спільної жовчної протоки застосовували комп'ютерну програму ImageJ. Результати дослідження свідчать, що через 2 тижні введення налбуфіну білим щурам виникало повнокров'я мікросудин стінки та достовірне збільшення поздовжнього діаметра просвіту спільної жовчної протоки. Через 4 тижні експерименту спільна жовчна протока дилатована, поперечний та поздовжній діаметри її просвіту зростали майже вдвічі, патологічні зміни її стінки мали всі ознаки запалення. На пізніх термінах експерименту (введення налбуфіну впродовж 6 тижнів) патологічні зміни наростали і проявлялися деструктуризацією стінки спільної жовчної протоки, дезорганізацією холангіоцитів, стоншенням клітинного пласту внаслідок відшарування холангіоцитів, поліморфізмом їхніх ядер, руйнуванням міжклітинних контактів, розшаруванням власної пластинки, вакуольною дистрофією м'язової оболонки, "варикозним" розширенням венул, виразною гладком'язовою гіперплазією артеріол, наявністю периваскулярних лімфоцитарних інфільтратів у стінці протоки.

Ключові слова: *мікроструктура, шляхи виведення жовчі, білий щур, налбуфін.*

МОРФОЛОГИЧЕСКИЕ ОСОБЕННОСТИ СТЕНКИ ОБЩЕГО ЖЕЛЧНОГО ПРОТОКА В УСЛОВИЯХ ЭКСПЕРИМЕНТАЛЬНОГО ВЛИЯНИЯ ОПИОИДА

Матешук-Вацеба Л.Р., Гирняк И.И., Пидвальна У.Е.

Морфологическое состояние путей вывода желчи остается одной из важнейших проблем современной медицинской науки. С целью получения анельгезирующего эффекта у пациентов с острым холангитом часто применяют опиоиды. Однако сведения об эффективности применения опиоидов для лечения патологических состояний желчных протоков противоречивы. Актуальным является дальнейшее исследование действия опиоидов на структурную организацию общего желчного протока. С целью установления морфологического состояния общего желчного протока в условиях длительного воздействия опиоида проведено исследование на 24 половозрелых белых крысах-самцах в возрасте 3,5-5,0 месяцев и массой тела 180-200 г, которым в течение 6 недель внутримышечно вводили налбуфин. Материал исследования представлен гистологическими препаратами общего желчного протока белых крыс. Для фотодокументирования полученных нами микропрепаратов была использована компьютерная система "Aver Media". Для измерения диаметра просвета и толщины стенки общего желчного протока применяли компьютерную программу ImageJ. Результаты исследования свидетельствуют, что через 2 недели введения налбуфина белым крысам возникало полнокровие микрососудов стенки и достоверное увеличение продольного диаметра просвета общего желчного протока. Через 4 недели эксперимента общий желчный проток дилятирован, поперечный и продольный диаметры его просвета увеличились почти вдвое, патологические изменения его стенки имели все признаки воспаления. На поздних сроках эксперимента (введение налбуфина в течение 6 недель) патологические изменения нарастали и проявлялись деструктуризацией стенки общего желчного протока, дезорганизацией холангиоцитов, истончением клеточного пласта в результате отслоения холангиоцитов, полиморфизмом их ядер, разрушением межклеточных контактов, расслоением собственной пластинки, вакуольной дистрофией мышечной оболочки, "варикозным" расширением венул, выраженной гладкомышечной гиперплазией артериол, наличием периваскулярных лимфоцитарных инфильтратов в стенке протока.

Ключевые слова: *микроструктура, пути выведения желчи, белая крыса, налбуфин.*

DOI: 10.31393/morphology-journal-2020-26(2)-05 Reports of Morphology, Vol. 26, №2, Pages 32-38

ISSN 1818-1295 eISSN 2616-6194

REPORTS OF MORPHOLOGY

Official Journal of the Scientific Society of Anatomists, Histologists, Embryologists and Topographic Anatomists of Ukraine

journal homepage: https://morphology-journal.com

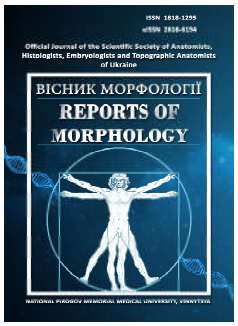

Grass pollen morphology investigation as a basis for monitoring of allergenic biological particles in an automatic mode

Yasniuk M.V., Kaminska O.A., Rodinkova V.V.
National Pirogov Memorial Medical University, Vinnytsia, Ukraine

ARTICLE INFO
Received: 14 June, 2020
Accepted: 10 July, 2020

UDC: 638.138:582.542:616-022.8

CORRESPONDING AUTHOR
e-mail: yasnyukmarina@gmail.com
Yasniuk M.V.

A clear distinction between the morphology of allergenic pollen grains of various genera of the Poaceae family is an important task in determining the causal allergenic factors in the population. It allows significant improvement of the efficiency of seasonal allergy diagnostics caused by grass pollen. Moreover, it let to perform better predictions of allergenic risks for people, suffering from pollinosis caused by Poaceae pollen. Therefore, the aim of our study was to establish the morphological difference between the pollen grains of plants of various species of Poaceae family in order to further determination of the possibility to use the established distinctions for the identification of pollen in aerobiological studies. For this, both herbarium samples and pollen of the studied plants were collected in the field during May-June 2019 in Vinnytsia. The pollen was shaken off the anthers directly onto a glass slide, immediately stained with basic fuchsin, and covered with a cover slip. The sizes of pollen grains - their width and length - were determined and analyzed using the PhotoM 1.21 program, and the obtained data on the sizes of pollen were divided into categories by the quartile method in Excel. Three categories of pollen sizes were identified: large, medium and small. Large grains had width and length parameters of 40 μm or more, average grains ranged from 26 to 39 μm, and small grains had a size of 26 μm or lesser in width and length. The large category includes the pollen of Hordeum morinum (39.5-53.1 μm), Elytrigia repens (41-48 μm), Secale cereale (48.4-62.5 μm) and Bromus arvensis (42.2-52.7 μm). The medium grain category included pollen from Dactylis glomerata (29.2-38.1 μm), Poa spp. (26.1-37.3 μm), Panicum capillare (33.3-39.5 μm), Lolium perenne (30.4-35.3 μm), Bromus sterilis (28.3-30.8 μm). The pollen size of B. ramosus ranged from 26.1 to 39.5 μm, and B. tectorum was from 35 to 38.4 μm. The pollen grains of Poa pratense (22.1-25.9 μm) and Piptatherum spp were assigned to the category of the smallest pollen (20.3-24.1 microns). Agrostis gigantea was the only grass pollen type whose size fitted for each category. We found out large, medium-sized and grains of 25.0-27.7 microns, which lie between categories 2 and 3, for different populations of this plant. Consequently, some genera and species of Poaceae can be distinguished by the size of their pollen, while in others the size of pollen grains varies considerably. It is necessary to carry out further research that will help to establish the morphology of pollen of a larger number of Grass family plants. This will significantly improve the diagnosis and prevention of seasonal allergy caused by grass pollen in Ukraine.

Key words: *allergenic pollen, allergenic biological particles, seasonal allergy, grass pollen, pollen sensitivity, pollinosis prevention.*

Introduction

Gramineae (Poaceae) or grasses are a large family of about 8,000 species. Representatives of this family are common herbs. They cover about 20% of the land surface. Grasses made a great contribution to the development of human culture, as they were one of the first plants grown by man, helping him to move from hunting and gathering the gifts of nature to agriculture. This happened about 10,000 years ago. Cereals such as wheat (Triticum) and barley (Hordeum) are still the most important sources of food for humans [27].

However, today the topic of grasses is becoming increasingly important given the high allergenicity of plants

of this family, including their pollen. After all, people are constantly exposed to it during the flowering of ornamental or those grasses that are used for landscaping lawns in settlements [16].

Thus, currently, the pollen of Poaceae family plants has become one of the most important factors of seasonal allergy in the world [5, 11]. In temperate climates, it contributes significantly in the level of sensitization of patients, along with pollen of ragweed and trees, in particular, birch [4, 8, 19]. According to molecular diagnostics of allergies [25], in Ukraine about 40% of patients with seasonal allergies are sensitive to grass pollen allergens. The same percentage of people with atopy react to grass pollen in Turkey. In other parts of the world, this number varies, but is also high. For example, in Switzerland, 12% of those with symptoms of seasonal allergy are sensitive to pollen [10], and in Australia, 29 to 41% of people with hay fever are sensitized to pollen too [6]. Therefore, it is not surprising that grass pollen is included into the list of pollen grain species for which allergy risk forecasts are most often made in Europe and in the world [15].

Moreover, both in Ukraine [25] and in the world [6], allergenicity of pollen of different species of the family Poaceae is considered [27]. These include Timothy (*Phleum pratensis*) and English ryegrass (*Lolium perenne*). Pollen allergens of these species are one of the main known factors of seasonal allergy [9, 26].

Thus, in Ukraine, 38.8% of people with hay fever are sensitive to meadow timothy' allergens, 28.8% - to English ryegrass, and 14.3% - to rye pollen [25]. There are also data on the allergenicity of pollen from other representatives of plants of the grass family - cock's-foot or orchard grass (*Dactylis glomerata*), Kentucky bluegrass (*Poa pratensis*) and Bermuda grass (Dhoob, dūrvā grass) (*Cynodon dactylon*) [2].

Flowering of all these species of Poaceae can both coincide and be observed in different periods of pollination of plants of the family. Therefore, pollen grains produced by plants at different times may be of clinical importance for different patients. From the point of view of the importance of these plants in terms of the ability to cause pathological symptoms in patients, it is important to inform them about the flowering of different species of plants at different times.

To date, the accuracy of aerobiological predictions of pollen distribution for plants of the Poaceae family is only relative: when counting and identifying pollen during aerobiological observations, grass pollen grains are gathered into one category - Poaceae. Therefore, when creating allergy forecasts [24], the risk levels due to the pollination of grasses are assessed for the family as a whole, and not for its individual species. However, as already mentioned, such an assessment could have a higher practical and clinical significance, given that it would allow for a more accurate diagnosis and prevention of pollinosis caused by grass pollen. This, in turn, could significantly save the population and the health care system' costs associated with treating seasonal allergies to grass pollen, in particular by allergen immunotherapy. The latter can last year-round in severe, late-diagnosed clinical casesand is expensive though [13].

Therefore, *the aim* of our study was to establish the morphological difference between the pollen grains of plants of different species of the family Poaceae to further determine the possibility of using the established difference in the identification of pollen in aerobiological studies.

Materials and methods

Pollen of the studied plants was collected in the city of Vinnytsia (Ukraine) directly from plant inflorescences (spikes or panicles) in the field during May and June 2019. Along with pollen samples, samples of the herbarium of selected plants were collected. The pollen was shaken out from the anthers directly onto a microscopic slide, immediately stained with a gelatin-based stain and stored in a thermos. The stain contained basic fuchsin. The chemical composition of the stain was identical to that, which is standardly used for staining pollen samples in aerobiological studies. After staining, the sample was covered with a cover glass. A total of 60 pollen samples from different plants were collected.

The first, test collection of pollen grains, was held on May 14, 2019. Its purpose was to determine the pollination activity of Poaceae family species that are among the first to emit pollen. In particular, wall barley (*Hordeum murinum*), rice grass (*Piptatherum spp.*), cock's-foot or orchard grass (*Dactylis glomerata*) and Kentucky bluegrass (*Poa pratensis*). At this time, the first 15 samples were collected, which did not show pollen grains. Therefore, despite the formed inflorescences, it was found out that the pollen of grasses at that time was still immature enough to be shaken off the anthers and, accordingly, cause symptoms of pollinosis.

A second attempt was made on May 30, 2019 and it had a positive result: 9 samples of pollen from different plants were obtained. During further collecting on June 1, 2019 and June 9, 2019 another 36 samples were collected. In total, grass pollen grains were detected in 45 samples. The obtained samples were analyzed using the method of light microscopy with a magnification of x400. This magnification is a standard for the identification of pollen grains.

Stained pollen grains were selected for getting their morphological parameters only after examination of the entire sample. This was done in order to be sure that pollen in one sample had the same size and shape, and to confirm that the collected pollen belongs to the same species.

When reviewing the selected samples, it was noteworthy that the pollen grains of grasses were of different shapes and sizes, had different structure and were differently saturated with the color of the stain, had different pore sizes.

Table 1. Indicators of width and length of pollen grains of the studied grass species (M±m), μm.

Species	Width	Length
Wall barley (*Hordeum morinum*)	45,68±4,47	47,60±3,41
Rye (*Secale cereale*)	61,60±0,90	51,20±2,80
Couch grass (*Elytrigia*)	45,68±4,32	47,60±3,05
Field brome (*Bromus arvensis*)	45,75±3,55	48,55±4,15
Cock's-foot or orchard grass (*Dactylis glomerata*)	30,97±2,93	33,23±2,72
Meadow-grass (*Poa*)	30,80±4,25	32,60±4,70
Annual meadow grass (*Poa annua*)	30,80±3,53	33,70±3,87
Downy brome (*Bromus tectorum*)	38,23±0,54	34,97±1,76
Barren brome (*Bromus sterilis*)	29,45±1,15	29,55±1,25
Hairy brome (*Bromus ramosus*)	31,77±4,05	35,20±3,64
Brome grasses (*Bromus*)	38,15±0,65	34,95±2,15
Kentucky bluegrass (*Poa pratensis*)	23,35±1,25	25,45±0,45
Ricegrass (*Piptatherum*)	20,65±0,35	23,45±0,65

Finally, a preliminary study found that pollen grain size varied the most (from 60 μm to 20 μm). Therefore, this parameter was chosen for further evaluation.

To get the linear dimensions, reference samples were selected without any mechanical damage. For pollen of each plant species, measurements were made at least three times to obtain their average value. For pollen grains of all categories, the average value of width and length, as well as the standard deviation were calculated (Table 1).

Grass species' definition was made in accordance with Ukrainian botanical atlases [20, 29] and Internet sources using the botanical specimens taken in a field after pollen collection.

PhotoM 1.21 program was used for accurate measurement of pollen grain size. This program made it possible to use photographs taken from a light microscope with a field of view having calibrated scale (Fig. 1). Analysis of sample sizes was continued in Excel using the quartile method.

The study of the morphology of grass pollen is a

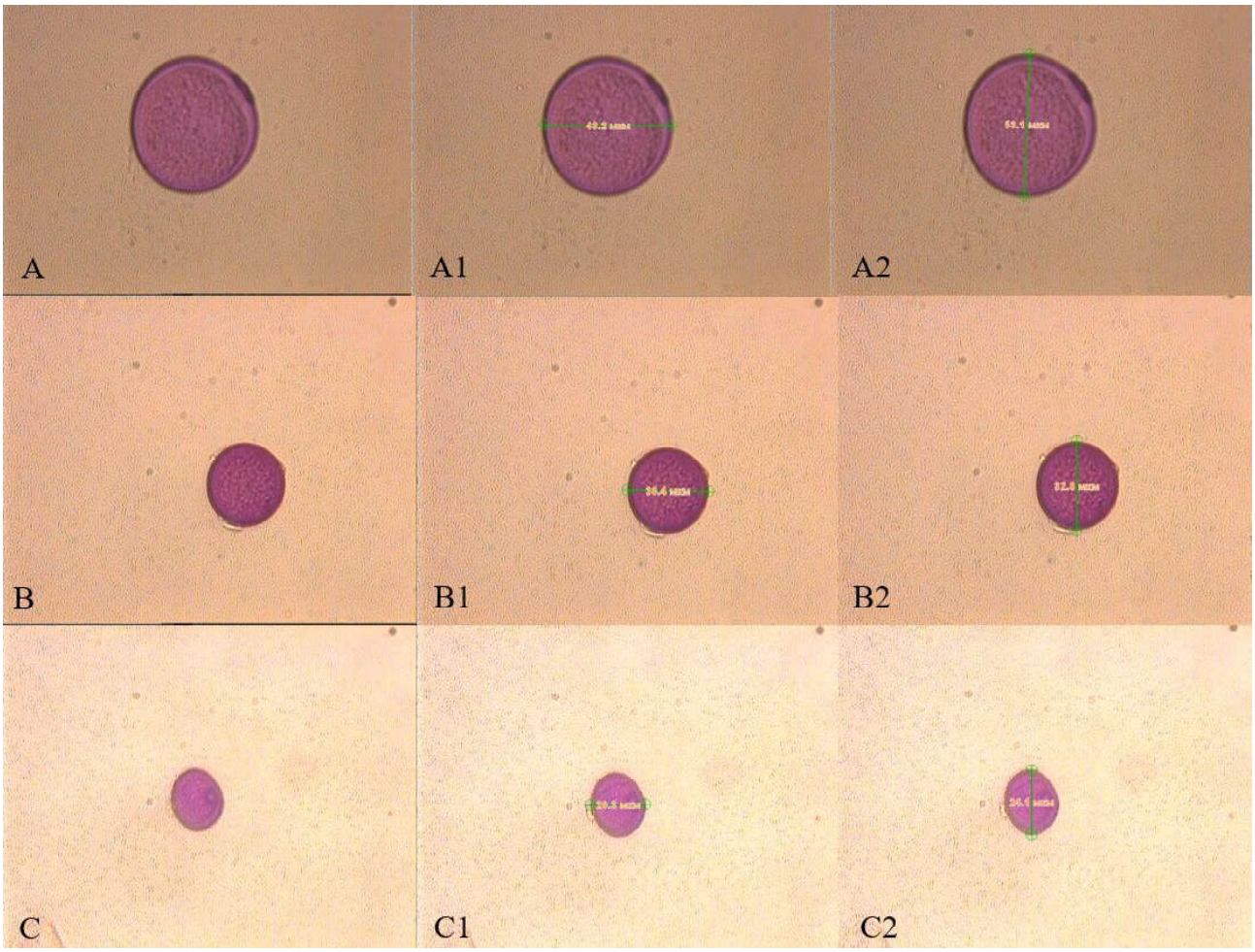

Fig. 1. Microscopic photos of pollen obtained in the program PhotoM 1.21. x400. Grass pollen of different categories: A - 1 category (Hordeum morinum), B - 2 category (Lolium perenne), C - 3 category (Piptatherum Spp.). A (Hordeum morinum): A1 - 48,2 μm of width and A2 -53,1 μm of length; B (Lolium perenne): B1 - width is 30,4 μm and B2 - length is 32,8 μm; C (Piptatherum Spp.): C1 - width is 20,3 μm and C2 - length is 24,1 μm.

promising scientific field in terms of diagnosis and prevention of hay fever. After all, pollen of grass species remains the leading allergenic agent of air. Moreover, the effectiveness of treatment of sensitivity to it depends on the exact definition of the causative agent of hay fever [18].

Results

The program divided the indicators of the linear size of the pollen into 4 quartiles as follows:

1st quartile: width - 62.5-38.4 μm, length 54.0-39.5 μm
2nd quartile: width - 37.5-32.1 μm, length 38.1-33.7 μm
3rd quartile: width - 31.7-26.1 μm, length 33.3-28.3 μm
4th quartile: width - 25.9-20.3 μm, length 27.9-22.8 μm.

Using the obtained data, with the help of "Excel" we obtained a clear selection of 3 categories of linear sizes of pollen grains (Fig. 2):

1. Large - width and length are greater than 40 μm;
2. Medium - width and length are in the range of26-39 μm;
3. Small - width and length are less than 26 μm.

The category of large pollen grains included pollen of *Hordeum morinum* (39.5-53.1 μm), *Elytrigia repens* (41-48 μm), *Secale cereale* (48.4-62.5 μm) and *Bromus arvensis* (42.2- 52.7 μm).

Medium-sized grains included pollen of *Dactylis glomerata* (29.2-38.1 μm), *Poa spp.* (26.1-37.3 μm), *Panicum capillare* (33.3-39.5 μm), *Lolium perenne* (30.4-35.3 μm), *Bromus sterilis* (28.3-30.8 μm). The pollen size of *B. ramosus* ranged from 26.1 to 39.5 μm, and *B. tectorum* from 35 to 38.4 μm.

The smallest category included pollen *Poa pratense* (22.1-25.9 μm) and *Piptatherum spp.* (20.3-24.1 μm).

The only species whose pollen size was suitable for all categories was *Agrostis gigantea*. For different populations of this plant, we found large, medium and grains of 25.0-27.7 μm, the size of which was between the categories of "medium" and "small" (Table 2).

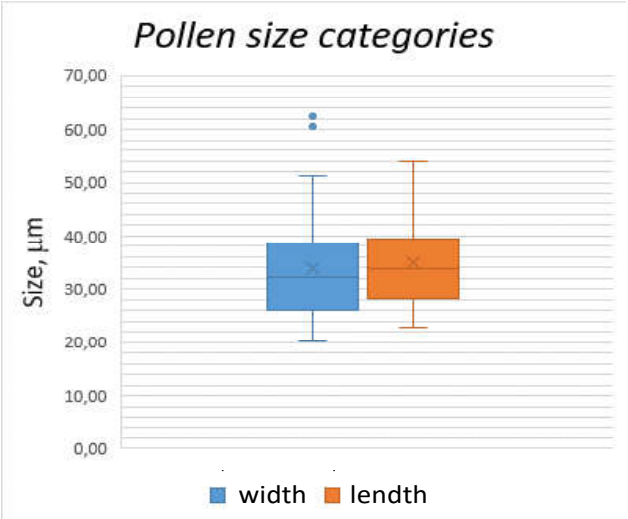

Fig. 2. Separation of grass pollen into categories by size (by width and length).

Table 2. Black bent (Agrostis gigantea). Variation of sizes on different samples of one specie (M±m), μm.

Agrostis gigantea			
sample	Width	Length	category
55	40,60±2,40	42,60±2,20	1
53	35,90±0,30	37,50±0,60	2
55A	30,10±0,75	30,40±1,90	2
52	25,90±0,20	27,70±2,90	3
54	26,10±0,12	27,00±2,40	3
53A	25,00±0,14	26,60±0,34	3

Table 3. Distribution of pollen grains sizes among the respective categories.

Species whose pollen has been identified	Date of collection	Pollen category
Wall barley (*Hordeum morinum*)	30.05.2019	1
Cock's-foot or orchard grass (*Dactylis glomerata*)	30.05.2019	2
Kentucky bluegrass (*Poa pratensis*)	30.05.2019	3
(Ricegrass (*Piptatherum*)	30.05.2019	3
Cock's-foot or orchard grass (*Dactylis glomerata*)	01.06.2019	2
Meadow-grass (*Poa*)	01.06.2019	2
Witchgrass (*Pancium capillare*)	01.06.2019	2
English ryegrass or perennial ryegrass (*Lolium perenne*)	01.06.2019	2
Barren brome (*Bromus sterilis*)	01.06.2019	2
Hairy brome (*Bromus ramosus*)	01.06.2019	2
Wall barley (*Hordeum morinum*)	09.06.2019	1
Couch grass (*Elytrigia*)	09.06.2019	1
Rye (*Secale cereale*)	09.06.2019	1
Field brome (*Bromus arvensis*)	09.06.2019	1
Cock's-foot or orchard grass (*Dactylis glomerata*)	09.06.2019	2
Annual meadow grass (*Poa annua*)	09.06.2019	2
Brome grasses (*Bromus*)	09.06.2019	2
Downy brome (*Bromus tectorum*)	09.06.2019	2
Kentucky bluegrass (*Poa pratensis*)	09.06.2019	3

To exclude the possibility of the impact of the gradual maturation of pollen on the final results, they were summarized in one table, which clearly showed that the size of the pollen did not depend on the time when it was collected.

Pollen of different categories was collected on each date indicated in the table. Pollen of the same species, which was collected on different dates, belonged to the same categories (Table 3).

Discussion

Grass pollen is not only the main factor of hay fever in the world [1], it also acts as an initiating factor that causes

the development of pollen allergy in general since childhood [19, 30].

However, insufficient attention is given in the scientific literature to the issue of studying the morphology of grass pollen. Available sources indicate the interest of scientists in studying the structure of pollen in agriculture [22], as well as - the interest in fossil pollen studies [12, 23].

At the same time, papers on the identification of grass pollen for aerobiological and allergological research are rare [8].

However, comparing the obtained data with the results of studying the morphology of grass pollen in the air, we can state that our data correlate with the data represented by other authors. In particular, rye pollen is known for its large size, and in our study it also got to the largest category. But *Agrostis* pollen, which in our study did not receive a clear category, was classified by L.N. Morgado and co-authors as pollen with small size [17]. These and other researchers [21] also divide grass pollen into three categories by size - large, medium and small. Moreover, the large pollen category includes pollen greater than 46 μm, and small - less than 22 μm, which roughly corresponds to the categories obtained in our study.

However, the morphology of grass pollen remains an unclear scientific question. This is because Poaceae family pollen is mostly spherical in size and has one pore. Therefore, scanning electron microscopy [3, 14] and spectroscopy [7] are used for its in-depth study. The latter technique can also be used to detect pollen automatically. However, there have been reports of evolutionary changes in the Poaceae family and the appearance of pollen with 2 pores [22]. The morphology of such pollen can be quickly determined using cheap and fast approaches used in aerobiology.

Therefore, the preliminary categorization of grass pollen and determination of their morphology using light microscopy remains an important approach of modern aerobiology.

The prospect of our further development and research is to further investigate the morphology of grass pollen that have already been selected for preliminary research, to expand the range of Poaceae family species under study, and to include in the morphological characteristics of pollen grains such indicators as pollen grain' volume, its width and length. Latter will lead to the determination of their shape.

These studies can be useful for both conventional aerobiological investigations and for automatic pollen monitoring.

Conclusions

Further study of the pollen morphology of Poaceae family plants is a promising practical area of both aerobiological and allergological research.

According to the linear sizes of pollen grain, three categories of grass pollen are defined - large, medium and small.

Some genera and species of the Poaceae family can be distinguished by the size and shape of their pollen, while in other cases the pollen varies considerably.

Further research is needed to determine the morphology of Poaceae pollen, the exact time of flowering of family species and the coincidence of periods of active pollination with data on exacerbations of human sensitivity to grass pollen in Ukraine.

References

[1] Al-Nesf, M. A., Gharbi, D., Mobayed, H. M., Dason, B. R., Ali, R. M., Taha, S. … del Mar Trigo, M. (2020). The association between airborne pollen monitoring and sensitization in the hot desert climate. *Clin. Transl. Allergy.*, 10, 35. doi: 10.1186/s13601-020-00339-6

[2] *Anallergo immunotherapy research,* n.d. Grass Mix Allergen Datasheet. Retrieved from: https://www.anallergo.it/en/patients/allergens/grass-pollens/grasses-(poaceae-or-gramineae)-mix.html

[3] Andersen, T. S., & Bertelsen, F. (1972). Scanning Electron Microscope Studies of Pollen of Cereals and other Grasses. *Grana,* 12(2), 79-86. doi: 10.1080/00173137209428830

[4] Bjerg, A., Ekerljung, L., Eriksson, J., Näslund, J., Sjölander, S., Rönmark, E. … Lundbäck, B. (2016). Increase in pollen sensitization in Swedish adults and protective effect of keeping animals in childhood. *Clinical & Experimental Allergy,* 46(10), 1328-1336. doi: 10.1111/cea.12757.

[5] Damialis A., Traidl-Hoffmann C., & Treudler R. (2019). Climate Change and Pollen Allergies. In: Marselle M., Stadler J., Korn H., Irvine K., Bonn A. (eds) *Biodiversity and Health in the Face of Climate Change*. Springer, Cham. doi: 10.1007/978-3-030-02318-8_3

[6] Davies, J. M., Berman, D., Beggs, P. J., Ramón, G. D., Peter, J., Katelaris, C. H., & Ziska, L. H. (2020). Global Climate Change and Pollen Aeroallergens; A Southern Hemisphere perspective. *Immunology and Allergy Clinics of North America*. doi: 10.1016/j.iac.2020.09.002

[7] Diehn, S., Zimmermann, B., Tafintseva, V.,Bagcioglu, M., Kohler, A., Ohlson, M. … Kneipp, J. (2020). Discrimination of grass pollen of different species by FTIR spectroscopy of individual pollen grains. *Analytical and Bioanalytical Chemistry*, 412, 6459-6474. doi: 10.1007/s00216-020-02628-2

[8] Douladiris, N., Garib, V., Focke-Tejkl, M., Valenta, R., Papadopoulos, N. G., & Linhart, B. (2018). Detection of genuine grass pollen sensitization in children by skin testing with a recombinant grass pollen hybrid. *Pediatric allergy and immunology,* 30(1), 59-65. doi: 10.1111/pai.12991

[9] Fernandez-Gonzalez, D., Rodriguez Rajo, F.J., Gonzalez Parrado, Z., Valencia Barrera, R. M., Jato, V., & Grau, S. M. (2011). Differences in atmospheric emissions of Poaceae pollen and Lol p 1 allergen. *Aerobiologia*, 27, 301-309. doi: 10.1007/s10453-011-9199-x

[10] Gangl, K., Niederberger, V., & Valenta, R. (2013). Multiple grass mixes as opposed to single grasses for allergen immunotherapy in allergic rhinitis. *Clin. Exp. Allergy,* 43(11), 1202-1216. doi: 10.1111/cea.12128

[11] Garcia-Mozo, H., (2017). Poaceae pollen as the leading aeroallergen worldwide: A review. *European journal of allergy and clinical immunology,* 72(12), 1849-1858. doi: 10.1111/all.13210.

[12] Liu, Q., Zhao, N-X., & Hao, G. (2004). Pollen morphology of the Chloridoideae (Gramineae), *Grana,* 43(4), 238-248. doi: 10.1080/00173130410000776

[13] Mahler, V., Zielen, S., & Rosewich, M. (2019). Year-round treatment initiation for a 6-grasses pollen allergoid in specific immunotherapy of allergic rhinoconjunctivitis and asthma. *Immunotherapy.* Retrieved from: https://www.futuremedicine.com/doi/10.2217/imt-2019-0086. doi: 10.2217/imt-2019-0086

[14] Mander, L., Li, M., Mio, W., Fowlkes, C. C., & Punyasena, S. W. (2013). Classification of grass pollen through the quantitative analysis of surface ornamentation and texture. *Proceedings of the Royal Society Biological Sciencies*, 280(1770). doi: 10.1098/rspb.2013.1905

[15] Maya-Manzano, J. M., Smith, M., Markey, E., Clancy, J. H., Sodeau, J., & O'Connor, D. J. (2020). Recent developments in monitoring and modelling airborne pollen, a review. *Grana.* doi: 10.1080/00173134.2020.1769176

[16] Mclnnes, R. N., Hemming, D., Burgess, P., Lyndsay, D., Osborne, N. J., Skjøth, C. A. … Vardoulakis, V. (2017). Mapping allergenic pollen vegetation in UK to study environmental exposure and human health. *The Science of the Total Environment*, 599-600, 483-499. doi: 10.1016/j.scitotenv.2017.04.136

[17] Morgado, L. N., Goncalves-Esteves, V., Resendes, R., & Mateus Ventura, M. A. (2015). Pollen morphology of Poaceae (Poales) in the Azores, Portugal. *Grana,* 54(4), 282-293. doi: 10.1080/00173134.2015.1096301

[18] Pfaar, O., Hohlfeld, J. M., Al-Kadah, B., Hauswald, B., Homey, B., Hunzelmann, N. … Klimek, L. (2017). Dose-response relationship of a new Timoty grass pollen allergoid in comparison with a 6-grass pollen allergoid. *Clinical Trial, Clin. Exp. Allergy,* 47(11), 144-1455. doi: 10.1111/cea.12977

[19] Pointner, L., Bethanis, A., Thaler, M., Traidl-Hoffmann, C., Gilles, S., Ferreira, F., & Aglas, L. (2020). Initiating pollen sensitization - complex source, complex mechanisms. *Clinical and Translational Allergy,* 10, 36. doi: 10.1186/s13601-020-00341-y

[20] Prokudyn, Y., & Vovk, A. (1977). *Grasses of Ukraine.* Kiev: Scientific Thought.

[21] Radaeski, J. N., Bauermann. S. G., & Pereira, A. B. (2016). Poaceae Pollen from Southern Brazil: Distinguishing Grasslands (Campos) from Forests by Analyzing a Diverse Range of Poaceae Species. *Frontiers in Plant Science*, 7(1833). doi: 10.3389/fpls.2016.01833

[22] Radaeski, J. N., Cunha, D. J., & Bauermann, S. G. (2017). Diporate pollen grains of Poaceae speices: high pollen resolution for reconstruction of grasslands vegetation. *Open access journal of agricultural research,* 2(3). doi: 10.23880/OAJAR-16000135

[23] Radaeski, J. N., Evaldt, A. N. P., & Bauermann, S. G. (2018). Anthropic pollen indicators: Poaceae pollen of non-native species in Southern Brazil. *Open Access Journal of Agricultural Research,* 2(2). doi: 10.15406/oajs.2018.02.00059

[24] Rodinkova, V. V. (2011). Pollen forecast is a service for doctors and patients that is developing in Vinnytsia. *"News of Medicine and Pharmacy" Allergology and Pulmonology.* Retrieved from: http://www.mif-ua.com/archive/issue-21193/

[25] Rodinkova, V., & Yuryev, S., (2019). The population sensitivity to the pollinosis factors in Ukraine according to the molecular allergy diagnosis ALEX. Clinical immunology. *Allergy. Infectology,* 2(115), 22-26. Retrieved from: https://kiai.com.ua/ua/archive/2019/2%28115%29/pages-22-26/chutlivist-naselennya-do-chinnikiv-polinozu-v-ukrayini-za-danimi-molekulyarnoyi-diagnostiki-alergiyi-alex-

[26] Ščevková, J., Vašková, Z., Sepšiová, R., Dušička, J., & Kováč, J. (2020). Relationship between Poaceae pollen and Phl p 5 allergen concentrationsand the imact of weather variables and air pollutants on their levels inthe atmosphere. *Heliyon* 6(7). doi: 10.1016/j.heliyon.2020.e04421

[27] Steinmann, H., & Ruden, S. (2004). *Grass pollens: Allergy - which allergens?* Uppsala: Pharmacia Diagnostics.

[28] Türe, C. (2016). Allergenic airborne Poaceae (grass) pollen around public transportation centers in Eskisehir, Turkey. *South Western Journal Horticulture, Biology and Environment,* 7(1), 1-14.

[29] Veselovskyi, I. V., Lysenko, A. K., & Manko, Y. P. (1988). *Atlas - determinant of weeds.* Kyiv: Harvest.

[30] Westman, M., Aberg, K., Apostolovic, D., Lupinek, C., Gattinger, P., Mittermann, I. … van Hage, M. (2020). Sensitization to grass pollen allergen molecules in a birth cohort-natural Phl p 4 as an early indicator of grass pollen allergy. *Journal of Allergy and Clinical Immunology,* 145(4), 1174-1181. doi: 10.1016/j.jaci.2020.01.006

ВИВЧЕННЯ МОРФОЛОГІЇ ПИЛКУ ЗЛАКІВ ЯК ПІДҐРУНТЯ МОНІТОРИНГУ АЛЕРГЕННИХ БІОЛОГІЧНИХ ЧАСТОК В АВТОМАТИЧНОМУ РЕЖИМІ

Яснюк М.В., Камінська О.А., Родінкова В.В.

Чітке розрізнення морфології алергенних пилкових зерен різних родів родини Тонконогових (Poaceae) є важливою задачею при визначенні чинників алергії у населення. Воно дозволяє як значно підвищувати ефективність діагностики сезонної алергії, викликаної пилком злаків, так і створювати більш точні прогнози сезонних ризиків для людей, котрі потерпають від алергії до пилку різних видів злаків. Відтак, метою нашого дослідження було встановлення морфологічної відмінності між пилковими зернами рослин різних видів родини Poaceae для подальшого визначення можливості використовувати встановлену відмінність при ідентифікації пилку в аеробіологічних дослідженнях. Для цього у польових умовах впродовж травня-червня місяця 2019 року у Вінниці збирали гербарні зразки й пилок досліджуваних рослин. Пилок струшували з пиляків безпосередньо на предметне скло і одразу забарвлювали основним фуксином та закривали покривним склом. Розміри пилкових зерен - їх ширину та довжину - визначали та аналізували за допомогою програми PhotoM 1.21, а квартильним методом у програмі Excel отримали цифрові дані щодо розмірів пилку, котрі в подальшому були розділені на 3 відповідні категорії: великий розмір пилку, середній та малий. Великі зерна мали параметри ширини й довжини 40 мкм і більше, середні зерна були від 26 до 39 мкм, а дрібний пилок становив 26 мкм та менше за шириною та довжиною. До категорії великих увійшов пилок Hordeum morinum (39,5-53,1 мкм), Elytrigia repens (41-48 мкм), Secale cereale (48,4-62,5 мкм) та Bromus arvensis (42,2-52,7 мкм). Категорія середніх зерен включала пилок Dactylis glomerata (29,2-38,1 мкм), Poa spp. (26,1-37,3 мкм), Panicum capillare (33,3-39,5 мкм), Lolium perenne (30,4-35,3 мкм), Bromus sterilis (28,3-30,8 мкм). Розмір пилку B. ramosus становив від 26,1 до 39,5 мкм, а B. tectorum - від 35 до 38,4 мкм. До категорії найменшого пилку були віднесені пилкові зерна Poa pratense (22,1-25,9 мкм) та Piptatherum spp. (20,3-24,1 мкм). Єдиним злаком, розмір пилку якого знаходився у кожній категорії, був Agrostis gigantea. Для різних популяцій цієї рослини ми виявили великі, середні розміри та зерна розміром 25,0-27,7 мкм, які

лежать між категоріями 2 та 3. Відтак, деякі роди та види Poaceae можна відрізнити за розмірами їхнього пилку, тоді як для інших розміри пилкових зерен значно варіюють. Необхідним є проведення подальших досліджень, які допоможуть встановити морфологію пилку більшої кількості рослин родини Тонконогових, що значно покращить в Україні діагностику та профілактику сезонної алергії, викликаної пилком злаків.
Ключові слова: *алергенний пилок, алергенні біологічні частки, сезонна алергія, пилок злаків, чутливість до пилку, профілактика полінозу.*

ИЗУЧЕНИЕ МОРФОЛОГИИ ПЫЛЬЦЫ ЗЛАКОВ КАК ОСНОВАНИЯ ДЛЯ МОНИТОРИНГА АЛЛЕРГЕННЫХ БИОЛОГИЧЕСКИХ ЧАСТИЦ В АВТОМАТИЧЕСКОМ РЕЖИМЕ

Яснюк М.В., Каминская О.А., Родинкова В.В.

Четкое отличие морфологии аллергенных зерен пыльцы различных родов семейства Тонконоговых (Poaceae) является важной задачей при определении факторов аллергии у населения. Оно позволяет как значительно повышать эффективность диагностики сезонной аллергии, вызванной пыльцой злаков, так и создавать более точные прогнозы сезонных рисков для людей, страдающих от аллергии на пыльцу разных видов злаков. Поэтому целью нашего исследования было установление морфологического различия между пыльцевыми зернами растений разных видов семейства Poaceae для дальнейшего определения возможности использования установленных отличий при идентификации пыльцы в аэробиологических исследованиях. Для этого в полевых условиях в течение мая-июня месяцев 2019 года в Виннице собирали гербарные образцы и пыльцу исследуемых растений. Пыльцу стряхивали с пыльников непосредственно на предметное стекло и сразу окрашивали основным фуксином и закрывали покровным стеклом. Размеры пыльцевых зерен - их ширину и длину - определяли и анализировали с помощью программы PhotoM 1.21, а квартильным методом в программе Excel получили цифровые данные размеров пыльцы, которые в дальнейшем были разделены на 3 соответствующие категории: большой размер пыльцы, средний и малый. Большие зерна имели параметры ширины и длины 40 мкм и более, средние зерна были от 26 до 39 мкм, а мелкая пыльца составляла 26 мкм и меньше по ширине и длине. В категорию больших вошла пыльца Hordeum morinum (39,5-53,1 мкм), Elytrigia repens (41-48 мкм), Secale cereale (48,4-62,5 мкм) и Bromus arvensis (42,2-52,7 мкм). Категория средних зерен включала пыльцу Dactylis glomerata (29,2-38,1 мкм), Poa spp. (26,1-37,3 мкм), Panicum capillare (33,3-39,5 мкм), Lolium perenne (30,4-35,3 мкм), Bromus sterilis (28,3-30,8 мкм). Размер пыльцы B. ramosus составлял от 26,1 до 39,5 мкм, а B. tectorum - от 35 до 38,4 мкм. К категории самой маленькой пыльцы были отнесены зерна пыльцы Poa pratense (22,1-25,9 мкм) и Piptatherum spp. (20,3-24,1 мкм). Единственным злаком, размер пыльцы которого находили в каждой категории, был Agrostis gigantea. Для разных популяций этого растения мы обнаружили большие, средние размеры и зерна размером 25,0-27,7 мкм, которые лежат между категориями 2 и 3. Следовательно, некоторые роды и виды Poaceae можно отличить по размерам их пыльцы, тогда как у других размеры пыльцевых зерен значительно варьируют. Необходимым является дальнейшее проведение исследований, которые помогут установить морфологию пыльцы большего количества растений семейства Тонконоговых, что значительно улучшит в Украине диагностику и профилактику сезонной аллергии, вызванной пыльцой злаков.
Ключевые слова: *аллергенная пыльца, аллергенные биологические частицы, сезонная аллергия, пыльца злаков, чувствительность к пыльце, профилактика поллиноза.*

DOI: 10.31393/morphology-journal-2020-26(2)-06 Reports of Morphology, Vol. 26, №2, Pages 39-44

ISSN 1818-1295 eISSN 2616-6194

REPORTS OF MORPHOLOGY

Official Journal of the Scientific Society of Anatomists, Histologists, Embryologists and Topographic Anatomists of Ukraine

journal homepage: https://morphology-journal.com

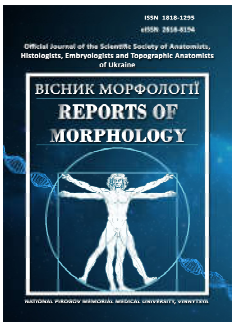

Comparative characteristics of the manifestations of damage and reparative processes in the mucous membrane of the duodenum of rats under the conditions of skin burns and skin burns associated with diabetes

Tymoshenko I.A.[1], Sokurenko L.M.[1], Yanchyshyn A.Ya.[1], Pastukhova V.A.[2]

[1]Bogomolets National Medical University, Kyiv, Ukraine

[2]National University of Ukraine on Physical Education and Sport, Kyiv, Ukraine

ARTICLE INFO

Received: 14 July, 2020

Accepted: 10 August, 2020

UDC: 616.342:599.323.4:616-001.17+616.379-008.64

CORRESPONDING AUTHOR

e-mail: iryna.tymoshenko@i.ua

Tymoshenko I.A.

Currently, severe thermal injury is becoming one of the most important problems of practical medicine. Diabetes is also recognized as another global medical and social challenge of our century. The emergency situation for the treatment and prevention of the consequences of these pathologies is a consequence of the lack of a reliable theoretical basis for solving specific clinical problems regarding the course of burns, diabetes and their complications. The aim of the study is to establish the patterns of structural changes in the mucous membrane of the duodenum after burn injury of the skin of rats under conditions of experimental diabetes mellitus. The study was performed on 63 laboratory white adult male rats weighing 180-210 g, which were divided into 3 groups: intact animals, rats with skin burns and rats with skin burns on the background of diabetes. The model of experimental diabetes mellitus was reproduced by administering Streptozotocin to rats intraperitoneally once at a dose of 50 mg/kg, pre-dissolved in 0.1 M citrate buffer solution (pH=4.5). The control of the development of hyperglycemia in the experimental groups was the level of glucose in the blood 24.24±0.79 mmol/l. In the control group this index was 8.03±0.4 mmol/l. Rats with skin burns revealed destructive manifestations, which are accompanied by an active inflammatory reaction and corresponding necrotic changes, while rats with skin burns on the background of diabetes mellitus pathological processes are not just "summed up", but in some way adaptively modified with the involvement of stress mechanisms of the endoplasmic reticulum and associated autophagy.

Key words: *duodenum, thermal trauma, diabetes.*

Introduction

Medium molecular weight proteins, which are products of proteolytic cleavage of blood plasma and tissue peptides, various toxins, proteolytic enzymes, mediators of immune reactions, prostaglandins, and cytokines, play an important role in the development of burn endogenous intoxication. The result of the rapid development of endogenous intoxication is the appearance of other disorders typical of burns - multiorgan failure syndrome, hypermetabolism syndrome, systemic inflammatory and apoptotic response. Thermal burn injury causes structural and functional changes in the small intestine, the nature and depth of which in some way correlate with the stage of the burn. Intestinal dysfunction (based on reactive, compensatory-adaptive and destructive changes in the cells of the digestive system) plays an important role in the development of multiorgan failure typical to burns.

Complications of diabetes mellitus and their symptoms are caused by abnormal gastrointestinal motility, which is a consequence of diabetic autonomic neuropathy. Currently, the most common is the streptozotocin model of experimental diabetes mellitus [2, 3, 10, 16, 17, 20]. Streptozotocin is an antibiotic (2-deoxy-2-methylnitrosamino-carbonyl-amino-O-glucopyranose) that is isolated during the fermentation of a culture of Streptomyces aerotogenes. Streptozotocin in the chemical sense is N-acetylglucosamine, which has in the position of acetate a residue of nitrosourea. According to the peculiarities of hormonal and metabolic changes, streptozotocin-induced

diabetes is similar to type 1 diabetes in humans, although under the conditions of this experimental model absolute insulin deficiency is a consequence of direct toxic damage to beta cells and occurs without autoimmune mechanisms, which is characteristic of their destruction. type 1 diabetes mellitus in humans.

It is generally accepted that the destructive processes of various genesis in the mucous membrane of the gastrointestinal tract not only cause changes in its barrier function, but also have critical effects on the course of carbohydrate, protein and lipid metabolism in the body [11, 14, 15, 19, 21]. Therefore, the study of polycaudal reaction [14] of the mucous membrane of the gastrointestinal tract, as part of the general maladaptation syndrome in diabetes mellitus (especially in combination with diabetes and other pathological conditions) remains relevant [19].

The aim of the study is to establish the patterns of structural changes in the mucous membrane of the duodenum after burn injury of the skin of rats under conditions of experimental diabetes mellitus.

Materials and methods

The study was performed on 63 laboratory white adult male rats weighing 180-210 g. The control group - 21 intact rats without signs of somatic pathology, the first experimental group included 21 rats with experimentally simulated skin burn injury, the second experimental group included 21 experimental rats simulated skin burn injury and diabetes. The experimental diabetes mellitus model was replicated by administering intraperitoneal streptozotocin to rats once at a dose of 50 mg/kg, pre-dissolved in 0.1 M citrate buffer solution (pH=4.5). The control of the development of hyperglycemia in the experimental groups was the level of glucose in the blood - 24.24±0.79 mmol/l. In the control group this level was 8.03±0.4 mmol/l.

The department of the duodenum was taken for morphological examinations, fragments of which were examined by light and electron microscopy.

Results

Damage to the epitheliocytes of the duodenal mucosa is based on deep destructive changes (mostly necrotic), which after 21 days (in the stage of septicotoxemia) are usually irreversible and develop against the background of significant intoxication of the body.

The revealed structural changes of epitheliocytes are evidence of violation of the structural integrity of the intestinal epithelial barrier (Fig. 1). In animals of the first experimental group, the damaged epithelium of the duodenal mucosa critically weakens the adequacy of its interface function between the mucosa and the intestinal lumen environment and is structurally unable to provide an effective barrier against toxins, pathogens and antigenic molecules.

The course of structural changes in the mucous membrane of rats of the first experimental group in terms of development over time is staged and it can be divided

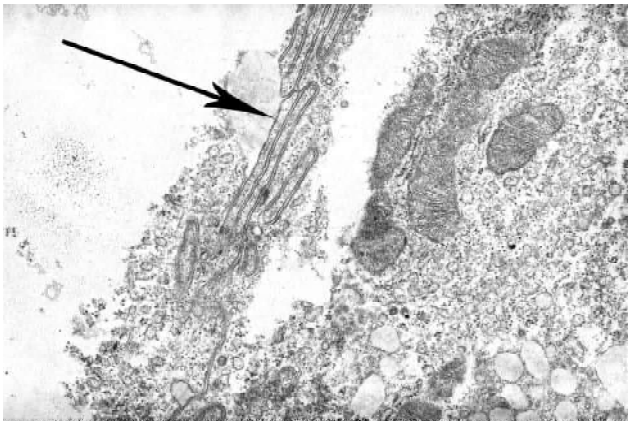

Fig. 1. Destruction of adjacent areas of adjacent epitheliocytes with a brush border in the duodenal mucosa of the rat of the first experimental group 7 days after the burn. The arrow marked the preserved area of intraepithelial contact, preserved in a fragment of intestinal cellular detritus. Electronic microphotography. x30000.

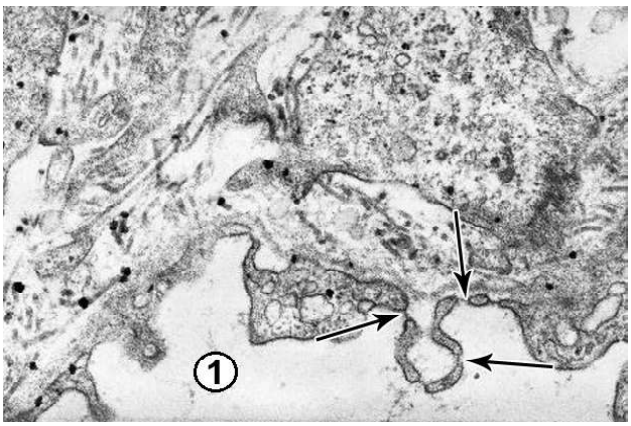

Fig. 2. Detachment of fenestrated blood capillary endothelium from the preserved basement membrane of the blood capillary in the loose connective tissue of the duodenal mucosa of the rat of the first experimental group 7 days after the burn. Arrows marked fenestrae in the endothelial cell. 1 - lumen of the blood capillary. Electronic microphotography. x30000.

into three stages and two phases. Seven days after the burn, structural manifestations of the overload stage are registered (which consists of a combination of total and subtotal destruction of some cells and with structural manifestations of the functional stress phase of other structurally preserved cells) (Fig. 2).

Fourteen days after the burn, a fixed structural picture of mucosal changes unfolds, which corresponds to the stage of relative stabilization of hyperfunction. Twenty-one days after the burn, the structural manifestations of gradual depletion and the development of decompensation are registered (Fig. 3).

The structural expression of the overload stage is not only the destruction of the plasmalemma followed by total or subtotal cell destruction, but also the changes of the organelles of the preserved cells detected by us (characteristic of the functional stress phase).

This is an expansion of the lumen and an increase in

Fig. 3. Cellular detritus (1) in the intestinal space of the duodenum of rats of the first experimental group 21 days after the burn. Electronic microphotography. x20000.

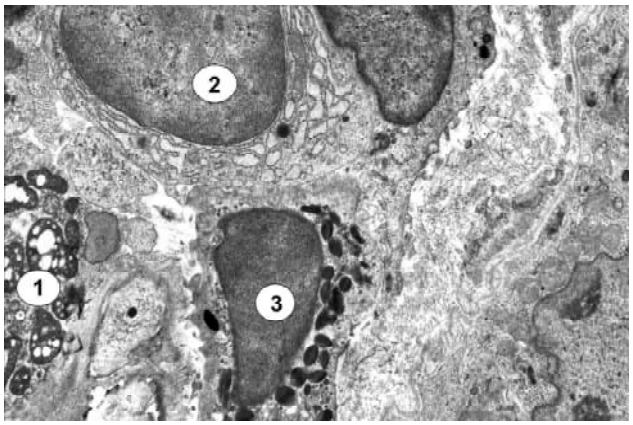

Fig. 4. Loose connective tissue of the duodenal mucosa of the rat of the third experimental group 21 days after the start of the experiment. 1 - accumulation of microbial bodies; 2 - plasma cell nucleus; 3 - leukocyte nucleus. Electronic microphotography. x10000.

the number of tubules of the granular endoplasmic reticulum (as well as an increase in the number of ribosomes attached to the tubular wall); increase in the number of ribosomes and polysomes; Golgi complex hypertrophy; increase in the number and variability of mitochondria (presence of large, old and small "young" mitochondria). But such intensive functioning, in our opinion, accelerates the rate of cell depletion, increases the accumulation in the cytoplasm of substances and damaged (defective) organelles, which activates intracellular mechanisms that lead to cell death (excessive autophagy and necrosis).

The phase of functional stress (and all its above manifestations) under the condition of favorable for the maintenance of cell life coincides with the phase of consolidation of compensatory-adaptive processes (which precedes the stage of relative stabilization of hyperfunction). But prolonged compensatory hyperfunction leads to the destruction of cellular organelles and cytoplasmic matrix, promotes the transition to the stage of gradual depletion and the development of decompensation.

Thus, not only the primary direct destruction of intestinal epithelial cells, but also organelle hyperplasia, probably leads to a disorder of the intracellular self-regulation system, disruption of intercellular interactions (including due to the destruction of dense intraepithelial contacts). It is probable that in the stage of stabilization of structural bases of function compensation the development of compensatory adaptations of intestinal epithelium ends and the point of dichotomy appears: the process goes towards full restoration of functions or towards decompensation of functions (in case of loss of structural support, even partial restoration of functions).

In contrast to the above changes, in the duodenal mucosa of rats of the second experimental group, the dynamics of morphological changes during different periods after burns (7 days - stage of shock and early toxemia; 14 days - stage of late toxemia; 21 days - stage of septicotoxicity) differs from this in animals of the first experimental group. Comparison of the obtained data with the previously revealed ones gives grounds to believe that the time intervals and the nature of the adaptive changes of the duodenal mucosa are significantly prolonged and worsened.

Significant lesions of the mucous membrane should lead to disruption of the digestive system, parietal digestion and absorption, as well as immunological protection (due to the fact that the mucous membranes are the first zone of contact with environmental antigens and a leading link in immune protection) which, no doubt, affects the condition of the body of the burned and, to a large extent, determines the development of burns, as well as the course of diabetes.

Evidence of dysfunction of the immune component of the intestinal barrier is our structural signs of stress function (adaptation) of various immunocompetent cells (lymphocytes, plasma cells, macrophages, which provide the functions of antigen presentation and secretion of local inflammatory response mediators), and subsequently to their partial destruction (failure of adaptation). This leads to the further development of an inflammatory reaction involving leukocytes, which also undergo a stage of activation and subsequent depletion (a sign of which is the destruction of leukocytes). These structural transformations are accompanied by the appearance in the cytoplasm of epitheliocytes and in the loose connective tissue of the duodenal mucosa of microbial bodies, which is a sign of microbial infiltration and general shifts of the intestinal microbiota (which, under normal conditions, acts as a biological intestinal filter) (Fig. 4).

The permeability of the duodenal mucosa barrier is also impaired in the association of experimental skin burn injury with streptozocin-induced diabetes mellitus. We have found structural transformations of goblet cells that produce intestinal mucus, which forms a layer on the surface of the intestinal mucosa.

A gradual change in the types of secretion of goblet

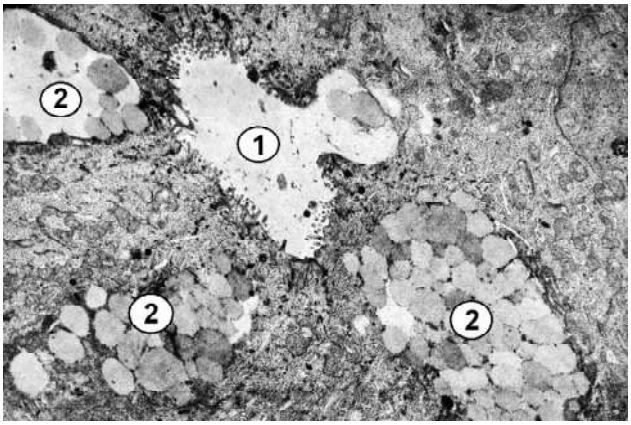

Fig. 5. Destruction of secretory granules with content of different degrees of electron density in the apical parts of goblet cells in the duodenal mucosa of rats of the third experimental group 21 days after the start of the experiment. 1 - lumen, 2 - secretory granules with content of different degrees of electron density. Electronic microphotography. x20000.

cells has been registered: from merocrine type (by exocytosis of mature secretory granules) to apocrine type (by rejection of the apical part of goblet cells together with secretory granules and individual organelles due to clasmatosis), and further - to the holocrine type (by complete destruction of the apical part of goblet cells and even complete destruction of these cells) (Fig. 5).

This leads to structural signs of changes in the intestinal mucosa (which at the electron microscopic level consists of small globular content of low electron density, secretory granules with preserved membrane and cell detritus, and on histological sections stained with hematoxylin and eosin in the lumen of the intestinal lumen). eosinophilic content). The structural changes of epitheliocytes detected under the conditions of the experiment are evidence of violation of the structural integrity of the intestinal epithelial barrier.

Thus, the permeability of the intestinal mucosal barrier is altered and these changes can be interpreted as contributing to microbial invasion. The results of studies have shown that the basis of damage to the epitheliocytes of the duodenal mucosa are profound destructive changes, which after 21 days (in the stage of septicotoxemia) are usually irreversible and develop against the background of significant intoxication. In animals of the second experimental group, the damaged epithelium of the duodenal mucosa critically weakens the adequacy of its function of the interface between the mucosa and the intestinal lumen environment and is structurally unable to provide an effective barrier against toxins, pathogens and antigenic molecules.

In particular, it should be noted that the structural changes of the mucous membrane in rats after burn injury of the skin associated with diabetes develop over time so rapidly that the stage of relative stabilization can be considered significantly unsettled.

The obtained results can be used to develop methods to prevent the development of negative changes in the intestinal epithelial barrier of the duodenum and enterocytes in particular and to effectively treat their possible consequences.

Discussion

The prevalence of diabetes, its specific complications, and the presence of other comorbidities that often accompany diabetes make it one of the major social and public health problems. The steady increase in information about the etiology and pathogenesis of diabetes mellitus, as well as its chronic complications, leads to the need for timely supplementation and clarification of existing scientific concepts, accompanied by constant reassessment of already established pathophysiological processes and structural mechanisms that provide them.

In the modern scientific literature there is an idea that "diabetes is predominantly an intestinal disease". It is well known [9] that the small intestine plays an important role in both digestion and the endocrine response in regulating blood glucose levels. Hormones (GLP-1 and GJP) released from the small intestinal mucosa in response to ingestion of nutrients modulate the secretory response of insulin and glucagon to this food.

The data obtained by us may indicate the greatest contribution to the development of diabetic enteropathy of structural changes in the mucous membrane of the duodenum. In addition, it should be noted that the structural transformation of the duodenal mucosa under the conditions of the applied model of experimental burns is deepened in its association with diabetes mellitus.

Also important is the dependence of morphological changes of the duodenal mucosa on the course characteristic of [4, 7, 12, 13, 18, 22] for burn disease complexes of syndromes (endotoxic syndrome, hypermetabolism syndrome, systemic inflammatory response and their general manifestation in the form of internal dysfunction). It should be noted that the excretion of toxins from the body of burnt [13] is carried out in several ways (skin, kidneys, lungs, liver and gastrointestinal tract), but these ways in the development of burn disease are blocked by "actual intraorgan afterburn pathology". In addition to the fact that the mucous membrane of the duodenum is affected by endotoxins of various origins (from foci of ischemia and necrosis in the burn area and from initially intact internal organs), It is worth noting the local pathogenic effects of leukocytes, which we found in large numbers in the mucous membrane of the duodenum of rats of the first and especially the third experimental group. It should be noted that their main foci of toxic products are formed due to the interaction of leukocytes and their main forms of oxygen with damaged cells. This phenomenon is called "oxygen-metabolic, or respiratory explosion" [8]. The chain connection of this phenomenon is that against the background of activation of neutrophils occurs almost fifteen times, which in turn induces the relaxation of smooth muscle. Under the combination of burn disease with diabetes mellitus, these

processes are superimposed on the typical for diabetic enteropathy changes in intestinal motility in the form of alternating diarrhea with constipation [1, 5, 6, 23-25], which should generate a vicious circle of temporary intraluminal intestinal endotoxins accumulation and subsequent intestinal release from them. In general, this variant of the dynamics of changes in pathological mechanisms, which increases the uncertainty and adds instability to the nature of intestinal motility, should affect the course of diabetic enteropathy in terms of its association with burn injury. These data obtained by us and made on the basis of their assumptions are theoretically plausible, but need to be confirmed in clinical trials.

Conclusions

In the mucous membrane of the duodenum after burn injury of the skin associated with diabetes there is a deterioration of the adaptive response and prolongation of destructive processes, accompanied by disruption of intercellular interactions in cytoarchitectonically altered and deformed villi and crypts. Structural changes in the duodenal mucosa of rats in experimental burn skin injury under experimental streptozotocin-induced diabetes mellitus 7, 14 and 21 days after the start of the experiment indicate structural features (peculiarity of morphological features) of enteropathy in burnt with diabetics.

References

[1] Anjaneyulu, M., & Ramarao, P. (2002). Studies on gastrointestinal tract functional changes in diabetic animals. *Methods Find. Exp. Clin. Pharmacol.,* 24(2), 71-5. https://www.ncbi.nlm.nih.gov/pubmed/12040885

[2] Azpiroz, F., & Malagelada, C. (2016). Diabetic neuropathy in the gut: pathogenesis and diagnosis. *Diabetologia*, 59, 404. https://doi.org/10.1007/s00125-015-3831-1

[3] Damasceno, D. C., Netto, A. O., Iessi, I. L., Gallego, F. Q., Corvino, S. B., Dallaqua, B., …. Rudge, M. V. C. (2014). Streptozotocin-Induced Diabetes Models: Pathophysiological Mechanisms and Fetal Outcomes. *BioMed. Research International*., 2014, 1-11. doi: 10.1155/2014/819065

[4] Deitch, E. A. (1990). Intestinal permeability is increased in burn patients shortly after injury. *Surgery*, 107(4), 411-416. doi: 10.1002/bjs.1800770541

[5] El-Salhy, M. (2001). Gastrointestinal transit in nonobese diabetic mouse: An animal model of human diabetes Type 1. *Journal of Diabetes and its Complications,* 15(5), 277-284. doi: 10.1016/S1056-8727(01)00158-1

[6] El-Salhy, M. (2002). Gastrointestinal Transit in an Animal Model of Human Diabetes Type 2: Relationship to gut neuroendocrine peptide contents, 107(2), 101-110. doi: 10.3109/2000-1967-133

[7] Epstein, M. D., Tchervenkov, J. I., Alexander, J. W, Johnson, J. R., & Vester, J. V. (1991). Increased gut permeability following burn trauma. *Arch. Surg.,* 126, 198-200. doi: 10.1001/arrchsurg/1991/01410260086012

[8] Evers, L. H. (2010). The biology of burn injury. *Exp. Dermatol.,* 19(2), 9, 777-783. doi: 10. 1111/j.1600-0625.2010.01105.x

[9] Gotfried, J., Priest, S., & Schey, R. (2017). Diabetes and the small intestine. *Curr. Treat. Options. Gastroenterol.*, 15(4), 490-507. doi: 10.1007/s11938-017-0155-x

[10] Goyal, S. N., Reddy, N. M., Patil, K. R., Nakhate, K. T., Ojha, S., Patil, C. R., & Agrawal, Y. O. (2016). Challenges and issues with streptozotocin-induced diabetes - A clinically relevant animal model to understand the diabetes pathogenesis and evaluate therapeutics. *Chem. Biol. Interact.,* 244, 49-63. doi: 10.1016/j.cbi.2015.11.032

[11] Khvorostinka, V. M., & Kryvonosova, O. M. (2009). Pathogenetic and therapeutic aspects of chronic diseases of the gastroduodenal system in patients with Diabetes Mellitus. *Problems of endocrine pathology,* 1, 18-24.

[12] Klymenko, M. O., & Netiukhailo, L. H. (2009). *Burn disease (pathogenesis and treatment)*. Poltava.

[13] Kozinets, G. P., Slesarenko, S. V., & Povstianoi, N. E. (2004). *Burn Intoxication. Pathogenesis, clinic, principles of treatment.* K.: Phoenix.

[14] Krivonosova, E. M. (2006). Morphological and functional mucous layer condition of stomach and duodenum in patients with diabetes mellitus. *The Journal of V.N.Karazin Kharkiv National University, series "Medicine",* 13(738), 35-39.

[15] Lopetuso, L. R., Scaldaferri, F., Bruno, G., Petito, V., Franceschi, F., & Gasbarrini, A. (2015). The therapeutic management of gut barrier leaking: the emerging role for mucosal barrier protectors. *Eur. Rev. Med. Pharmacol. Sci.,* 19(6), 1068-1076.

[16] Lukashevych, P. Yu., Orlenko, V. L., & Tronko, M. D. (2017). Modern approaches to providing antidiabetic therapy to patients with diabetes in Ukraine. *Endocrinology,* 1(22), 45-51.

[17] Mankovskii, B. N. (2018). Diabetology today. Is there a breakthrough in treatment? *Diabetes. Adiposity. Metabolic syndrome,* 2, 39-44.

[18] Martusevich, A. K., Peretiagin, S. P., & Pogodin, I. E. (2009). Metabolic aspects of the pathogenesis of burn endotoxicosis. Pathological Physiology and Experimental Therapy, 1, 30-32.

[19] Radionova, T. O. (2017). Peculiarities of the course of diseases of the upper gastrointestinal tract in patients with type 2 diabetes mellitus. *Actual problems of modern medicine*, 17, 4(2), 207-210.

[20] Sah, S. P., Singh, B., Choudhary, S., & Kumar, A. (2016). Animal models of insulin resistance: A review. *Pharmacol. Rep.,* 68(6), 1165-1177. doi: 10.1016/j.pharep.2016.07.010

[21] Scaldaferri F., Pizzoferrato, M., Gerardi, V., Lopetuso, L., & Gasbarrini, A. (2012). The gut barrier: new acquisitions and therapeutic approaches. *J. Clin. Gastroenterol.,* 46, 12-17. doi: 10.1097/MCG.0b013e31826ae849

[22] Turner, J. R. (2009). Intestinal mucosal barrier function in health and disease. *Nat. Rev. Immunol.*, 9(11), 799-809. doi: 10.1038/nri2653

[23] Zhao, J., Chen, P., & Gregersen, H. (2013). Changes of phasic and tonic smooth muscle function of jejunum in type 2 diabetic Goto-Kakizaki rats. *World J. Diabetes*, 4(6), 339-348. doi: 10.4239/wjd.v4.i6.339

[24] Zhao, J., Chen, P., & Gregersen, H. (2013). Stress-strain analysis of jejunal contractility in response to flow and ramp distension in type 2 diabetic GK rats: effect of carbachol stimulation. *J. Biomech.*, 27, 46(14), 2469-2476. doi: 10.1016/j.jbiomech.2013.07.019

[25] Zhao, J., Chen, P., & Gregersen, H. (2015). Stress-strain analysis of contractility in the ileum in response to flow and ramp distension in streptozotocin-induced diabetic rats--association with advanced glycation end product formation. *Journal of Biomechanics,* 48(6), 1075-1083. doi: 10.1016/j.jbiomech.2015.01.027

ПОРІВНЯЛЬНА ХАРАКТЕРИСТИКА ПРОЯВІВ ПОШКОДЖЕННЯ ТА РЕПАРАТИВНИХ ПРОЦЕСІВ У СЛИЗОВІЙ ОБОЛОНЦІ ДВАНАДЦЯТИПАЛОЇ КИШКИ ЩУРІВ ЗА УМОВ ОПІКОВОЇ ТРАВМИ ШКІРИ ТА ОПІКОВОЇ ТРАВМИ ШКІРИ, АСОЦІЙОВАНОЮ З ЦУКРОВИМ ДІАБЕТОМ

Тимошенко І.О., Сокуренко Л.М., Янчишин А.Я., Пастухова В.А.

На даний час важка термічна травма стає однією з найважливіших проблем практичної медицини. Ще одним глобальним медико-соціальним викликом нашого століття визнано також цукровий діабет. Надзвичайна ситуація щодо профілактики, лікування та попередження наслідків цих патологій є наслідком відсутності надійного теоретичного підґрунтя у вирішенні конкретних клінічних проблем щодо перебігу опікової хвороби, цукрового діабету та їх ускладнень. Метою дослідження є встановлення закономірностей структурних змін в слизовій оболонці дванадцятипалої кишки після опікової травми шкіри щурів за умов експериментального цукрового діабету. Дослідження здійснено на 63 лабораторних білих статевозрілих щурах-самцях масою 180-210 г, котрі були розподілені на 3 групи: інтактні тварини, щурі з опіковою травмою шкіри та щурі з опіковою травмою шкіри на тлі цукрового діабету. Модель експериментального цукрового діабету відтворювали шляхом введення щурам стрептозотоцину внутрішньоочеревенно одноразово в дозі 50 мг/кг, попередньо розчинивши його в 0,1 М цитратному буферному розчині (pH=4,5). Контролем розвитку гіперглікемії в екпериментальних групах був рівень глюкози в крові 24,24±0,79 ммоль/л. В контрольній групі цей показник становив 8,03±0,4 ммоль/л. У щурів з опіковою травмою шкіри виявлені деструктивні прояви, котрі супроводжуються активною запальною реакцією і відповідними некротичними змінами, в той час як у щурів з опіковою травмою шкіри на тлі цукрового діабету патологічні процеси не просто "сумуються", а певним чином адаптивно модифікуються із залученням механізмів стресу ендоплазматичного ретикулума та асоційованої з ним автофагії.

Ключові слова: *дванадцятипала кишка, термічна травма, діабет.*

СРАВНИТЕЛЬНАЯ ХАРАКТЕРИСТИКА ПРОЯВЛЕНИЙ ПОВРЕЖДЕНИЯ И РЕПАРАТИВНЫХ ПРОЦЕССОВ В СЛИЗИСТОЙ ОБОЛОЧКЕ ДВЕНАДЦАТИПЕРСТНОЙ КИШКИ КРЫС В УСЛОВИЯХ ОЖОГОВОЙ ТРАВМЫ КОЖИ И ОЖОГОВОЙ ТРАВМЫ КОЖИ, АССОЦИИРОВАННОЙ С САХАРНЫМ ДИАБЕТОМ

Тимошенко И.О., Сокуренко Л.М., Янчишин А.Я., Пастухова В.А.

В данное время тяжелая термическая травма становится одной из наиболее важных проблем практической медицины. Еще одним глобальным медико-социальным вызовом нашего столетия признан также сахарный диабет. Чрезвычайная ситуация по профилактике, лечению и предупреждению последствий этих патологий является следствием отсутствия надежного теоретического основания в решении конкретных клинических проблем о ходе ожоговой болезни, сахарного диабета и их осложнений. Целью исследования является установление закономерностей структурных изменений в слизистой оболочке двенадцатиперстной кишки после ожоговой травмы кожи крыс в условиях экспериментального сахарного диабета. Исследование проведено на 63 лабораторных белых половозрелых крысах-самцах массой 180-210 г, которые были разделены на 3 группы: интактные животные, крысы с ожоговой травмой кожи и крысы с ожоговой травмой кожи на фоне сахарного диабета. Модель экспериментального сахарного диабета воспроизводили путем введения крысам стрептозотоцина внутрибрюшинно однократно в дозе 50 мг/кг, предварительно растворив его в 0,1 М цитратном буферном растворе (pH=4,5). Контролем развития гипергликемии в екпериментальных группах был уровень глюкозы в крови 24,24±0,79 ммоль/л. В группе контроля 8,03±0,4 ммоль/л. У крыс с ожоговой травмой кожи обнаружены деструктивные проявления, которые сопровождаются активной воспалительной реакцией и соответствующими некротическими изменениями, в то время как у крыс с ожоговой травмой кожи на фоне сахарного диабета патологические процессы не просто "суммируются", а определенным образом адаптивно модифицируются с привлечением механизмов стресса эндоплазматического ретикулума и ассоциированной с ним автофагии.

Ключевые слова: *двенадцатиперстная кишка, термическая травма, диабет.*

DOI: 10.31393/morphology-journal-2020-26(2)-07 Reports of Morphology, Vol. 26, №2, Pages 45-50

ISSN 1818-1295 eISSN 2616-6194

REPORTS OF MORPHOLOGY

Official Journal of the Scientific Society of Anatomists, Histologists, Embryologists and Topographic Anatomists of Ukraine

journal homepage: https://morphology-journal.com

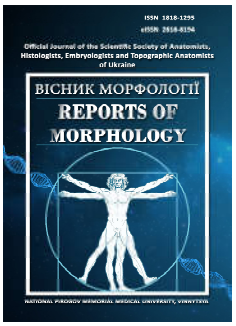

The role of sorbents and probiotics in prevention of structural and morphological disorders in the small intestine of animals developing in dysbiosis

Bobyr V.V.[1], Stechenko L.O.[1], Shirobokov V.P.[1], Nazarchuk O.A.[2], Rymsha O.V.[2]

[1]O.O.Bogomolets National Medical University, Kyiv, Ukraine
[2]National Pirogov Memorial Medical University, Vinnytsya, Ukraine

ARTICLE INFO
Received: 14 July, 2020
Accepted: 10 August, 2020

UDC: 616.34:615.211.099

CORRESPONDING AUTHOR
e-mail: nazarchukoa@gmail.com
Nazarchuk O.A.

The past decade is characterized by a noticeable increase in the interest of physicians in all areas of activity in the development of new and improvement of existing approaches to the correction of dysbiotic disorders. Among them, the concept of using probiotics occupies a leading position. At the same time, some enterosorbents, the mechanism of action of which is largely due to the sanitation of the intestinal lumen and due to this improvement of conditions for the vital activity of the physiological microbiota, can be attributed to the group of means of improving the normal microflora. In the context of an increase in the level of resistance to antibacterial agents, the inclusion of enterosorbents in the complex therapy of dysbiosis is an important and pathogenetically justified approach. The aim of the work was to clarify the effectiveness of the use of sorbents and probiotics for the prevention of structural and morphological disorders in the small intestine of white mice developing against the background of antibiotic-induced dysbiosis. Electron-microscopic methods showed that in the mucous membrane of the small intestine of mice after using the probiotic "Simbiter" the extinction of manifestations of cytodestructive disorders is observed. In addition, the obtained electron microscopic data, indicating the ability of probiotic drugs with the simultaneous introduction into the body of animals with a complex of antibiotics, to stimulate the body's immune response. As a result of ultrastructural analysis of the mucous membrane of the small intestine of mice, the formation of dysbiosis in which occurred against the background of the use of enterosorbents, a decrease in the severity of structural damage was found, compared with the group of animals that received only antibiotics. After using "Symbiogel", activation of plasma cells was registered, which can be an indicator of the inflammatory process and the activity of the immune response in general, as evidenced by the detection of plasma cells with dilated tubules. In general, it should be noted that the use of "Symbiogel" for the prevention of dysbiotic disorders contributes to the formation of a more pronounced immune response, compared with probiotic drugs. So, on the model of antibiotic-induced dysbiosis at the ultrastructural level, the ability of multiprobiotics "Simbiter®" and sorbent "Symbiogel" to reduce cytodestructive changes in the mucous membrane of the small intestine of mice and normalize morphoimunogenesis was proved.

Key words: *microbiota, probiotics, enterosorbents.*

Introduction

Nowadays, the interest of scientists in studying the normal human microflora is growing. In recent years, the term "normal microflora" is often replaced by the term "microbiome" [9]. It should be noted that progress in the study of the microbiome and its role in maintaining human health is considered one of the key achievements of modern biology and medicine [11].

Many convincing evidences of huge potential of action of a microbiome on various processes of functioning of a human body are received. Experts now consider the microbiome as an additional human organ, which, actively participating in digestion, management of metabolic processes, maintaining the integrity of the epithelial barrier, development and strengthening of the immune system and

a number of other physiological functions, optimizes conditions for normal life [1, 2, 4, 5, 8, 10, 14, 18].

However, recent scientific studies show that from 70 to 90% of the world's population suffers from dysbiosis of varying degrees, which, of course, indicates their significant social and environmental significance [7, 13]. Among the many causes of dysbiotic disorders in the first place is the use of chemotherapeutic antimicrobials, often broad-spectrum and with an oral mechanism of administration. Particularly dangerous in this regard is the use of antibiotics for prophylactic purposes. However, some other groups of drugs can contribute to the formation of dysbiosis by affecting the kinetics of the epithelium of mucous membranes and, accordingly, the composition of mucin (nonsteroidal anti-inflammatory drugs, laxatives, cholagogues, enveloping agents with sorbent properties and some others) [23, 25].

The past decade has been marked by increase in the interest of physicians in all areas of activity in the development of new and improvement of existing approaches to the correction of dysbiotic disorders. Among them, the concept of probiotics occupies a leading position. According to the WHO, probiotics are "living microorganisms that, when used in adequate quantities, have a beneficial effect on the host" [22]. The mechanisms responsible for various probiotic effects are usually associated with the ability of probiotics to inhibit the development of pathogenic microbes, exhibit immunomodulatory properties, stimulate the proliferation and differentiation of epithelial cells and strengthen the intestinal barrier [12, 17, 19].

Some types of enterosorbents can be referred to the group of means of improvement of normal microflora. The mechanism of their action is largely due to the rehabilitation of the intestinal lumen and the improvement due to this conditions for the functioning of the physiological microbiota. Enterosorption is a non-invasive method of efferent therapy and when choosing an adequate sorbent can help effectively cleanse the body of allergens, mediators, products of allergic or inflammatory reactions, metabolites, toxins, viruses and other components. Rehabilitation of habitats can optimize the conditions for the functioning of normal human microflora. With increasing levels of resistance to antibacterial agents, the inclusion of enterosorbents in the complex therapy of dysbiosis is an important and pathogenetically sound approach [6, 20, 21].

In recent years, much attention has been paid to enterosorbents based on clay minerals, among which bentonite clays are one of the most studied. Today, bentonites are so-called "edible" minerals with proven anti-inflammatory, antitoxic and ion exchange properties [15, 16, 24].

Objective of work: to determine the effectiveness of sorbents and probiotics for the prevention of structural and morphological disorders in the small intestine of mice developing on the background of antibiotic-induced dysbiosis.

Materials and methods

White laboratory mice of the *BALB/c* line were selected as a model for studying morphofunctional changes of the small intestinal mucosa in antibiotic-induced dysbiosis and after their correction with probiotics and enterosorbents. The formation of dysbiotic conditions in animals was performed according to the previously described method [3]. In addition, these antibiotics were added to a glass of water (1 g of Ampicillin, 1 g of Metronidazole and 290 mg of Gentamicin per 1000 ml of water).

A total of 80 mice were involved in the experiment. The first group - control, formed from intact animals, was 20 individuals; group 2 - animals with established intestinal dysbiosis; group 3 - animals that in the process of modeling dysbiotic conditions orally received "Symbiter® M concentrated"; group 4 - animals that received "Symbiogel" orally during the entire period of dysbiosis modeling.

Animals were removed from the experiment 5 days after the start of modeling dysbiosis. Probiotics and sorbents were administered intragastrically to animals for 5 days in a volume of 200 μl 6 hours after receiving antimicrobial drugs to form dysbiosis.

Results

As a result of the analysis of structural and morphological changes of the small intestine of mice with antibiotic-induced dysbiosis (experimental group 2) the expressed disturbances accompanying this process are recorded: shortening of microvilli length and their partial reduction or destruction with subsequent disintegration, absence of brush border, mitochondria and the presence of autophagosomes (Fig. 1A), as well as an increase in the number of eosinophils, which are an indicator of allergic reactions, as they are directly involved in protective allergic and anaphylactic reactions of the body (Fig. 1B).

In the mucous membrane of the small intestine of mice after the use of probiotics there was a visual attenuation of cytodestructive disorders, namely a decrease in the number of desquamated microvilli, the vast majority of enterocytes retained the brush border, compared with the experimental group of animals №2 (animals with dysbiosis) (Fig. 2). The desquamation of microvilli was local in nature with a partial absence of a brush border and a slight smoothness of the plasma membrane.

It should also be noted about the intensive formation of autophagosomes in enterocytes after the use of "Simbiter" (Fig. 3). Electron microscopic studies showed no signs of cell displacement to the basement membrane, compaction of the cytoplasm, organelles and precursors of apoptotic cells, as well as other apoptotic disorders. The number of detected Paneth cells was statistically higher, but specific changes were recorded in their granules: granules, which apparently contained defensins, gradually lost their content and transformed into structures with an electron-transparent rim. Such granules can be considered as

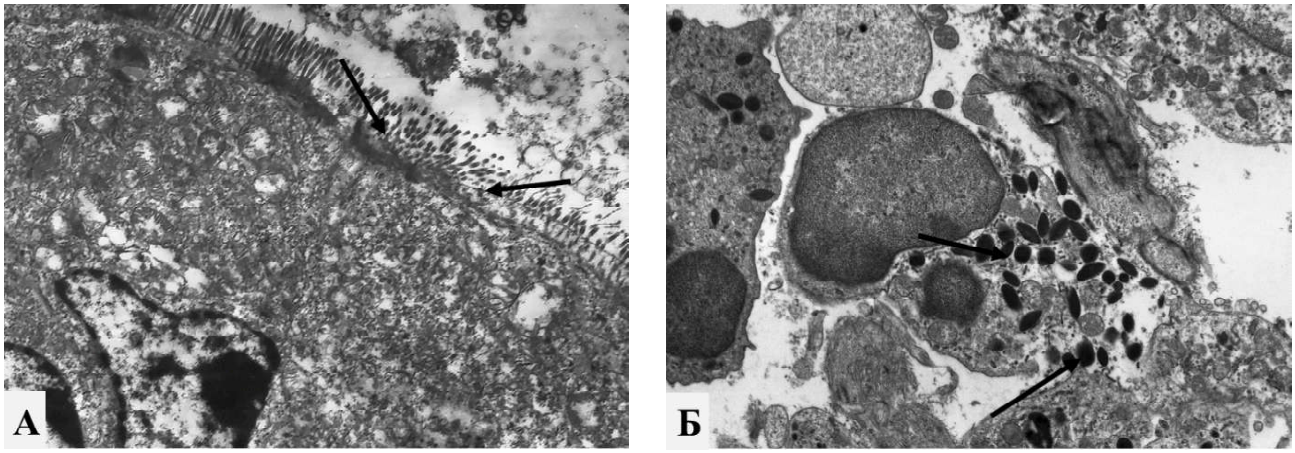

Fig. 1. Electronic microphotography. A - local reduction of the brush border of mouse small intestine enterocytes in antibiotic-induced dysbiosis (↑). x6200; B - eosinophil (1) with characteristic elongated granules with a crystalloid (↑). x8000.

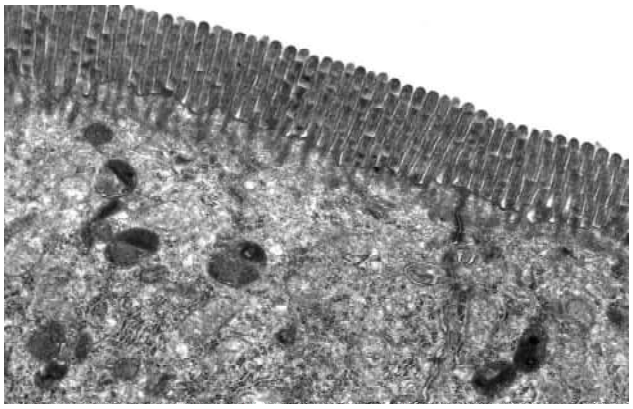

Fig. 2. Electronic microphotography. Local desquamation, signs of partial absence of the brush border, smoothing of the plasma membrane of the microvilli of the small intestine of animals with dysbiosis after the use of probiotics. x8000.

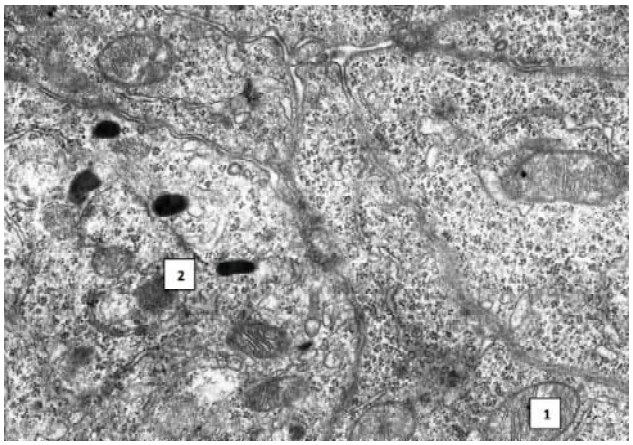

Fig. 3. Electronic microphotography. Mitochondrial edema (1) and intensive formation of autophagosomes (2) in enterocytes on the background of probiotic use. x3600.

objects that are at different stages of functional activity and, obviously, are proteins (Fig. 4).

The obtained data may indicate the ability of probiotic drugs when simultaneously administered to animals with a complex of antibiotics to stimulate the body's immune response. In addition, in contrast to the control, the expansion of the tubules of plasma cells due to their filling with antibodies was not recorded at all. Blood vessels also remained unchanged. At the same time, when using probiotics, there was a visual decrease in the number of eosinophils and basophils.

Based on the data obtained, it cannot be claimed that the probiotic strains administered to mice colonized the intestine. However, it should not be ruled out the possibility of probiotics to actively secrete metabolites when passing through the gastrointestinal tract. The latter can have a positive effect on the barrier function of the intestine. However, after the use of probiotics in the modeling of antibiotic-induced dysbiosis, microecological changes and cytodestructive manifestations in the intestines of animals were less pronounced, compared with the group where animals received only antibiotics.

As a result of ultrastructural analysis of the mucous membrane of the small intestine of mice, the formation of dysbiosis in the background of the use of enterosorbents, a decrease in the severity of structural damage, compared with the group of animals receiving only antibiotics was

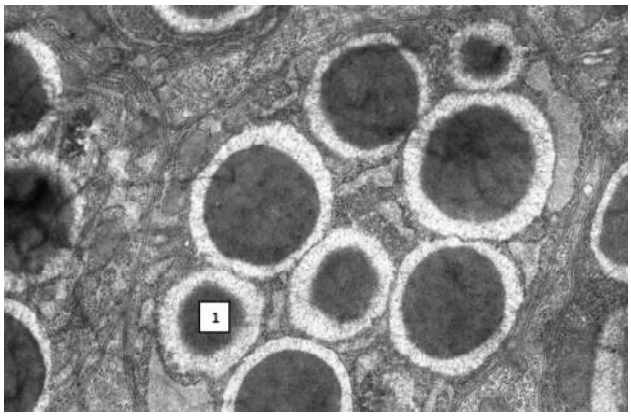

Fig. 4. Electronic microphotography. Transformation of Paneth cell granules (1) with the formation of cytosegresome (2). x3600.

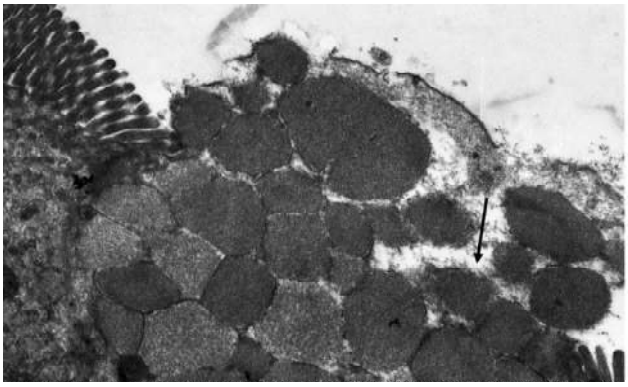

Fig. 5. Electronic microphotography. Local desquamation of microvilli with partial absence of microvilli destruction (↑) and unexpressed smoothness of enterocyte plasma membrane after Symbiogel use. x8000.

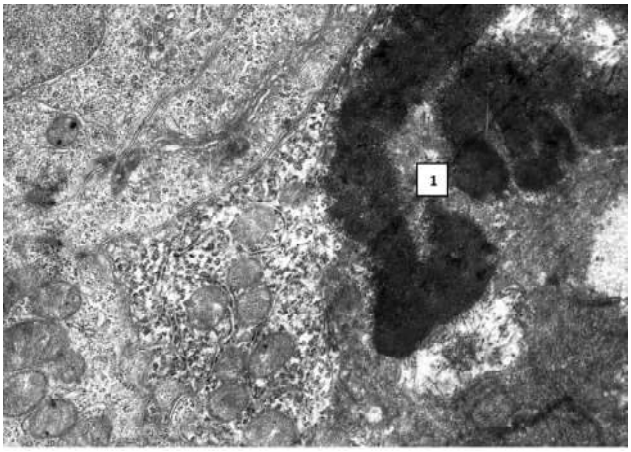

Fig. 6. Electronic microphotography. Compacted enterocytes (1). x6000.

established. Although in some places in the mucous membrane of the small intestine was observed a visual shortening of the length of the microvilli, cases of their complete desquamation or disintegration were not recorded (Fig. 5). After using Symbiogel, we registered the activation of plasma cells, which may be an indicator of the inflammatory process and the activity of the immune response in general, as evidenced by the detection of plasma cells with dilated tubules, apparently filled with antibodies (Fig. 6).

In general, it should be noted that the use of Symbiogel for the prevention of dysbiotic disorders contributes to the formation of a more pronounced immune response, compared with probiotic drugs. At the same time, no changes were observed in the circulatory system, and it is likely that the development of antibiotic-induced dysbiosis is not reflected in the hemomicrocirculatory tract. There are no direct signs that would indicate the intensive development of apoptosis with the formation of apoptotic cells that move to the basement membrane.

It should be noted that, in general, when receiving electron microscopic sections of the mucous membrane of the small intestine, microbial cells cannot always be registered, while after the use of Symbiogel in the intestinal lumen more often noted their presence. It should also be noted that we have recorded isolated cases of the presence of metamyelocytes and plasma cells in the own plate of the mucous membrane of the small intestine.

Discussion

With increasing levels of resistance to antibacterial agents, the inclusion of probiotics and enterosorbents in the complex therapy of dysbiosis is an important and pathogenetically sound approach. The feasibility of correction of intestinal dysbiosis in various pathological conditions with probiotic drugs was confirmed in the Practical Recommendations of the World Gastroenterological Organization (WGO) 2002, 2008, 2011, 2012, 2014 [7, 9, 22].

An important advantage of probiotics with their inherent wide range of antagonistic activity against pathogenic and opportunistic microorganisms is that, unlike antibiotics, they do not cause the formation of resistant forms of bacteria. In addition, they have a multifaceted positive effect on the body, which consist, in particular, in ability of probiotics to reduce the permeability of tissue barriers to toxins, to have a detoxifying effect on compounds produced in the host by the pathogen. Unlike antibiotics that suppress the immune system, probiotics stimulate the production of antibodies and its non-specific factors. By producing biological substances, they promote the production of mediators by the macroorganism, which has a positive effect on the functions of the digestive tract, liver, cardiovascular, circulatory systems and metabolic processes in the body of the host; involved in the synthesis and absorption of vitamins. When interacting with immune and intestinal epithelial cells, the active signaling components of probiotics interact with antigen-recognizing receptors (TLRs - Toll-like receptors, NLRs - The NOD-like receptors or Nucleotide Oligomerization Domain receptors) and other surface receptors, and as a consequence cause - lymphocytes in Peyer's patches (CD4+ Th1, CD4+ Th2, CD8+ cytotoxic T-lymphocytes) and their production of various chemokines and cytokines [7, 23, 24].

The results of electron microscopic examination indicate that during the correction of experimental chemotherapeutic dysbiosis in laboratory animals the use of probiotic "Simbiter" allows not only to stop the destructive-dystrophic changes in the mucous membrane of the small intestine, but also stimulates repair processes.

Based on the data obtained in the study, the stimulating effect of "Symbiogel" was proved, which significantly contributes to the restoration of parietal microflora of the small intestine and eradication of translocated intestinal microflora. Under such conditions, the introduction of immobilized probiotics achieves an early therapeutic effect in comparison with therapy with free probiotic cells and enterosorbents.

Conclusions

The results of experiments showed the property of probiotic drugs and sorbents to reduce the depth of cytodestructive changes in the mucous membrane of the small intestine in the formation of antibiotic-induced dysbiosis and normalization of immune responses that accompany the development of such disorders.

Advances in DNA sequencing and computational technology have revolutionized the field of microbiology, but many fundamental questions remain to be answered. Obviously, future research will focus on elucidating the more precise mechanisms responsible for the interaction between the microbiome and the human body, as well as on improving the effectiveness of therapeutic approaches to the assessment and treatment of conditions associated with microbiome disorders.

References

[1] Barko, P. C., McMichael, M. A., Swanson, K. S., & Williams, D. A. (2018). The Gastrointestinal Microbiome: A Review. *Journal of Veterinary Internal Medicine,* 32(1), 9-25. https://doi.org/10.1111/jvim.14875

[2] Bengmark, S. (2013). Gut microbiota, immune development and function. *Pharmacological research,* 69(1), 87-113. https://doi.org/10.1016/j.phrs.2012.09.002

[3] Bobyr, V. V, Poniatovskyi, V. A, Dyuzhikova, O. M., & Shirobokov, V. P. (2015). Methods of modeling dysbiotic disorders in laboratory animals. *Biomedical and Biosocial Anthropology,* 26, 230-233.

[4] Harris, L. A., & Baffy, N. (2017). Modulation of the gut microbiota: a focus on treatments for irritable bowel syndrome. *Postgrad. Med.,* 129(8), 872-888. doi: 10.1080/00325481.2017.1383819

[5] Heintz-Buschart, A., & Wilmes, P. (2018). Human Gut Microbiome: Function Matters. *Trends in microbiology,* 26(7), 563-574. https://doi.org/10.1016/j.tim.2017.11.002

[6] Howell, C. A., Mikhalovsky, S. V., Markaryan, E. N., & Khovanov, A. V. (2019). Investigation of the adsorption capacity of the enterosorbent Enterosgel for a range of bacterial toxins, bile acids and pharmaceutical drugs. *Scientific reports,* 9(1), 5629. https://doi.org/10.1038/s41598-019-42176-z

[7] Knight R., Callewaert Ch., Marotz C., Hyde E. R., Debelius J. W., McDonald D., Sogin M. L. (2017). The Microbiome and Human Biology. *Ann. Review of Genomics and Human Genetics,* 18, 65-86. https://doi.org/10.1146/annurev-genom-083115-022438

[8] McNally, L., & Brown, S. P. (2015). Building the microbiome in health and disease: niche construction and social conflict in bacteria. *Philosophical transactions of the Royal Society of London. Series B, Biological sciences*, 370(1675), 20140298. https://doi.org/10.1098/rstb.2014.0298.

[9] Mohajeri, M. H., Brummer, R., Rastall, R. A., Weersma, R. K., Harmsen, H., Faas, M., & Eggersdorfer, M. (2018). The role of the microbiome for human health: from basic science to clinical applications. *European journal of nutrition*, 57 (Suppl 1), 1-14. https://doi.org/10.1007/s00394-018-1703-4 .

[10] Nagpal, R., Mainali, R., Ahmadi, S., Wang, S., Singh, R., Kavanagh, K. … Yadav, H. (2018). Gut microbiome and aging: Physiological and mechanistic insights. *Nutrition and healthy aging,* 4(4), 267-285. https://doi.org/10.3233/NHA-170030.

[11] Pennisi, E. (2010). Body's hardworking microbes get some overdue respect. *Science*, 330, 16-19. doi: 10.1126/science.330.6011.1619

[12] Preidis, G. A., & Versalovic, J. (2009). Targeting the human microbiome with antibiotics, probiotics, and prebiotics: gastroenterology enters the metagenomics era. *Gastroenterology,* 136(6), 2015-2031. https://doi.org/10.1053/j.gastro.2009.01.072.

[13] Sakhnyuk, O. M., Surmasheva, O. V., Nastoyascha, N. I., Kryvoshlik, M. O., & Nikonova, N. O. (2011). Role of milk acidic bacteria for human dysbacteriosis correction and contemporary problems of probiotic preparations working out and hygienic estimation (literature survey). *Hygiene of populated areas,* 58, 373-383.

[14] Seidel, J., & Valenzano, D. R. (2018). The role of the gut microbiome during host ageing. *F1000Research*, 7, F1000 Faculty Rev-1086. https://doi.org/10.12688/f1000research.15121.1.

[15] Shirobokov, V. P., Yankovskyi, D. S., & Dyment, G. S. (2013). At the dawn of the origin of life: the role of clay minerals. *Outlook*, 39(1), 58-65.

[16] Shirobokov, V. P., Yankovskyi, D. S., & Dyment, G. S. (2012). The world of clays and human health. *Outlook,* 34(2), 6-17.

[17] Thomas, C., & Versalovic, J. (2010). Probiotics-host communication: modulation of signaling pathways in the intestine, *Gut. Microbes,* 1, 148-163.

[18] Tremaroli, V., & Backhed F. (2012). Functional interactions between the gut microbiota and host metabolism. *Nature,* 489, 242-249 https://doi.org/10.1038/nature11552.

[19] Van Tassell, M. L., & Miller, M. J. (2011). Lactobacillus adhesion to mucus. *Nutrients*, 3(5), 613-636. https://doi.org/10.3390/nu3050613.

[20] Wang, M., Hearon, S. E., & Phillips, T. D. (2019). Development of enterosorbents that can be added to food and water to reduce toxin exposures during disasters. *Journal of environmental science and health. Part. B, Pesticides, food contaminants, and agricultural wastes,* 54(6), 514-524. https://doi.org/10.1080/03601234.2019.1604039.

[21] Wang, M., Hearon, S. E., & Phillips, T. D. (2020). A high capacity bentonite clay for the sorption of aflatoxins. *Food additives & contaminants. Part A, Chemistry, analysis, control, exposure & risk assessment,* 37(2), 332-341. https://doi.org/10.1080/19440049.2019.1662493.

[22] Wischmeyer, P. E., McDonald, D., & Knight, R. (2016). Role of the microbiome, probiotics, and 'dysbiosis therapy' in critical illness. *Current opinion in critical care,* 22(4), 347-353. https://doi.org/10.1097/MCC.0000000000000321.

[23] Yankovskyi, D. S, Shirobokov, V. P, & Dyment, G. S. (2017). *Microbiome*. Kiev: FLP Veres O.I.

[24] Yankovskyi, D. S., Shirobokov, V. P., & Dyment, G. S. (2013). Creation of new complex preparations based on the biomass of probiotic bacteria and smectite gel. *Prophylactic medicine,* 21(3-4), 108-115.

[25] Yankovskyi, D. S., Shirobokov, V. P., & Dyment, G. S. (2018). Innovation technologies for human microbiome improvement. *Science and Innovation*, 14(6), 11-21. https://doi.org/10.15407/scine14.06.011

РОЛЬ СОРБЕНТІВ ТА ПРОБІОТИКІВ У ПРОФІЛАКТИЦІ СТРУКТУРНО-МОРФОЛОГІЧНИХ ПОРУШЕНЬ У ТОНКОМУ КИШКІВНИКУ ТВАРИН, ЩО РОЗВИВАЮТЬСЯ ПРИ ДИСБІОЗІ

Бобир В.В., Стеченко Л.О., Широбоков В.П., Назарчук О.А., Римша О.В.

Минуле десятиліття характеризується помітним зростанням зацікавленості медиків усіх напрямків діяльності питаннями

розробки нових та вдосконалення існуючих підходів до корекції дисбіотичних порушень. Серед них концепція використання пробіотиків займає провідні позиції. Разом із тим, до групи засобів оздоровлення нормальної мікрофлори можна віднести і деякі ентеросорбенти, механізм дії яких в значній мірі обумовлений санацією просвіту кишки і поліпшенням за рахунок цього умов для життєдіяльності фізіологічної мікробіоти. В умовах зростання рівня резистентності до антибактеріальних засобів включення до комплексної терапії дисбіозу ентеросорбентів є важливим та патогенетично обґрунтованим підходом. Метою роботи було з'ясування ефективності використання сорбентів та пробіотиків для профілактики структурно-морфологічних порушень у тонкому кишківнику білих мишей, що розвиваються на фоні антибіотикоіндукованого дисбіозу. Електронно-мікроскопічними методами показано, що в слизовій оболонці тонкої кишки мишей після використання пробіотику "Симбітеру" спостерігається згасання проявів цитодеструктивних порушень. Крім того, отримані електронно-мікроскопічні дані, які свідчать про здатність пробіотичних препаратів при одночасному введенні в організм тварин з комплексом антибіотиків стимулювати імунну відповідь організму. В результаті ультраструктурного аналізу слизової оболонки тонкого кишківника мишей, формування дисбіозу у яких відбувалось на фоні вживання ентеросорбентів, встановлено зниження виразності структурних ушкоджень порівняно з групою тварин, які отримували лише антибіотики. Після використання "Симбіогелю" зареєстровано активізацію плазматичних клітин, які можуть бути показником запального процесу та активності імунної відповіді в цілому, про що свідчить виявлення плазматичних клітин з розширеними канальцями. В цілому слід відмітити, що використання "Симбіогелю" для профілактики дисбіотичних розладів сприяє формуванню більш вираженої імунної відповіді у порівнянні з пробіотичним препаратами. Отже, на моделі антибіотикоіндукованого дисбіозу на ультраструктурному рівні доведена здатність мультипробіотику "Симбітер®" та сорбенту "Симбіогель" зменшувати цитодеструктивні зміни в слизовій оболонці тонкого кишківника мишей та нормалізувати морфоімуногенез.
Ключові слова: *мікробіота, пробіотики, ентеросорбенти.*

РОЛЬ СОРБЕНТОВ И ПРОБИОТИКОВ В ПРОФИЛАКТИКЕ СТРУКТУРНО-МОРФОЛОГИЧЕСКИХ НАРУШЕНИЙ В ТОНКОМ КИШЕЧНИКЕ ЖИВОТНЫХ, РАЗВИВАЮЩИХСЯ ПРИ ДИСБИОЗЕ

Бобирь В.В., Стеченко Л.А., Широбоков В.П., Назарчук А.А., Рымша Е.В.

Прошедшее десятилетие характеризуется заметным ростом заинтересованности медиков всех направлений деятельности вопросами разработки новых и совершенствования существующих подходов к коррекции дисбиотических нарушений. Среди них концепция использования пробиотиков занимает ведущие позиции. Вместе с тем, в группу средств оздоровления нормальной микрофлоры можно отнести и некоторые энтеросорбенты, механизм действия которых в значительной степени обусловлен санацией просвета кишки и улучшением за счет этого условий для жизнедеятельности физиологической микробиоты. В условиях роста уровня резистентности к антибактериальным средствам включение в комплексную терапию дисбиоза энтеросорбентов является важным и патогенетически обоснованным подходом. Целью работы было выяснение эффективности использования сорбентов и пробиотиков для профилактики структурно-морфологических нарушений в тонком кишечнике белых мышей, развивающихся на фоне антибиотикоиндуцированного дисбиоза. Электронно-микроскопическими методами показано, что в слизистой оболочке тонкой кишки мышей после использования пробиотика "Симбитера" наблюдается угасание проявлений цитодеструктивных нарушений. Кроме того, получены электронно-микроскопические данные, которые свидетельствуют о способности пробиотических препаратов при одновременном введении в организм животных с комплексом антибиотиков стимулировать иммунный ответ организма. В результате ультраструктурного анализа слизистой оболочки тонкого кишечника мышей, формирование дисбиоза у которых происходило на фоне употребления энтеросорбентов, установлено снижение выраженности структурных повреждений по сравнению с группой животных, получавших только антибиотики. После использования "Симбиогеля" зарегистрирована активизация плазматических клеток, которые могут быть показателем воспалительного процесса и активности иммунного ответа в целом, о чем свидетельствует обнаружение плазматических клеток с расширенными канальцами. В целом следует отметить, что использование "Симбиогеля" для профилактики дисбиотических расстройств способствует формированию более выраженного иммунного ответа по сравнению с пробиотическим препаратами. Итак, на модели антибиотикоиндуцированного дисбиоза на ультраструктурном уровне доказана способность мультипробиотика "Симбитер®" и сорбента "Симбиогель" уменьшать цитодеструктивные изменения в слизистой оболочке тонкого кишечника мышей и нормализовать морфоиммуногенез.
Ключевые слова: *микробиота, пробиотики, энтеросорбенты.*

DOI: 10.31393/morphology-journal-2020-26(2)-08 Reports of Morphology, Vol. 26, №2, Pages 51-61

ISSN 1818-1295 eISSN 2616-6194

REPORTS OF MORPHOLOGY

Official Journal of the Scientific Society of Anatomists, Histologists, Embryologists and Topographic Anatomists of Ukraine

journal homepage: https://morphology-journal.com

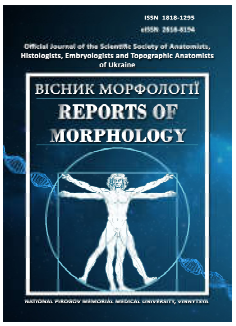

Features of correlations of the sizes of molars with cephalometric indicators of men of the western region of Ukraine

***Gunas V.I.*[1], *Kotsyura O.O.*[1], *Babych L.V.*[1], *Shevchuk Yu.G.*[1], *Cherkasova O.V.*[2]**

[1]National Pirogov Memorial Medical University, Vinnytsya, Ukraine
[2]Bogomolets National Medical University, Kyiv, Ukraine

ARTICLE INFO
Received: 17 July, 2020
Accepted: 18 August, 2020

UDC: 611.314:616.714.1-071.3:79-055.1(477)

CORRESPONDING AUTHOR
e-mail: igor.v.gunas@gmail.com
Gunas V.I.

Expanding the theoretical knowledge of medical anthropology in the modern field of dental services is one of the main drivers of progress in the orthodontic field. The only way to successfully develop the relationship of these disciplines is to create and fill a database of normative data and search for correlations between various, both obviously related and, at first glance, completely unrelated structures of the human body. The purpose of the study was to determine the features of the relationship between the linear dimensions of molars with the cephalometric parameters of practically healthy men of the first mature age, residents of the western region of Ukraine. Cone-beam computed tomography was performed in 36 practically healthy men of the first mature age, residents of the western region of Ukraine (from Rivne, Volyn, Chernivtsi, Lviv, Ternopil, Khmelnytsky, Ivano-Frankivsk and Zakarpattia regions) followed by odontometry research and cephalometry. Statistical processing of the results was performed in the license package "Statistica 6.1" using non-parametric Spearman's statistics. As a result of quantitative analysis of reliable and average strength of unreliable correlations of linear computed tomographic sizes of molars with cephalometric indicators and indices of practically healthy men of the western region of Ukraine it is established that the percentage, mainly direct, reliable and average strength of unreliable correlations of linear sizes of molars with cephalometric indices and with indicators of the cerebral or facial skull is almost no different. The largest number of reliable and medium-strength unreliable correlations of linear molars sizes with cranial indices was found with vestibular-lingual and mesio-distal tooth sizes (20.5% with upper molars and 25.0% with lower molars). The highest number of reliable and medium-strength unreliable correlations of linear molars sizes with facial skull indices was found for upper molars with tooth height, crowns and root length (10.8%) and vestibular-lingual and mesio-distal dimensions (12.8%), and for lower molars - only with vestibular-lingual and mesio-distal dimensions (19.4%). The obtained data testify to the prospects of the chosen scientific direction of research, which will further improve the work of physicians in various fields of medicine, including preventive.

Keywords: *computed tomography, molars, odontometry, cephalometry, correlations, practically healthy men, administrative-territorial regions of Ukraine.*

Introduction

The human dental apparatus has undergone successive development from a simple organ that provides food grinding to an organ that participates in word-formation function, thus forming speech. Recently, this device has received a new function - aesthetic, thus forming the image of man. All this led to the formation of dentistry as an industry that embraces only the problems of the dental apparatus and in the future, its active branching into other, more specific areas. In particular, one of these branches is orthodontics - a branch of dentistry that deals with the treatment, study of etiology and prevention of abnormalities of the dental system [6, 13, 15, 16].

However, the last component, namely prevention, is the least studied and possibly underestimated by both representatives of the theoretical and practical direction of orthodontics. The ability to identify population risk groups for a disease using simple and at the same time, scientifically sound methods would seem to be a kind of

"utopia" for medicine. But in fact such works already exist and new ones are being developed - with the use of medical anthropology [3, 7, 17]. The dental industry is no exception, where it is also used to build the ideal proportions of the face and dental system. The latter becomes possible due to the use of various cranial values and their further comparison with human orthodontic indicators [12, 14]. Thus, a group of Indian authors [10] found a positive correlation between the size of the human iris and the mesiodistal width of the central incisor of the upper jaw for men and women.

The difficulty of the widespread implementation of the results of anthropological research is that they require research on different groups of the population - both by age and sex. It is proved that there is a difference in such indicators as length, the ratio of width/length of the teeth of the upper jaw and the width of their crowns, between males and females [27]. It is also necessary to take into account the ethnic and regional affiliation of individuals [9]. It is established that the largest odontometric indicators have representatives of African races, smaller Japanese and the smallest Europeans [4]. Thus, there is a need for research to find relationships between cephalometric and orthodontic indicators that take into account all of the above variables (gender, age, and ethnic or regional affiliation).

The purpose of the study was to determine the features of the relationship between the linear dimensions of molars with the cephalometric parameters of practically healthy men of the first mature age, residents of the western region of Ukraine.

Materials and methods

As a result of the study, 36 practically healthy men of the first mature age, residents of the western region of Ukraine from Rivne, Volyn, Chernivtsi, Lviv, Ternopil, Khmelnytsky, Ivano-Frankivsk and Zakarpattia regions, with favorable, moderately favorable and satisfactory ecological living conditions were selected. Committee on Bioethics of National Pirogov Memorial Medical University, Vinnytsya found that the research does not contradict the basic bioethical norms of the Council of Europe Convention on Human Rights and Biomedicine (1977) and the Declaration of Helsinki.

Computed tomography was performed using a Veraviewepocs-3D dental cone-beam tomograph (Morita, Japan). Odontometric examination was performed in the software shell i-Dixel One Volume Viewer (Ver.1.5.0, J Morita Mfg. Cor.). Measurements of the first and second molars of the right and left sides of the upper and lower jaws included determination of tooth height and tooth crown, length of palatal medial and distal roots, vestibular-lingual and mesio-distal dimensions of the crown and neck of the tooth [23]. For the convenience of recording, the digital designation of teeth was used: 16 - upper right first molar; 17 - upper right second molar; 26 - upper left first molar; 27 - upper left second molar; 36 - lower left first molar; 37 - lower left second molar; 46 - lower right first molar; 47 - lower right second molar

Cephalometric study of the parameters of the cerebral and facial parts of the head was performed in accordance with generally accepted recommendations and anatomical guidelines and points [2]. The shape of the head [28] and the type of face were also determined [20].

The correlations between odonto- and cephalometric parameters were evaluated in the licensed package "Statistica 6.1" using non-parametric Spearman statistics.

Results

The correlations obtained by us between the sizes of molars of the upper and lower jaws with cephalometric indicators of the brain and facial skull of practically healthy men of the western administrative-territorial region of Ukraine are presented in Tables 1-6.

Table 1. Correlations of the sizes of molars of an upper jaw with cephalometric indicators of a brain skull of a man of the western region of Ukraine (n=16-36).

Sizes of molars	Cephalometric indicators						
	DUG_GOP	DUGS_GOP	DUG_AUAU	G_OP	FMT_FMT	EY_EY	KRANIO
17HZ	-0.01	-0.03	0.25	-0.02	0.09	0.00	-0.02
17HKZ	-0.15	-0.09	0.05	-0.18	0.17	0.00	0.11
17HRZ1	-0.06	-0.07	0.22	0.10	-0.06	-0.07	-0.12
17HRZ2	0.19	0.25	0.32	0.32	0.24	0.10	-0.07
17HRZ3	0.03	-0.01	0.13	0.20	-0.05	0.03	-0.18
17VO_K	-0.09	0.03	0.07	-0.08	**0.37**	0.29	0.25
17VO_S	-0.14	0.15	0.02	-0.09	0.30	0.28	0.29
17MD_K	0.23	0.17	-0.05	0.31	-0.24	-0.21	**-0.41**
17MD_S	0.27	0.28	0.02	**0.36**	-0.13	-0.22	**-0.43**
16HZ	0.13	0.03	0.30	0.01	0.20	0.16	0.11
16HKZ	-0.14	-0.06	0.15	-0.15	0.15	-0.06	-0.02

Continuation of table 1.

Sizes of molars	Cephalometric indicators						
	DUG_GOP	DUGS_GOP	DUG_AUAU	G_OP	FMT_FMT	EY_EY	KRANIO
16HRZ1	0.09	0.33	0.29	0.26	0.14	0.04	-0.14
16HRZ2	0.09	0.02	0.21	0.07	0.06	0.00	-0.03
16HRZ3	0.17	0.22	0.25	0.32	0.14	0.17	-0.08
16VO_S	0.17	**0.34**	0.14	**0.39**	0.05	0.02	-0.19
16VO_K	0.04	0.23	0.18	0.13	0.14	0.19	0.08
16MD_S	0.14	0.18	0.06	0.28	-0.06	-0.18	**-0.38**
16MD_K	0.09	0.09	-0.07	0.22	-0.02	-0.20	-0.33
26HZ	0.16	-0.01	0.24	0.05	0.03	-0.02	-0.06
26HKZ	-0.02	-0.15	0.17	-0.08	0.05	-0.02	0.01
26HRZ1	-0.10	0.04	0.00	0.20	0.08	-0.09	-0.23
26HRZ2	0.09	0.06	0.17	0.10	0.05	-0.03	-0.10
26HRZ3	0.21	0.22	0.22	0.24	0.07	0.09	-0.04
26VO_K	0.21	**0.39**	0.32	**0.33**	0.17	0.24	0.01
26VO_S	0.03	0.24	0.19	0.24	0.19	0.15	-0.02
26MD_K	0.09	0.14	0.06	0.31	-0.12	-0.20	**-0.41**
26MD_S	-0.02	0.05	0.00	0.18	-0.06	-0.21	-0.27
27HZ	-0.14	-0.06	0.17	0.05	-0.11	-0.23	-0.25
27HKZ	**-0.33**	-0.24	-0.02	-0.19	0.05	-0.03	0.10
27HRZ1	0.02	0.06	0.32	0.25	-0.12	-0.18	-0.29
27HRZ2	0.12	0.16	0.18	0.28	0.08	-0.18	-0.33
27HRZ3	0.03	0.04	0.29	0.11	0.00	0.00	-0.07
27VO_K	-0.25	-0.11	-0.04	-0.02	0.19	0.25	0.23
27VO_S	0.01	0.08	0.08	0.05	0.30	**0.34**	0.23
27MD_K	0.14	0.16	0.02	0.29	-0.30	-0.28	**-0.48**
27MD_S	0.17	0.18	-0.05	0.32	-0.32	-0.30	**-0.49**

Notes: here and in the following tables, bold and red, or blue, respectively, are significant reliable medium-strength direct and inverse correlations; underlining and sand, or green color, respectively, unreliable medium-strength direct and inverse correlations; HZ - tooth height; HKZ - height of the tooth crown; HRZ1 - length of the palatine root of the upper molars; HRZ2 - length of the dorsal proximal root of the upper molars; HRZ3 - length of the parietal distal root of the upper molars; VO_K - vestibular-lingual size of the tooth crown; VO_S - vestibular-lingual size of the neck of the tooth; MD_K - mesio-distal size of the tooth crown; MD_S - mesio-distal size of the tooth neck; DUG_GOP - the largest head circumference; DUGS_GOP - sagittal arch; DUG_AUAU - transverse arc; G_OP - the largest length of the head; FMT_FMT - the smallest width of the head (frontal diameter); EU_EU - the largest width of the head (occipital diameter); KRANIO - cranial index.

Table 2. Correlations of the sizes of molars of a mandible with cephalometric indicators of a brain skull of men of the western region of Ukraine (n=16-36).

Sizes of molars	Cephalometric indicators						
	DUG_GOP	DUGS_GOP	DUG_AUAU	G_OP	EY_EY	FMT_FMT	KRANIO
47HZ	-0.14	-0.07	-0.08	-0.13	-0.10	0.00	-0.02
47HKZ	-0.25	-0.22	-0.19	-0.19	-0.14	-0.14	0.01
47HRZ4	-0.12	-0.14	0.01	-0.21	-0.20	-0.27	-0.04
47HRZ5	-0.09	0.11	0.24	0.13	0.20	**0.33**	0.10
47VO_K	0.06	0.30	0.26	0.31	0.30	0.31	-0.02
47VO_S	0.04	0.26	0.16	0.17	**0.41**	0.28	0.19
47MD_K	0.21	0.24	0.16	0.23	0.29	0.06	0.03

Continuation of table 2.

Sizes of molars	Cephalometric indicators						
	DUG_GOP	DUGS_GOP	DUG_AUAU	G_OP	EY_EY	FMT_FMT	KRANIO
47MD_S	0.08	0.01	0.03	0.11	0.15	0.05	0.05
46HZ	-0.06	-0.07	-0.10	0.07	-0.05	-0.14	-0.11
46HKZ	0.02	-0.01	0.10	-0.12	0.07	-0.05	0.10
46HRZ4	0.08	0.07	0.14	-0.03	-0.10	-0.12	-0.15
46HRZ5	-0.01	-0.17	0.00	0.19	-0.18	-0.21	-0.25
46VO_K	0.13	0.14	0.01	0.28	0.26	0.01	0.06
46VO_S	0.17	**0.35**	-0.08	0.32	**0.41**	0.27	0.15
46MD_K	0.17	**0.35**	0.24	0.28	**0.48**	**0.34**	0.19
46MD_S	0.18	0.31	0.22	0.18	0.28	0.28	0.15
36HZ	-0.06	-0.05	-0.02	0.04	-0.28	-0.27	-0.31
36HKZ	0.00	0.05	0.07	-0.06	-0.13	-0.24	-0.14
36HRZ4	-0.09	-0.09	-0.02	-0.09	-0.18	-0.18	-0.20
36HRZ5	0.03	-0.03	0.01	0.28	-0.24	-0.17	**-0.34**
36VO_K	0.29	**0.34**	0.27	**0.39**	**0.35**	0.10	0.09
36VO_S	0.20	**0.38**	0.13	**0.42**	**0.37**	0.20	0.05
36MD_K	0.15	0.31	0.30	0.24	**0.51**	0.30	0.26
36MD_S	0.08	0.25	0.13	0.20	**0.37**	0.26	0.20
37HZ	-0.01	-0.06	0.03	-0.04	-0.13	-0.01	-0.11
37HKZ	-0.11	-0.19	-0.10	-0.21	-0.11	-0.07	0.01
37HRZ4	-0.17	-0.27	-0.07	-0.27	-0.27	-0.23	-0.04
37HRZ5	-0.04	0.15	0.19	0.17	0.10	**0.34**	0.03
37VO_K	0.04	0.26	0.17	0.26	**0.36**	**0.36**	0.07
37VO_S	0.00	0.11	0.17	0.16	0.33	**0.38**	0.15
37MD_K	0.07	0.20	0.01	0.17	0.31	0.08	0.09
37MD_S	0.03	0.09	0.04	0.06	0.24	0.10	0.13

Notes: here and in the following tables, HRZ4 - the length of the near root of the lower molars; HRZ5 - the length of the distal root of the lower molars.

Table 3. Correlations of molar sizes of the upper jaw with cephalometric indicators of the facial skull of men from the western region of Ukraine (n=16-36).

Sizes of molars	Cephalometric indicators								
	ZY_ZY	ZM_ZM	TR_GN	TR_N	N_GN	N_PRN	N_SN	GO_GO	N_STO
17HZ	0.00	-0.04	-0.08	-0.11	0.19	-0.13	-0.15	0.09	0.05
17HKZ	0.05	-0.13	-0.03	-0.09	0.20	-0.10	-0.13	-0.12	0.14
17HRZ1	-0.08	-0.04	-0.16	0.19	-0.16	-0.11	-0.08	-0.20	0.13
17HRZ2	0.08	0.08	-0.04	**0.37**	-0.16	-0.13	-0.02	-0.12	-0.04
17HRZ3	0.12	-0.21	0.16	-0.10	**0.50**	0.13	0.08	0.16	0.21
17VO_K	**0.36**	-0.22	0.29	0.14	0.09	**0.39**	0.32	0.03	0.25
17VO_S	**0.38**	-0.29	0.19	0.04	0.11	0.32	0.26	0.10	0.03
17MD_K	-0.02	-0.31	0.04	0.00	0.18	0.00	0.06	0.12	-0.13
17MD_S	0.04	**-0.34**	0.08	0.10	0.10	0.00	0.11	0.01	-0.10
16HZ	0.09	-0.02	0.08	0.13	0.15	-0.06	-0.05	0.13	0.11

Continuation of table 3.

Sizes of molars	Cephalometric indicators								
	ZY_ZY	ZM_ZM	TR_GN	TR_N	N_GN	N_PRN	N_SN	GO_GO	N_STO
16HKZ	0.10	-0.28	-0.08	-0.05	0.03	-0.12	-0.15	-0.17	0.11
16HRZ1	0.23	**-0.40**	0.21	0.28	0.16	0.10	0.13	-0.06	-0.02
16HRZ2	0.01	-0.02	-0.02	**0.34**	-0.06	-0.11	-0.04	-0.14	-0.18
16HRZ3	0.22	0.06	0.20	0.10	**0.39**	0.16	0.19	0.12	**0.55**
16VO_S	0.10	-0.22	0.31	**0.38**	0.06	0.14	0.18	0.13	0.02
16VO_K	0.20	-0.25	0.14	-0.02	-0.05	0.11	0.11	0.31	-0.21
16MD_S	-0.08	-0.05	-0.15	-0.02	-0.11	-0.30	-0.19	0.16	-0.11
16MD_K	-0.05	-0.09	-0.12	-0.03	-0.12	-0.32	-0.21	0.11	-0.13
26HZ	0.01	0.11	-0.05	0.04	0.07	-0.28	-0.25	0.18	0.00
26HKZ	0.04	-0.22	-0.16	-0.11	-0.04	-0.23	-0.22	-0.11	-0.01
26HRZ1	0.14	-0.17	-0.25	-0.10	0.10	-0.30	-0.27	-0.04	0.11
26HRZ2	0.07	0.00	-0.05	0.30	0.14	-0.15	-0.15	-0.05	-0.02
26HRZ3	0.24	0.14	0.12	0.12	0.25	0.10	0.14	0.26	**0.33**
26VO_K	0.23	-0.24	0.31	**0.39**	0.10	0.25	0.32	0.05	0.26
26VO_S	0.23	-0.32	0.17	0.02	0.00	0.16	0.22	0.07	0.07
26MD_K	-0.20	0.04	-0.16	-0.07	-0.09	-0.22	-0.12	0.09	-0.10
26MD_S	-0.16	-0.01	-0.27	-0.13	-0.20	-0.28	-0.16	0.03	-0.17
27HZ	-0.19	0.02	-0.14	-0.16	0.13	-0.11	-0.11	-0.13	0.08
27HKZ	-0.09	0.04	-0.27	**-0.34**	0.15	-0.25	-0.30	-0.19	0.16
27HRZ1	-0.04	-0.09	-0.09	0.17	-0.05	-0.08	-0.02	-0.11	0.10
27HRZ2	0.06	0.01	-0.10	**0.37**	-0.07	-0.32	-0.29	0.02	-0.06
27HRZ3	-0.02	-0.02	0.03	0.01	0.22	0.08	0.10	-0.07	0.12
27VO_K	0.13	-0.13	0.15	0.01	0.05	0.24	0.16	0.06	0.17
27VO_S	**0.41**	**-0.34**	0.25	0.17	0.00	0.21	0.16	0.17	-0.05
27MD_K	-0.16	-0.14	-0.01	-0.10	0.16	0.03	0.08	0.11	-0.12
27MD_S	-0.14	-0.20	-0.09	-0.12	0.14	-0.01	0.04	0.11	-0.14

Notes: here and in the following tables, inaccurate mean correlations of inverse correlations are highlighted by underlining and green color; ZY_ZY - face width (distance between zygomatic points); ZM_ZM - average width of the face; TR_GN - physiological length of the face; TR_N - forehead height; N_GN - morphological length of the face; N_PRN - length of the nose; N_SN - nose height; GO_GO - width of the lower jaw (width between the corners of the lower jaw); N_STO - height of the upper part of the face.

Table 4. Correlations of the sizes of molars of a mandible with cephalometric indicators of a facial skull of men of the western region of Ukraine (n=16-36).

Sizes of molars	Cephalometric indicators								
	ZY_ZY	ZM_ZM	TR_GN	TR_N	N_GN	N_PRN	N_SN	GO_GO	N_STO
47HZ	-0.06	0.04	-0.23	-0.24	0.24	-0.08	-0.11	-0.25	0.10
47HKZ	-0.21	0.07	-0.31	-0.32	0.13	-0.09	-0.15	-0.16	-0.01
47HRZ4	-0.19	0.01	-0.32	-0.20	0.01	-0.25	-0.24	-0.11	-0.28
47HRZ5	0.17	0.05	0.13	0.16	0.21	0.14	0.12	-0.24	0.29
47VO_K	0.30	-0.07	0.18	0.20	0.10	0.26	0.30	-0.07	**0.36**
47VO_S	0.28	-0.14	0.25	-0.04	0.14	0.21	0.22	0.20	0.20
47MD_K	0.21	-0.17	0.29	0.11	0.28	0.27	0.27	0.18	0.23
47MD_S	0.17	-0.15	0.13	0.02	0.14	0.01	0.03	0.22	0.03

Continuation of table 4.

Sizes of molars	Cephalometric indicators								
	ZY_ZY	ZM_ZM	TR_GN	TR_N	N_GN	N_PRN	N_SN	GO_GO	N_STO
46HZ	-0.17	-0.01	-0.32	-0.25	0.01	-0.07	-0.05	-0.25	0.02
46HKZ	0.01	-0.10	-0.11	-0.05	0.10	0.16	0.10	0.01	0.03
46HRZ4	-0.05	-0.19	-0.17	-0.12	0.00	-0.16	-0.23	0.06	-0.23
46HRZ5	-0.23	0.12	-0.04	0.08	0.13	-0.15	-0.08	-0.10	0.05
46VO_K	0.08	0.13	0.07	-0.03	0.14	0.01	0.12	0.11	0.23
46VO_S	0.31	-0.23	0.23	0.10	0.17	0.25	**0.35**	0.14	**0.34**
46MD_K	**0.39**	-0.22	**0.35**	0.10	0.19	0.24	0.25	0.25	0.28
46MD_S	0.33	-0.14	0.26	0.15	0.02	0.09	0.12	0.22	0.07
36HZ	-0.19	0.02	**-0.39**	-0.22	0.03	-0.21	-0.23	-0.12	-0.06
36HKZ	-0.08	-0.14	-0.11	-0.07	0.16	-0.02	-0.06	0.06	-0.02
36HRZ4	-0.13	-0.14	-0.25	-0.23	0.08	-0.19	-0.26	-0.09	-0.13
36HRZ5	-0.12	0.16	-0.11	0.01	0.11	-0.16	-0.10	-0.02	0.06
36VO_K	0.18	0.09	0.15	0.08	-0.03	0.22	**0.35**	0.14	0.17
36VO_S	0.23	-0.10	0.15	0.04	0.05	0.28	**0.40**	0.13	0.31
36MD_K	0.29	-0.04	0.27	0.03	0.15	0.30	0.30	0.19	0.29
36MD_S	0.27	-0.14	0.25	0.04	0.02	0.17	0.20	0.21	0.11
37HZ	0.02	-0.07	-0.28	-0.11	0.16	-0.23	-0.26	-0.03	-0.04
37HKZ	-0.08	0.02	-0.26	-0.23	0.16	-0.17	-0.24	0.04	-0.07
37HRZ4	-0.18	0.02	**-0.37**	-0.22	-0.05	-0.30	-0.31	-0.12	**-0.34**
37HRZ5	0.29	-0.20	-0.06	0.19	0.07	-0.07	-0.07	-0.06	0.01
37VO_K	**0.34**	-0.02	0.13	0.13	0.07	0.28	0.32	-0.10	**0.38**
37VO_S	**0.37**	-0.18	0.10	-0.02	0.05	0.06	0.09	0.15	0.18
37MD_K	0.20	-0.23	0.26	0.01	**0.34**	0.31	0.28	0.16	0.29
37MD_S	0.14	-0.10	0.22	-0.03	0.21	0.31	0.26	0.20	0.15

Table 5. Correlations of molar sizes of the upper jaw with cephalometric indicators of the facial skull of men in the western region of Ukraine (n=16-36).

Sizes of molars	Cephalometric indicators								
	SN_PRN	AL_AL	CHI_CHI	EK_EK	MF_MF	N_I	PGO_GN	IGO_GN	IN_GARS
17HZ	0.16	-0.29	0.03	0.28	0.06	0.24	0.01	0.01	0.15
17HKZ	0.27	**-0.35**	-0.24	0.07	0.02	0.14	0.05	0.00	0.21
17HRZ1	0.02	-0.04	-0.04	0.22	-0.22	-0.18	**0.49**	**0.45**	-0.06
17HRZ2	-0.01	0.24	0.00	**0.40**	0.23	-0.11	0.23	0.18	-0.23
17HRZ3	0.19	**-0.36**	-0.03	0.14	-0.01	**0.61**	-0.16	-0.23	0.47
17VO_K	0.31	-0.08	-0.06	0.23	0.07	0.20	0.18	0.13	0.01
17VO_S	0.20	-0.02	-0.08	0.17	-0.06	0.15	0.26	0.25	0.07
17MD_K	-0.12	-0.02	0.02	0.09	-0.31	0.25	-0.09	-0.03	**0.42**
17MD_S	-0.18	-0.04	0.00	0.03	**-0.34**	0.10	-0.04	0.05	-0.31
16HZ	0.29	-0.11	0.14	**0.37**	0.16	0.15	0.19	0.18	0.07
16HKZ	0.04	-0.32	-0.20	0.08	0.10	0.05	0.03	-0.08	0.14
16HRZ1	-0.02	-0.08	-0.23	0.07	-0.02	0.04	0.11	0.04	0.26
16HRZ2	0.12	**0.37**	0.07	**0.46**	0.08	-0.15	**0.42**	**0.37**	-0.01

Continuation of table 5.

Sizes of molars	Cephalometric indicators								
	SN_PRN	AL_AL	CHI_CHI	EK_EK	MF_MF	N_I	PGO_GN	IGO_GN	IN_GARS
16HRZ3	0.29	**-0.37**	-0.11	0.18	-0.02	**0.43**	-0.04	0.01	0.12
16VO_S	0.04	0.07	0.27	**0.34**	0.15	0.03	0.19	0.21	0.16
16VO_K	0.10	0.15	-0.02	0.31	0.10	0.04	0.25	0.22	-0.01
16MD_S	-0.05	0.13	0.23	0.31	0.01	-0.07	0.02	0.10	0.00
16MD_K	-0.09	0.04	0.21	0.16	0.01	-0.04	-0.10	-0.01	0.07
26HZ	0.26	0.02	0.21	**0.43**	0.13	0.09	0.18	0.24	0.02
26HKZ	0.12	-0.19	0.04	0.12	-0.15	-0.08	0.25	0.22	0.12
26HRZ1	0.15	-0.14	0.00	0.06	-0.07	-0.03	0.06	0.07	0.13
26HRZ2	0.12	0.18	-0.19	**0.39**	0.22	0.07	0.23	0.20	0.10
26HRZ3	0.30	-0.16	0.15	**0.33**	0.06	0.27	-0.03	0.06	-0.04
26VO_K	0.22	0.05	0.08	0.23	-0.05	-0.03	**0.34**	**0.38**	0.10
26VO_S	0.18	0.12	-0.04	0.17	-0.13	0.08	0.27	0.32	0.12
26MD_K	-0.07	0.15	0.23	0.24	-0.01	0.01	-0.06	0.04	0.04
26MD_S	-0.05	0.09	0.21	0.19	-0.02	-0.09	-0.01	0.07	0.01
27HZ	0.23	-0.27	-0.06	0.09	-0.10	0.13	-0.03	-0.05	0.21
27HKZ	0.24	**-0.48**	-0.15	-0.15	-0.07	0.11	-0.14	-0.20	0.14
27HRZ1	0.15	-0.05	-0.11	0.30	-0.22	-0.10	**0.43**	**0.35**	0.00
27HRZ2	-0.05	0.08	-0.11	**0.52**	**0.48**	-0.05	0.17	0.10	-0.09
27HRZ3	0.18	-0.11	0.09	0.25	-0.01	0.32	-0.05	-0.08	0.22
27VO_K	**0.38**	-0.02	0.12	0.23	-0.09	0.15	0.31	0.25	0.04
27VO_S	0.11	0.08	-0.15	0.28	0.06	0.14	**0.36**	**0.34**	0.02
27MD_K	0.01	0.00	0.08	0.06	-0.31	0.19	-0.07	0.01	**0.34**
27MD_S	-0.02	-0.02	0.05	0.03	-0.30	0.17	-0.09	-0.02	**0.35**

Notes: here and in the following tables, SN_PRN -the depth of the nose; AL_AL - width of the base of the nose (distance between alar points); CHI_CHI - width of the oral slit; EK_EK - extraocular width (biorbital width); MF_MF - interorbital width (anterior interorbital width); N_I - the distance between the nasion and the intercanine point; RGO_GN - body length of the lower jaw on the right; LGO_GN - body length of the lower jaw on the left; IN_GARS - Garson's morphological index.

Table 6. Correlations of the sizes of molars of a mandible with cephalometric indicators of a facial skull of men of the western region of Ukraine (n=16-36).

Sizes of molars	Cephalometric indicators								
	SN_PRN	AL_AL	CHI_CHI	EK_EK	MF_MF	N_I	PGO_GN	IGO_GN	IN_GARS
47HZ	0.18	-0.14	-0.27	-0.09	0.04	0.24	-0.25	-0.28	0.23
47HKZ	0.18	-0.05	-0.19	-0.07	-0.01	0.20	-0.15	-0.20	0.21
47HRZ4	-0.01	0.05	-0.21	0.11	-0.11	-0.01	-0.01	0.01	0.15
47HRZ5	0.27	-0.23	-0.12	-0.02	0.25	0.24	-0.17	-0.22	0.06
47VO_K	0.23	0.10	-0.13	**0.40**	0.15	0.33	0.16	0.09	-0.08
47VO_S	0.14	0.00	-0.06	**0.33**	0.07	**0.41**	0.11	0.10	0.02
47MD_K	0.30	0.19	-0.07	**0.43**	-0.05	**0.41**	0.28	0.24	0.15
47MD_S	0.21	0.17	-0.02	**0.45**	-0.05	0.21	**0.42**	**0.47**	0.14
46HZ	0.03	0.15	-0.06	-0.06	-0.13	0.18	-0.13	-0.19	0.16
46HKZ	-0.03	0.00	-0.08	0.02	0.05	0.18	-0.01	-0.04	0.13
46HRZ4	-0.03	0.00	-0.04	0.06	0.10	0.04	-0.07	-0.16	0.14

Continuation of table 6.

Sizes of molars	Cephalometric indicators								
	SN_PRN	AL_AL	CHI_CHI	EK_EK	MF_MF	N_I	PGO_GN	IGO_GN	IN_GARS
46HRZ5	-0.04	0.10	0.09	0.22	0.03	0.30	-0.12	-0.09	0.24
46VO_K	**0.37**	0.04	0.10	0.15	**-0.33**	0.23	0.10	0.20	-0.01
46VO_S	**0.35**	0.02	0.00	0.17	-0.15	0.31	0.16	0.18	0.13
46MD_K	**0.46**	-0.11	0.04	0.30	-0.14	0.31	**0.33**	0.29	0.02
46MD_S	**0.44**	0.15	0.07	**0.33**	-0.05	0.05	**0.36**	**0.43**	-0.06
36HZ	-0.03	0.06	-0.10	0.00	0.06	0.11	-0.21	-0.25	0.17
36HKZ	-0.07	-0.07	-0.15	0.05	0.03	0.13	-0.01	-0.05	0.25
36HRZ4	-0.04	-0.03	-0.14	0.02	0.06	0.12	-0.07	-0.15	0.24
36HRZ5	-0.02	0.03	0.13	0.12	0.18	0.24	-0.29	-0.29	0.12
36VO_K	0.27	0.10	0.14	0.12	-0.33	0.11	0.19	0.28	-0.20
36VO_S	0.29	0.06	0.07	0.19	-0.16	0.22	0.21	0.24	-0.03
36MD_K	**0.52**	-0.06	0.04	0.23	-0.15	0.29	0.29	0.26	-0.08
36MD_S	**0.47**	0.14	0.09	0.22	-0.17	0.08	**0.36**	**0.40**	-0.05
37HZ	0.05	-0.13	-0.27	0.11	0.15	0.13	-0.02	-0.06	0.17
37HKZ	0.11	-0.12	-0.18	0.07	0.11	0.16	-0.07	-0.08	0.17
37HRZ4	-0.07	-0.03	-0.19	0.09	-0.01	-0.06	-0.02	0.04	0.13
37HRZ5	0.10	-0.13	-0.07	0.20	0.25	0.08	0.12	0.01	0.05
37VO_K	0.25	0.14	-0.09	0.32	0.09	0.29	0.16	0.11	-0.14
37VO_S	0.12	-0.11	-0.14	**0.36**	0.11	0.26	0.29	0.30	-0.04
37MD_K	**0.35**	0.08	-0.12	**0.33**	-0.10	**0.46**	0.25	0.20	0.26
37MD_S	**0.37**	0.10	-0.03	0.27	-0.02	0.30	0.28	0.29	0.13

Discussion

In a survey of 200 people of North African ethnic group, it was found that there is a pronounced correlation between the shape of the face and the shape of the central incisor of the upper jaw ($p<0.05$) [1]. Also, statistically significant relationships between orthodontic and cephalometric indicators were found in the study of ethnic groups of Malays and Chinese [11]. Brazilian scientists have found the most pronounced correlations between the size of the anterior maxillary incisor and the oval shape of the face [18].

At the same time, Indian scientists have not found a relationship between the indicators of the central incisor and the height of the face [5] and the indicators of the front maxillary teeth and the lower height or shape of the face [8, 26].

When presenting a study involving 149 students aged 18-30 years with subsequent statistical processing of the data on cephalometric and orthodontic examination, correlations were found between the proportions of the subjects and the size of the maxillary central incisor [21]. Similar data were also obtained by a group of Indian scientists led by N. Raghavendra [22], Brazilian [24] and Jordanian researchers [25] on local populations.

Quantitative analysis of reliable and average unreliable correlations of linear computed tomographic dimensions of molars with cephalometric indicators and indices of practically healthy men of the western region of Ukraine revealed the following distribution of connections:

between the upper molars and cranial skull indicators 31 correlation out of 252 possible (12.3%), of which, 2.8% of direct reliable average forces, 4.8% of direct unreliable average forces, 2.8% of inverse reliable average forces and 2.0% of inverse unreliable average forces; among which - with the first molars teeth 12 correlation from 126 possible (3.2% of direct reliable average force, 4.0% of direct unreliable average force, 1.6% of inverse reliable average force and 0.8% of return unreliable average force); with the second molars teeth 19 correlation from 126 possible (2.4% of direct reliable average force, 5.6% of direct unreliable average force, 4.0% of inverse reliable average force and 3.2% of inverse unreliable average force); with the height of the teeth, their crowns and the length of the roots of 8 correlation out of 140 possible (4.3% of direct unreliable medium strength, 0.7% of inverse reliable medium strength and 0.7% of inverse unreliable medium strength); with vestibular-lingual and mesio-distal dimensions, 23 correlation out of 112 possible (6.3% of direct reliable medium forces, 5.4% of direct unreliable

medium forces, 5.4% of reverse reliable medium forces and 3.6% of inverse unreliable medium forces);

between lower molars and cranial skull indicators 32 correlation out of 224 possible (14.3%), of which, 8.5% of direct reliable average forces, 4.9% of direct unreliable average forces, 0.4% of inverse reliable average forces and 0.4% of inverse unreliable average forces; among which - with the first molars teeth 20 correlation from 112 possible (11.6% of direct reliable average forces, 4.5% of direct unreliable average forces, 0.9% of inverse reliable average forces and 0.9% of return unreliable average forces); with the second molars teeth 12 correlation from 112 possible (5.4% of direct reliable average force and 5.4% of direct unreliable average force); with the height of the teeth, their crowns and the length of the roots, only 4 correlation out of 112 possible (1.8% of direct reliable average forces, 0.9% of inverse reliable average forces and 0.9% of inverse unreliable average forces); with vestibular-lingual and mesio-distal dimensions of 28 correlation out of 112 possible (15.2% of direct reliable average forces and 9.8% of direct unreliable average forces);

between the upper molars and facial skull indicators 76 correlation out of 648 possible (11.7%), of which, 0.2% direct reliable strong, 6.0% direct reliable medium strength, 2.3% direct unreliable medium strength, 1.4% inverse reliable medium strength and 1.9% of reverse unreliable average forces; among which - with the first molars teeth 34 correlation from 324 possible (5.6% of direct reliable average force, 2.8% of direct unreliable average force, 0.6% of inverse reliable average force and 1.5% of inverse unreliable average force); with the second molars teeth 42 correlation from 324 possible (0.3% of direct reliable strong, 6.5% of direct reliable average force, 1.9% of direct unreliable average force, 2.2% of return reliable average force and 2.2% of inverse unreliable average force); with the height of the teeth, their crowns and the length of the roots 39 correlation out of 360 possible (0.3% direct reliable strong, 6.7% direct reliable medium force, 1.1% direct unreliable medium force, 1.7% reverse reliable medium force and 1.1% reverse unreliable medium force); with vestibular-lingual and mesio-distal dimensions, 37 correlation out of 288 possible (5.2% of direct reliable medium forces, 3.8% of direct unreliable medium forces, 1.0% of inverse reliable medium forces and 2.8% of inverse unreliable middle forces);

between the lower molars and facial skull indicators 66 correlation out of 576 possible (11.5%), of which, 6.3% direct reliable medium strength, 3.3% direct unreliable medium strength, 0.7% reverse reliable medium strength and 1.2% reverse unreliable average strength; among which - with the first molars teeth 31 correlation from 288 possible (6.3% of direct reliable average forces, 3.1% of direct unreliable average forces, 0.7% of inverse reliable average forces and 0.7% of inverse unreliable average forces); with the second molars teeth 35 correlation from 288 possible (6.3% of direct reliable average forces, 3.5% of direct unreliable average forces, 0.7% of return reliable average forces and 1.7% of inverse unreliable average forces); with the height of the teeth, their crowns and the length of the roots 10 correlation out of 288 possible (0.3% of direct unreliable average forces, 1.0% of inverse reliable average forces and 2.1% of inverse unreliable average forces); with vestibular-lingual and mesio-distal dimensions 56 correlation out of 288 possible (12.5% of direct reliable medium forces, 6.3% of direct unreliable medium forces, 0.3% of inverse reliable medium forces and 0.3% of inverse unreliable middle forces).

Our results for men from the southern region of Ukraine differ from similar studies of the relationship between the size of molars with cephalometric indicators of men from the northern region of Ukraine [19], which confirms the need to take into account regional characteristics.

Thus, the data obtained by us are fully consistent with the results of both domestic and foreign studies, which indicates the viability of the chosen area of research and requires subsequent collection and analysis of data on other groups of the population of Ukraine.

Conclusions

1. The percentage of mostly direct, reliable and medium-strength unreliable correlations of linear sizes of molars with cephalometric indicators and indices of practically healthy men of the western region of Ukraine with indicators of cerebral or facial skull practically does not differ (12.3% between upper molars and indicators of a brain skull - 11.7% between the upper molars and indicators of the facial skull and 14.3% between the lower molars and the indicators of the skull - 11.5% between the lower molars and the indicators of the facial skull).

2. The largest number of reliable and medium-strength unreliable correlations of linear sizes of molars with indicators of a skull is established with vestibular-lingual and mesio-distal sizes of teeth (20.5% with upper molars and 25.0% with lower molars).

3. The largest number of reliable and medium-strength unreliable correlations of linear molars sizes with facial skull indices was established for upper molars with tooth height, crowns and root length (10.8%) and vestibular-lingual and mesio-distal dimensions (12.8%), and for lower molars - only with vestibular-lingual and mesio-distal dimensions (19.4%).

References

[1] Boujoual, I., Mouhibi, A., Mbarki, E., & Andoh, A. (2018). Correlation between the form of the maxillary central incisor and the inverted form of the face (Part II: statistical study on a Moroccan sample). *International Journal of Information Research and Review,* 5(10), 5770-5773.

[2] Bunak, V. V. (1941). *Anthropometry: a practicalcourse.* M.: Uchpedgiz.

[3] Dmitriev, M. O., Chernysh, A. V., & Gunas, I. V. (2019). Features

of the cephalometric profile of ukrainian youth by methods of Ricketts R. M., Burstone C. J. and Harvold E. P. *World Science,* 3, 6(46), 4-11. doi: 10.31435/rsglobal_ws/30062019/6569

[4] Fernandes, T. M. F., Sathler, R., Natalicio, G. L., Henriques, J. F. C., & Pinzan, A. (2013). Comparison of mesiodistal tooth widths in Caucasian, African and Japanese individuals with Brazilian ancestry and normal occlusion. *Dental press Journal of Orthodontics,* 18(3), 130-135. doi: 10.1590/S2176-94512013000300021

[5] Furtado, G. C., Furtado, A., El Haje, O. A., Butignon, L. E., Pesqueira, A. A., & Paranhos, L. R. (2014). Relationship between the morphology of the maxillary central incisor and horizontal and vertical measurements of the face. *Indian Journal of Dental Research,* 25(2), 178-183. doi: 10.4103/0970-9290.135914

[6] Glushak, A. A., & Gunas, I. V. (2015). Models of individual linear dimensions required to build the correct shape of the dental arch in boys and girls with different head shapes. *Ukrainian Scientific and Medical Youth Journal,* (1), 34-38.

[7] Gunas, I. V., Dmitriev, M. O., Prokopenko, S. V., Shinkaruk-Dykovytska, M. M., & Yeroshenko, G. A. (2017). Determination of regulatory cephalometric parameters according to Charles H. Tweed International Foundation analysis for Ukrainian boys and girls. *World of Medicine and Biology,* 4(62), 27-31. doi: 10.26724/2079-8334-2017-4-62-27-31

[8] Gyawali, R., & Singh, V. P. (2017). Analysis of maxillary anterior teeth proportion in relationship with lower facial height and malocclusion. *Journal of College of Medical Sciences-Nepal,* 13(2), 262-267. doi: 10.3126/jcmsn.v13i2.16717

[9] Hassan, A. H. (2011). Mandibular cephalometric characteristics of a Saudi sample of patients having impacted third molars. *The Saudi Dental Journal,* 23(2), 73-80. doi: 10.1016/j.sdentj.2010.11.001

[10] Hemalatha, K., Chander, N. G., & Anitha, K. V. (2018). Correlation between iris diameter and the width of the maxillary central incisor with digital image analysis. *The Journal of Prosthetic Dentistry,* 119(3), 450-454. doi: 10.1016/j.prosdent.2017.04.011

[11] Isa, Z. M., Tawfiq, O. F., Noor, N. M., Shamsudheen, M. I., & Rijal, O. M. (2010). Regression methods to investigate the relationship between facial measurements and widths of the maxillary anterior teeth. *The Journal of Prosthetic Dentistry,* 103(3), 182-188. doi: 10.1016/S0022-3913(10)60028-5

[12] Jain, A. R., Nallaswamy, D., & Ariga, P. (2019). Determination of the correlation of width of maxillary anterior teeth using extraoral factor (intercanthal width) in Indian population. Drug Invention Today, 11(5), 1082-1090.

[13] Marchenko, A. V., Gunas, I. V., Petrushanko, T. O., Serebrennikova, O. A., & Trofimenko, Y. Y. (2017). Computer-tomographic characteristics of root length incisors and canines of the upper and lower jaws in boys and girls with different craniotypes and physiological bite. *Wiadomosci Lekarskie* (Warsaw, Poland: 1960), 70(3 pt 1), 499-502. PMID: 28711896

[14] Mehndiratta, A., Bembalagi, M., & Patil, R. (2019). Evaluating the Association of Tooth Form of Maxillary Central Incisors with Face Shape Using AutoCAD Software: A Descriptive Study. *Journal of Prosthodontics,* 28(2), e469-e472. doi: 10.1111/jopr.12707

[15] Mokhtarpour, H., Ebrahimi Saravi, M., Ghabel, S., Yazdani Charati, J., & Armin, M. (2019). Relationship between Length and Width of Maxillary Central Teeth and Facial Indices in Patients with Complete Denture. *Journal of Mazandaran University of Medical Sciences,* 29(178), 127-133.

[16] Neda, A. K., & Garib, B. T. (2016). Selecting maxillary anterior tooth width by measuring certain facial dimensions in the Kurdish population. *The Journal of Prosthetic Dentistry*, 115(3), 329-334. doi: 10.1016/j.prosdent.2015.08.012

[17] Paranhos, L. R., Zaroni, M., Carli, J. P. D., Okamoto, R., Zogheib, L. V., & Torres, F. C. (2014). Association between the facial type and morphology of the upper central incisor in normal occlusion subjects. *The Journal of Contemporary Dental Practice*, 15(1), 29-33. doi: 10.5005/jp-journals-10024-1183

[18] Pedrosa, V. O., Franca, F. M. G., Florio, F. M., & Basting, R. T. (2011). Study of the morpho-dimensional relationship between the maxillary central incisors and the face. *Brazilian Oral Research,* 25(3), 210-216. doi: 10.1590/S1806-83242011005000010

[19] Polishchuk S. S., Kotsyura O. O., Dmitriev M. O., Orlovskiy V. O., & Popov M. V. (2020). Correlations of linear sizes of molars with cephalometric indicators of practically healthy men of the northern region of Ukraine. *Reports of Morphology,* 26(1), 37-47. doi: 10.31393/morphology-journal-2020-26(1)-06

[20] Proffit, U. R. (translation from English; Ed. L.S. Persina) (2015). *Modern Orthodontics*. M.: Medpress-inform. ISBN: 978-5-00030-236-1

[21] Radia, S., Sherriff, M., McDonald, F., & Naini, F.B. (2016). Relationship between maxillary central incisor proportions and facial proportions. *The Journal of Prosthetic Dentistry,* 115(6), 741-748. doi: 10.1016/j.prosdent.2015.10.019

[22] Raghavendra, N., Kamath, V. V., Satelur, K. P., & Rajkumar, K. (2015). Prediction of Facial Profile Based on Morphometric Measurements and Profile Characteristics of Permanent Maxillary Central Incisor Teeth. *Journal of Forensic Science and Medicine*, 1(1), 26-32. doi: 10.4103/2349-5014.155550

[23] Samusev, R. P., Krayushkin, A. I., & Dmitrienko, S. V. (Ed. M.R.Sapin) (2002). *Basics of Clinical Morphology of Teeth: a Tutorial.* M: OOO "Publishing House ONIX21 vek": OOO "World and Education". ISBN: 5-329-00426-8

[24] Sharma, S., Nagpal, A., & Verma, P. R. (2012). Correlation Between Facial Measurements And The Mesiodistal Width Of The Maxillary Anterior Teeth. *Indian Journal of Dental Sciences,* 4(3), 20-24.

[25] Shaweesh, A. I., Al-Dwairi, Z. N., & Shamkhey, H. D. (2015). Studying the relationships between the outlines of the face, maxillary central incisor, and maxillary arch in Jordanian adults by using Fourier analysis. *The Journal of Prosthetic Dentistry,* 113(3), 198-204. doi: 10.1016/j.prosdent.2014.08.009

[26] Shrestha, S., Pandey, K. K., Verma, A. K., Ali, M., Katiyar, P., Gaur, A., & Tarannum, F. (2019). Comparison of relationship between intercondylar width and maxillary inter-canine width. *International Journal of Research and Reports in Dentistry,* 2(1), 1-6.

[27] Yuan, P. H., Evangelina, I. A., & Gayatri, G. (2018). Comparison of crown width, length, width/length ratio of maxillary anterior teeth between male and female dental students. *Padjadjaran Journal of Dentistry,* 30(3), 170-177. doi: 10.24198/pjd.vol30no3.19275

[28] Zubov, A. A. (1968). *Odontology. Methodology of anthropological research.* M.: Science.

ОСОБЛИВОСТІ КОРЕЛЯЦІЙ РОЗМІРІВ ВЕЛИКИХ КУТНІХ ЗУБІВ ІЗ КЕФАЛОМЕТРИЧНИМИ ПОКАЗНИКАМИ ЧОЛОВІКІВ ЗАХІДНОГО РЕГІОНУ УКРАЇНИ

Гунас В.І., Коцюра О.О., Бабич Л.В., Шевчук Ю.Г., Черкасова О.В.

Розширення теоретичних знань медичної антропології в сучасній сфері надання стоматологічних послуг є одним з головних

рушіїв прогресу у ортодонтичній галузі. Єдиним шляхом успішного розвитку взаємовідносин даних дисциплін є створення і наповнення бази нормативних даних та пошук у ній зв'язків між різноманітними, як очевидно пов'язаними, так і на перший погляд, абсолютно не пов'язаними структурами тіла людини. Мета дослідження - визначити особливості зв'язків лінійних розмірів великих кутніх зубів (ВКЗ) із кефалометричними показниками практично здорових чоловіків першого зрілого віку, жителів західного регіону України. У 36 практично здорових чоловіків першого зрілого віку, жителів західного регіону України (із Рівненської, Волинської, Чернівецької, Львівської, Тернопільської, Хмельницької, Івано-Франківської та Закарпатської областей) проведено конусно-променеву комп'ютерну томографію з наступною одонтометрією великих кутніх зубів і кефалометричне дослідження. Статистичну обробку результатів проведено у ліцензійному пакеті "Statistica 6.1" за допомогою непараметричної статистики Спірмена. В результаті кількісного аналізу достовірних і середньої сили недостовірних кореляцій лінійних комп'ютерно-томографічних розмірів ВКЗ із кефалометричними показниками та індексами практично здорових чоловіків західного регіону України встановлено, що відсоток, переважно прямих, достовірних і середньої сили недостовірних кореляцій лінійних розмірів ВКЗ із кефалометричними показниками та індексами з показниками мозкового, або лицевого черепу практично не відрізняється. Найбільша кількість достовірних і середньої сили недостовірних кореляцій лінійних розмірів ВКЗ із показниками мозкового черепу встановлена з присінково-язиковими та мезіо-дистальними розмірами зубів (20,5% із верхніми ВКЗ та 25,0% із нижніми ВКЗ). Найбільша кількість достовірних і середньої сили недостовірних кореляцій лінійних розмірів ВКЗ із показниками лицевого черепу встановлена для верхніх ВКЗ з висотою зубів, їх коронок і довжиною коренів (10,8%) та присінково-язиковими та мезіо-дистальними розмірами (12,8%), а для нижніх ВКЗ - лише з присінково-язиковими та мезіо-дистальними розмірами (19,4%). Отримані дані засвідчують перспективність обраного наукового напрямку досліджень, що в подальшому дозволить покращити роботу лікарів у різних напрямках медицини, зокрема і превентивної.

Ключові слова: *комп'ютерна томографія, великі кутні зуби, одонтометрія, кефалометрія, кореляції, практично здорові чоловіки, адміністративно-територіальні регіони України.*

ОСОБЕННОСТИ КОРРЕЛЯЦИЙ РАЗМЕРОВ БОЛЬШИХ КОРЕННЫХ ЗУБОВ С КЕФАЛОМЕТРИЧЕСКИМИ ПОКАЗАТЕЛЯМИ МУЖЧИН ЗАПАДНОГО РЕГИОНА УКРАИНЫ

Гунас В.И., Коцюра О.А., Бабич Л.В., Шевчук Ю.Г., Черкасова Е.В.

Расширение теоретических знаний медицинской антропологии в современной сфере предоставления стоматологических услуг является одним из главных двигателей прогресса в ортодонтической области. Единственным путем успешного развития взаимоотношений данных дисциплин является создание и наполнение базы нормативных данных и поиск в ней связей между различными, как очевидно связанными, так и на первый взгляд, совершенно не связаннми структурами тела человека. Цель исследования - определить особенности связей линейных размеров больших коренных зубов (БКЗ) с кефалометрическими показателями практически здоровых мужчин первого зрелого возраста, жителей западного региона Украины. У 36 практически здоровых мужчин первого зрелого возраста, жителей западного региона Украины (с Ровенской, Волынской, Черновицкой, Львовской, Тернопольской, Хмельницкой, Ивано-Франковской и Закарпатской областей) проведено конусно-лучевую компьютерную томографию с последующей одонтометриею больших коренных зубов и кефалометрическое исследование. Статистическую обработку результатов проведено в лицензионном пакете "Statistica 6.1" с помощью непараметрической статистики Спирмена. В результате количественного анализа достоверных и средней силы недостоверных корреляций линейных компьютерно-томографических размеров БКЗ с кефалометрическими показателями и индексами практически здоровых мужчин западного региона Украины установлено, что процент, преимущественно прямых, достоверных и средней силы недостоверных корреляций линейных размеров БКЗ с кефалометрическими показателями и индексами с показателями мозгового или лицевого черепа практически не отличается. Наибольшее количество достоверных и средней силы недостоверных корреляций линейных размеров БКЗ с показателями мозгового черепа установлена с преддверно-языковыми и мезио-дистальными размерами зубов (20,5% с верхними БКЗ и 25,0% с нижними БКЗ). Наибольшее количество достоверных и средней силы недостоверных корреляций линейных размеров БКЗ с показателями лицевого черепа установлена для верхних БКЗ с высотой зубов, их коронок и длиной корней (10,8%) и преддверно-языковыми и мезио-дистальными размерами (12,8%), а для нижних БКЗ - только с преддверно-языковыми и мезио-дистальными размерами (19,4%). Полученные данные свидетельствуют о перспективности выбранного научного направления исследований, и в дальнейшем позволит улучшить работу врачей в разных направлениях медицины, в том числе и превентивной.

Ключевые слова: *компьютерная томография, большие коренные зубы, одонтометрия, кефалометрия, корреляции, практически здоровые мужчины, административно-территориальные регионы Украины.*

DOI: 10.31393/morphology-journal-2020-26(2)-09 Reports of Morphology, Vol. 26, №2, Pages 62-66

ISSN 1818-1295 eISSN 2616-6194

REPORTS OF MORPHOLOGY

Official Journal of the Scientific Society of Anatomists, Histologists, Embryologists and Topographic Anatomists of Ukraine

journal homepage: https://morphology-journal.com

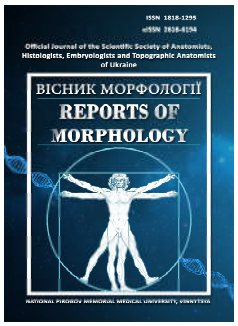

Use of azimuthal-invariant Mueller-matrix images of linear dichroism of histological sections of brain substance for diagnosis of hemorrhage genesis

Garazdiuk M.S.[1], Dubolazov O.V.[2], Malanchuk S.M.[3]

[1]Bukovinian State Medical University, Chernivtsi, Ukraine
[2]Institute of Physical, Technical and Computer Sciences of Chernivtsi National University named after Yu. Fedkovych, Chernivtsi, Ukraine
[3]Municipal Non-Commercial Enterprise "City Children's Polyclinic" Chernivtsi City Council, Chernivtsi, Ukraine

ARTICLE INFO
Received: 21 June, 2020
Accepted: 31 July, 2020

UDC: 340.6:616.831-005.1-073.55:535.515

CORRESPONDING AUTHOR
e-mail: sudmed@bsmu.edu.ua
Garazdiuk M.S.

Differential diagnosis of the cause of death (CD) from ischemic cerebral infarction (ICI), hemorrhages of traumatic (HTG) and non-traumatic (HNG) genesis exclude the violent nature of death. The aim of our work was to develop forensic criteria for hemorrhage differentiation of traumatic and non-traumatic genesis and ICI by azimuthal-invariant Mueller-matrix images of linear dichroism of histological sections of brain substance (HBS). For the study were used native sections of HBS from 130 corpses in the case of: death from coronary heart disease - 40 of native sections (group 1 - control); HTG - 30 sections (group 2), ICI - 30 native sections (group 3), HNG - 30 native sections (group 4). Measuring the coordinate allocation meanings of parameters of polarization in the points of microscopic images was carried out at the location of the standard stokes-polarimeter. The effectiveness of intergroup differentiation of samples of deaths from traumatic hemorrhage and ischemic cerebral infarction reaches a satisfactory level and is 76-83%. Efficiency between group differentiation of samples of deaths from nontraumatic and traumatic hemorrhages reaches a satisfactory level and is 75-82%. As for differentiation between ischemic cerebral infarction and nontraumatic hemorrhages thise method is ineffective.

Keywords: *hemorrhages of traumatic genesis, hemorrhages of non-traumatic genesis, ischemic cerebral infarction, Muller-matrix mapping.*

Introduction

Traumatic brain injury is one of the most common types of mechanical damage to the human body [7, 8, 9, 10, 12, 24]. Quite often, in forensic practice there are cases when the body was found at home under unexplained circumstances and later during the autopsy hemorrhage into the substance of the human brain (HBS) was detected. In this case forensic authorities raise questions about the genesis of hemorrhage: traumatic or non-traumatic. There are studies in which it is noted that traumatic brain injury (TBI) and strokes can coexist or occur one on background of another one, which further complicates the situation [22]. Therefore, differential diagnosis of the cause of death (CD) from ischemic cerebral infarction (ICI), hemorrhages of traumatic (HTG) and non-traumatic (HNG) genesis excluded the violent nature of death [10, 12, 23]. It should also be noted that the incidence of hemorrhage in the brain necessitates the study of structural alterations of HBS and the determination of reliable criteria for hemorrhage differentiation.

Typically, physicians in routine practice for differential diagnosis within the group of acute cerebrovascular disorders use computed tomography (CT) and general clinical data, but there is very little data on the differentiation of strokes of ischemic and hemorrhagic genesis and hemorrhage in HBS of traumatic origin [10, 12, 24]. A team of scientists led by Panzer S noted the feasibility of performing pre-mortem CT to compare it with CT immediately after injury of HBS, as well as the subsequent comparison of all CT images with autopsy results [10]. Comparison between primary CT and recent CT scans revealed marked changes in the presence and severity of signs of HBS injury, especially in patients with severe TBI. They also noted that the comparison of autopsy and CT data revealed a high level of diagnostic specificity (≥80%)

in the studied cases.

Recently in forensic practice optical methods of biological tissue research using lasers have positively proved themselves, which by studying the phenomena of light scattering make it possible to obtain reliable objective data of the dynamics of pre- and post-mortem changes of the studied tissues of the human body and to diagnose with greater accuracy prescription of pathological process in biological tissues and liquids [1, 2, 3, 4, 5, 11, 13, 14, 15, 16, 17, 18, 19, 20, 21].

The aim of our work: was to develop forensic criteria for hemorrhage differentiation of traumatic and non-traumatic genesis and ICI by azimuthal-invariant Mueller-matrix images of linear dichroism of histological sections of HBS.

Materials and methods

For the study were used native sections of HBS from 130 corpses in the case of: death from coronary heart disease - 40 (31%) of native sections (group 1 - control); HTG - 30 (23%) sections (group 2), ICI - 30 (23%) native sections (group 3), HNG - 30 (23%) native sections (group 4).

For the study, the preparations were previously subjected to rapid freezing, then histologic sections were made. Subsequently, the samples were sent to the laboratory of the Yuriy Fedkovych Institute of Physical, Technical and Computer Sciences, where they were investigated using the azimuthal-invariant Muller-matrix mapping method, the way of application of the method is described in sources [5, 13, 15].

Measuring the coordinate allocation meanings of parameters of polarization in the points of microscopic images was carried out at the location of the standard stokes-polarimeter [3].

Experimental measurements of Stokes-parametric images of biological layers were carried out according to the method presented in these publications [3, 5, 15]. Subsequently, statistical processing of the obtained data was performed [6].

Results

Figure 1 shows Results of azimuthal-invariant Mueller-matrix mapping of topographic maps (fragments (1), (3), (5), (7)) and histograms of probability distribution values(fragments (2), (4), (6), (8))of Mueller-matrix invariant (MMI) of linear dichroism (LD), which characterizes the polarization manifestations of linear dichroism of spatial structured fibrillar networks of nervous tissue of the deceaseds from groups 1-4.

A comparative analysis of the results of the Muller-matrix mapping of the polarization manifestations of LD of fibrillar networks of brain samples revealed: significant topographic heterogeneity of MMI LD maps of histological sections of the brain of the dead from all groups (Fig. 1, Fragments (1), (3), (5), (7)); series of distributions of the value of MMI LD fibrillar networks of samples of histological sections of the brain from all (control 1 and experimental 2-4) groups are characterized by individual and significant variations in the magnitude of the central statistical moments of the 2nd - 4th orders (Fig. 1, Fragments (2), (4), (6), (8)).

Table 1 shows the statistical analysis of MMI of LD maps of HBS.

Comparison of statistical analysis data revealed diagnostic sensitivity of the set of central statistical moments of the 2nd - 4th orders (highlighted in gray - Table 1) for azimuthal-invariant Mueller-matrix differentiation of manifestations of linear dichroism of spatially structured fibrillar networks of samples of nerve tissue samples both control group 1 and all experimental groups 2-4 ($p<0.05$). Along with this, there are possibility of intergroup (experimental groups 2-4) statistical differentiation of coordinate distributions of the MMI of LD of experimental representative samples of histological sections of the brain

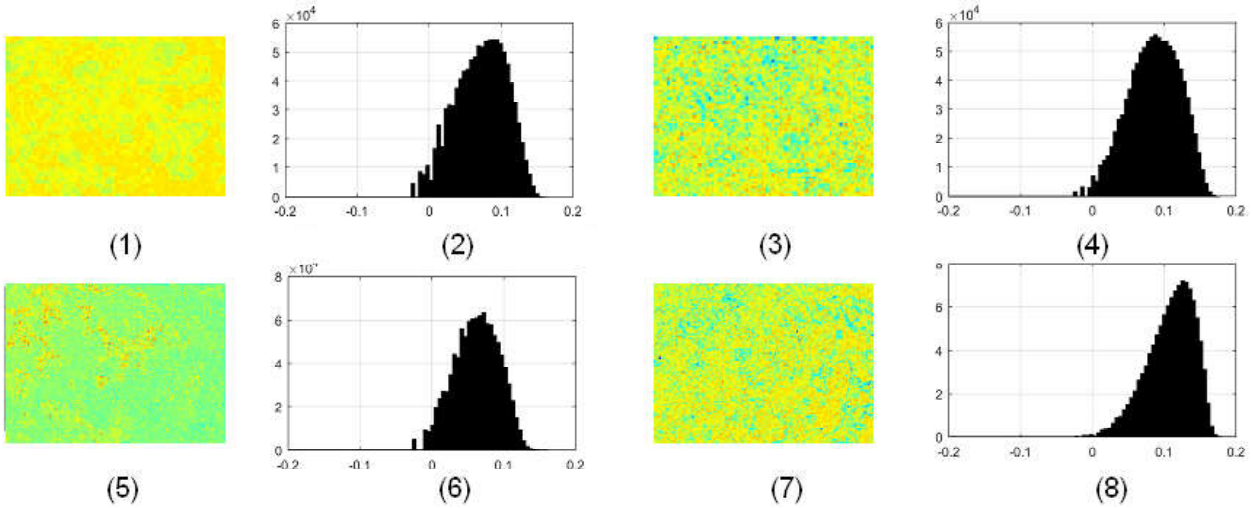

Fig. 1. Maps ((1), (3), (5), (7)) and histograms ((2), (4), (6), (8)) of the magnitudes of the distributions of the MMI LB of HBS histological sections from group 1 ((1), (2)), group 2 ((3), (4)), group 3 ((5), (6)) and group 4 ((7), (8)).

Table 1. Statistical moments of 1-4-th order characterizing the MMI of LD values distributions of histological sections of the brain of groups 1 - 4.

Parameters	Group 1	Group 2	Group 3	Group 4
SM_1	0.240±0.009	0.221±0.011	0.251±0.01	0.210±0.008
p_1		p<0.05	p<0.05	p<0.05
p_2		p>0.05		p>0.05
p_3		p>0.05	p>0.05	
p_4		p>0.05		
SM_2	0.212±0.011	0.271±0.017	0.321±0.016	0.370±0.014
p_1		p<0.05	p<0.05	p<0.05
p_2		p>0.05		p>0.05
p_3		p>0.05	p>0.05	
p_4		p>0.05		
SM_3	0.691±0.027	0.872±0.034	0.981±0.035	1.110±0.044
p_1		p<0.05	p<0.05	p<0.05
p_2		p>0.05		p<0.05
p_3		p>0.05	p>0.05	
p_4		p>0.05		
SM_4	0.891±0.041	1.120±0.048	1.221±0.051	1.431±0.059
p_1		p<0.05	p<0.05	p<0.05
p_2		p>0.05		p>0.05
p_3		p>0.05	p>0.05	
p_4		p>0.05		

- "group 2 - group 4" ($p<0.05$) and "group 2 and group 3" ($p<0.05$).

The values of operational characteristics that characterize the strength of the method of azimuthal-invariant Mueller-matrix polarimetry of the distributions of the linear dichroism of a set of brain tissue samples for objective statistical differentiation of causes of death are presented in table 2.

An increase in the value of sensitivity, specificity and balanced accuracy by 14-19% compared with the data of the Muller-matrix polarimetry of distributions of the Muller-matrix invariant of linear birefringence of samples of HBS [14, 16].

For a set of central statistical moments of the 1st, 3rd and 4th orders, which characterize the distributions of circular dichroism, the method of Mueller matrix microscopy in the differentiation of samples of control and experimental groups reaches a satisfactory level 78-84%.

Between control group 1 (ischemic heart disease) and all experimental groups 1-3 the azimuthal-invariant Muller-matrix mapping of the polarization manifestations of LB of fibrillary nerve tissue networks of the dead demonstrates a good level of differentiation, which is 79-83%.

Diagnostic efficiency of the Mueller-matrix mapping method of polarization manifestations of LD for intergroup differentiation of samples of deaths from HTG (group 2) and ICI (group 3) reaches a satisfactory level and is 76-83%. A similar (satisfactory 75-82%) level of differentiation is achieved for samples of histological sections of deaths from HNG (group 4) and HTG (group 2).

As for differentiation between ICI (group 3) and HNG (group 4) thise method is ineffective, as the level of differentiation is from 60 to 70%.

Table 2. Specificity, sensitivity, accuracy of the method of statistical analysis of MMI of LB maps of histological sections of the brain.

Groups "1 - 2+3+4"			
Parameters	sensitivity Se, %	specificity Sp, %	accuracy Ac, %
SM_1	a=99; b=31	c=93; d=37	n=130
	80	**75**	**77,5**
SM^2	a=99; b=31	c=93; d=37	n=130
	80	**75**	**77,5**
SM_3	a=108; b=22	c=105; d=25	n=130
	83	**79**	**81**
SM_4	a=108; b=22	c=105; d=25	n=130
	83	**79**	**81**
Groups "2 - 3"			
SM_1	a=90; b=40	c=102; d=28	n=130
	69	**64**	**66,5**
SM^2	a=90; b=40	c=102; d=28	n=130
	69	**64**	**66,5**
SM_3	a=108; b=22	c=99; d=31	n=130
	83	**76**	**79,5**
SM_4	a=108; b=22	c=99; d=31	n=130
	83	**76**	**79,5**
Groups "2 - 4"			
SM_1	a=82;b=48	c=78; d=52	n=130
	63	**60**	**61,5**
SM^2	a=82;b=48	c=81; d=49	n=130
	65	**62**	**63,5**
SM_3	a=107;b=23	c=98; d=32	n=130
	82	**75**	**78,5**
SM_4	a=107; b=23	c=98; d=32	n=130
	82	**75**	**78,5**
Groups "3 - 4"			
SM_1	a=82; b=48	c=78; d=52	n=130
	63	**60**	**61,5**
SM^2	a=82; b=48	c=79; d=51	n=130
	63	**61**	**62**
SM_3	a=87; b=43	c=82; d=48	n=130
	67	**63**	**65**
SM_4	a=87; b=43	c=82; d=48	n=130
	67	**63**	**65**

Discussion

Methods of polarization tomography, based on the results of numerical display of instrumental measurement of parameters, are one of the most objective and accurate for recording changes that occurred in a biological object under the influence of environmental factors and changes in biological tissues (BT) during the pathological process. They also have the main requirement for the introduction of modern research methods in the practice of any expert field - the ability not to change the properties and condition of the object under study in its evaluation [3, 19, 20, 21].

The method of polarization laser microscopy allows to obtain important information about the morphological structure and properties of human BT. From the optical point of view on BT they consist of 2 phases: amorphous and optically anisotropic (crystalline) [3]. Crystal structures include coaxial fibrils, which form collagen, elastin, myosin organic fibers, surrounded by fluids and media of the human body. An important feature of these fibrillar proteins is their clear order. It should be noted that polarization microscopy carries information about the degree of ordering and crystallization of the structure of BT [3].

Conclusions

1. The magnitudes of operational characteristics that characterize the power of the method of azimuthal-invariant Mueller-matrix images of linear dichroism of histological sections of human brain substance demonstrate the possibility of objective statistically significant differences by this method.

2. The effectiveness of intergroup differentiation of samples of deaths from traumatic hemorrhage and ischemic cerebral infarction reaches a satisfactory level and is 76-83%.

3. Efficiency between group differentiation of samples of deaths from nontraumatic and traumatic hemorrhages reaches a satisfactory level and is 75-82%.

4. As for differentiation between ischemic cerebral infarction and nontraumatic hemorrhages thise method is ineffective.

References

[1] Angelsky, O. V., Ushenko, Y. A., & Balanetska, V. O. (2011). *The degree of mutual anisotropy of biological liquids polycrystalline nets as a parameter in diagnostics and differentiations of hominal inflammatory processes.* Proc. SPIE 8338. In Tenth International Conference on Correlation Optics. 83380S. doi: 10.1117/12.920065

[2] Angelsky, O. V., Ushenko, A. G., Angelska, A. O., & Ushenko, Y. A. (2007). *Polarization correlometry of polarization singularities of biological tissues object fields*. Proc. SPIE 6616, Optical Measurement Systems for Industrial Inspection. 66160V. doi: 10.1117/12.725980

[3] Bachinskiy, V. T., Boichuk, T. M. & Ushenko, A. G. (2017). *Laser polarimetry of biological tissues and fluids.* LAP LAMBERT Academic Publishing.

[4] Bachynskyi, V. T., Hurov, O. M., Sarkisova, Yu. V., & Ushenko, O. H. (2017). Basic principles of morphological assessment of the state of biological tissues using laser polarimetric methods for solving forensic medicine problems. *Clinical and experimental pathology,* 16(1), 20-23.

[5] Garazdyuk, M., Savka, I., Tomka, Y., Soltys, I., Dubolazov, O., & Dvorjak, V. (2020). *Azimuthally invariant Mueller-matrix microscopy in the differential diagnosis of cerebral infarction*. In Optics and Photonics for Information Processing XIV (Vol. 11509, p. 115090T). International Society for Optics and Photonics. doi: 10.1117/12.2568436

[6] Glanc, S. (1999). *Biomedical statistics*. M.: Praktika.

[7] Finnie, J.W. (2016) Forensic Pathology of Traumatic Brain Injury. *Vet. Pathol.*, 53(5), 962-978. doi: 10.1177/0300985815612155

[8] Hohlov, V. V. (2010). *Forensic Medicine: A Guide*. Smolensk.

[9] Konovalov, A. N., Lihtermana, L. B. & Potapova, A. A. (Ed.). (2001). *Clinical Guide to Traumatic Brain Injury.* M.: Antidor.

[10] Panzer, S., Covaliov, L., Augat, P. & Peschel, O. (2017) Traumatic brain injury: Comparison between autopsy and ante-mortem CT. *J. Forensic Leg. Med.,* 52, 62-69. doi: 10.1016/j.jflm.2017.08.007

[11] Pavlyukovych, O. V. (2011). D*etermination of the age of death in some types of mechanical asphyxia and massive blood loss by laser polarimetry*. Kyiv.

[12] Pigolkina, E. Ju., Dorosheva, Zh. V., Sidorovich, V. & Bychkov, A. A. (2012). Modern aspects of forensic diagnosis of traumatic brain injury. *Forensic-medical examination*, 55(1), 38-40.

[13] Ushenko, Y. A., Dubolazov, A. V., Karachevtsev, A. O., Sakhnovskiy, M. Y., Bizer, L. I., & Bodnar, O. B. (2014). *Multidimensional Mueller matrices microscopy of biological crystal networks structure.* In: 7th International Workshop on Advanced Optical Imaging and Metrology Fringe 2013. New York: Springer.

[14] Ushenko, A. G., Dubolazov, A. V., Ushenko, Y. A., Tomka, Y. Y., Karachevtsev, A. O., Sidor, M. I. & Prydiy, A. (2020). *Differential diagnosis of the limitation of the formation of hemorrhages of traumatic origin, cerebral infarction, ischemic and hemorrhagic genesis by polarization-phase tomography.* Proc. SPIE 0277-786X. In Fourteenth International Conference on Correlation Optics. 11369. doi: 10.1117/12.2553989

[15] Ushenko, A. G., Dubolazov, A. V., Ushenko, V. A., Ushenko, Y. A., Pidkamin, L. Y., Soltys, I. V. … Pavlyukovich, N. (2016). Mueller-matrix mapping of optically anisotropic fluorophores of molecular biological tissues in the diagnosis of death causes. Proceedings of SPIE - The International Society for Optical Engineering, 9971, №99712L.

[16] Ushenko, Y., Grytsyuk, M., Sakhnovskiy, M., Zhytaryuk, V., Slyotov, M., Soltys, I., & Motrich, A. (2020). *Forensic medical evaluation of cerebral infarction of hemorrhagic formations of hemorrhages of traumatic genesis using polarization-phase tomography.* In Fourteenth International Conference on Correlation Optics. 11369. doi: 10.1117/12.2553991

[17] Ushenko, V. A., Sdobnov, A. Y., Mishalov, W. D., Dubolazov, A. V., Olar, O. V., Bachinskyi, V. T. … Meglinski, I. (2019). Biomedical applications of Jones-matrix tomography to polycrystalline flms of biological fuids. *Journal of Innovative Optical Health Sciences,* 12(6), 1950017-1-13. doi: 10.1142/S1793545819500172

[18] Ushenko, Y. A., Trifonyuk, L. Y., Dubolazov, A. V., & Karachevtsev, A. O. (2014). Fourier-domain Jones-matrix mapping of a complex degree of mutual anisotropy in differentiation of biological tissues' pathological states. *Applied*

Optics, 53(10), B205-B214.
[19] Vanchulyak, O. Ya. (2016). *Expert assessment of acute myocardial ischemia by polarization-correlation methods*. Kyiv.
[20] Vanchulyak, O., Ushenko, Y., Galochkin, O., Sakhnovskiy, M., Kovalchuk, M., Dovgun, A., … Bodnar, G. (2019). Azimuthal fractalography of networks of biological crystals. *Proceedings of SPIE - The International Society for Optical Engineering.,* 11105, №1110517.
[21] Vanchulyak, O., Ushenko, Y., Galochkin, O., Sakhnovskiy, M., Kovalchuk, M., Dovgun, A. ... Bodnar, G. (2019). Azimuthal fractalography of networks of biological crystals. Proceedings of SPIE, 11105, *Novel Optical Systems, Methods, and Applications.* XXII, 1110517. (doi: 10.1117/12.2529337)
[22] Vorlou, Ch. P., Dennis, M. S., & Gejn, Zh. (1998). *Stroke. A practical guide to patient management.* S.-Pb.: Politehnika.
[23] Walsh, K. B. (2019). Non-invasive sensor technology for prehospital stroke diagnosis: Current status and future directions. *Int. J. Stroke*. 14(6), 592-602. doi: 10.1177/1747493019866621
[24] Zasler, N. D. & Bender, S. D. (2019). Validity assessment in traumatic brain injury impairment and disability evaluations. *Physical Medicine and Rehabilitation Clinics,* 30(3), 621-636. doi: 10.1016/j.pmr.2019.03.009

ВИКОРИСТАННЯ ЛІНІЙНОГО ДИХРОЇЗМУ АЗИМУТАЛЬНО-ІНВАРІАНТНИХ МЮЛЛЕР-МАТРИЧНИХ ЗОБРАЖЕНЬ ГІСТОЛОГІЧНИХ ЗРІЗІВ РЕЧОВИНИ ГОЛОВНОГО МОЗКУ ДЛЯ ДІАГНОСТИКИ ҐЕНЕЗУ КРОВОВИЛИВУ

Гараздюк М.С., Дуболазов О.В., Маланчук С.М.

Диференційна діагностика причини смерті (ПС) від ішемічного інфаркту мозку (ІІМ), крововиливів травматичного (КТҐ) та нетравматичного (КНҐ) ґенезу дозволяє виключити насильницький характер смерті. Метою роботи була розробка судово-медичних критеріїв для диференціації крововиливів травматичного та нетравматичного ґенезу та ІІМ за допомогою азимутально-інваріантних зображень матриці Мюллера лінійного дихроїзму гістологічних зрізів речовини головного мозку (РГМ). Для дослідження були використані нативні зрізи РГМ від 130 трупів у разі: смерті від ішемічної хвороби серця (ІХС) - 40 нативних зрізів (група 1 - контроль); КТҐ - 30 зрізів (група 2), ІІМ - 30 зрізів (група 3), КНҐ - 30 зрізів (група 4). Вимірювання значень розподілу координатних параметрів поляризації в точках мікроскопічних зображень проводилося в місці розташування стандартного стокс-поляриметра. Ефективність міжгрупової диференціації зразків мозку померлих від травматичних крововиливів та ішемічного інфаркту мозку досягає задовільного рівня і становить 76-83%. Ефективність міжгрупової диференціації зразків у випадках смерті від крововиливів травматичного та нетравматичного ґенезу є задовільного рівня і становить 75-82%. Що стосується диференціації між ІІМ та КНҐ, то цей метод є неефективним.

Ключові слова: *крововиливи травматичного ґенезу, крововиливи нетравматичного ґенезу, ішемічний інфаркт мозку, Мюллер-матричне картографування.*

ИСПОЛЬЗОВАНИЕ ЛИНЕЙНОГО ДИХРОИЗМА АЗИМУТАЛЬНО-ИНВАРИАНТНЫХ МЮЛЛЕР-МАТРИЧНЫХ ИЗОБРАЖЕНИЙ ГИСТОЛОГИЧЕСКИХ СРЕЗОВ ВЕЩЕСТВА ГОЛОВНОГО МОЗГА ДЛЯ ДИАГНОСТИКИ ГЕНЕЗА КРОВОИЗЛИЯНИЯ

Гараздюк М.С., Дуболазов А.В., Маланчук С.М.

Дифференциальная диагностика причины смерти (ПС) от ишемического инфаркта мозга (ИИМ), кровоизлияний травматического (КТГ) и нетравматического (КНГ) генеза позволяет исключить насильственный характер смерти. Целью работы была разработка судебно-медицинских критериев для дифференциации кровоизлияний травматического и нетравматического генеза и ИИМ с помощью азимутально-инвариантных изображений матрицы Мюллера линейного дихроизма гистологических срезов вещества головного мозга (ВГМ). Для исследования были использованы нативные срезы ВГМ от 130 трупов в случае: смерти от ишемической болезни сердца (ИБС) - 40 нативных срезов (группа 1 - контроль); КТГ - 30 срезов (группа 2), ИИМ - 30 срезов (группа 3), КНГ - 30 срезов (группа 4). Измерение значений распределения координатных параметров поляризации в точках микроскопических изображений проводили в месте расположения стандартного стокс-поляриметра. Эффективность межгрупповой дифференциации образцов мозга умерших от травматических кровоизлияний и ишемического инфаркта мозга достигает удовлетворительного уровня и составляет 76-83%. Эффективность межгрупповой дифференциации образцов в случаях смерти от кровоизлияния травматического и нетравматического генеза является удовлетворительного уровня и составляет 75-82%. Что касается дифференциации между ИИМ и КНГ, то этот метод неэффективен.

Ключевые слова: *кровоизлияния травматического генеза, кровоизлияния нетравматического генеза, ишемический инфаркт мозга, Мюллер-матричное картографирование.*

DOI: 10.31393/morphology-journal-2020-26(2)-10 Reports of Morphology, Vol. 26, №2, Pages 67-73

ISSN 1818-1295 eISSN 2616-6194

REPORTS OF MORPHOLOGY

Official Journal of the Scientific Society of Anatomists, Histologists, Embryologists and Topographic Anatomists of Ukraine

journal homepage: https://morphology-journal.com

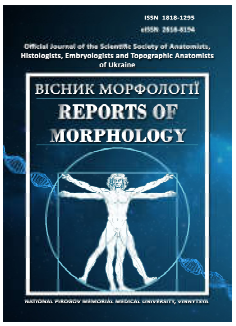

Fractal dimension of phylogenetically different parts of the human cerebellum (magnetic resonance imaging study)

Maryenko N.I., Stepanenko O.Yu.
Kharkiv National Medical University, Kharkiv, Ukraine

ARTICLE INFO
Received: 29 July, 2020
Accepted: 3 September, 2020

UDC: 611:57.086:517:530.191

CORRESPONDING AUTHOR
e-mail: maryenko.n@gmail.com
Maryenko N.I.

In recent years, fractal analysis has been increasingly used as a morphometric method, which allows to assess the complexity of the organization of quasi-fractal biological structures, including the cerebellum. The aim of the study was to determine the value of fractal dimension of phylogenetically different parts of the cerebellum by studying magnetic resonance imaging of the brain using the method of pixel dilation and to identify gender and age characteristics of individual variability of fractal dimension of the cerebellum and its external linear contour. The study was performed on the magnetic resonance images of the brain of 120 relatively healthy patients in age 18-86 years (65 women, 55 men). T2 weighted tomographic images were investigated. Fractal analysis was performed using the method of pixel dilation in the author's modification. Fractal dimension (FD) values were determined for cerebellar tomographic images segmented with brightness values of 100 (FD_{100}), 90 (FD_{90}) and in the range of 100-90 (FD_{100-90} or fractal dimension of the outer cerebellar contour) in its upper and lower lobes, which include phylogenetically different zones. The obtained data were processed using generally accepted statistical methods. The average value of FD_{100} of the upper lobe of the cerebellum was 1.816±0.005, the lower lobe - 1.855±0.005. The average value of FD_{90} of the upper lobe of the cerebellum was 1.734±009, the lower lobe - 1.768±0.009. The average value of FD_{100-90} of the upper lobe of the cerebellum was 1.370±0.009, the lower lobe - 1.431±0.008. All three values of the fractal dimension of the lower lobe, which lobules have a lower phylogenetic age, are statistically significantly higher than the corresponding values of the fractal dimension of the upper lobe, have a more pronounced correlation with age than in the upper lobe. The developed research algorithm can be used to assess the condition of the cerebellum as an additional morphometric method during magnetic resonance imaging study of the brain.
Key words: *fractal analysis, cerebellum, magnetic resonance imaging.*

Introduction

Modern diagnostic methods of neuroimaging (CT, MRI and others) are the methods of choice for lifelong assessment of the morphofunctional state of various brain structures and the diagnosis of various pathological changes and diseases of the nervous system. Images of different brain structures obtained using these diagnostic methods allow to determine different qualitative characteristics (shape, individual anatomical features, the presence of foci of pathological changes, etc.) and quantitative characteristics (linear dimensions, area of different structures, brightness values, etc.). To determine the quantitative characteristics of brain structures on tomograms mainly use the methods of traditional morphometry, which allow to determine simple geometric characteristics - linear dimensions, area, volume [5, 7, 9, 10, 14].

Among the various structures of the CNS, the cerebellum has the most geometrically complex shape and spatial configuration, the cortex of which, forming its outer contour, forms a complex three-dimensional convoluted structure, which is difficult to quantify using morphometry methods commonly used to assess tomograms.

In recent years, fractal analysis has been increasingly used to assess complex branched biological structures. This method as a morphometric allows to estimate the degree of complexity of the organization and filling of space with quasi-fractal structures that have the properties of fractals - self-similarity, self-repetition and large-scale

invariance. The value determined by fractal analysis is a fractal index or fractal dimension (FD), which can take values from 1 to 2 [3, 4].

Various modifications of fractal analysis are used to study the cerebellum and other CNS structures [3, 4, 6, 8, 11, 12, 15-17, 19-21], the most commonly used of which is the box counting method [1, 2, 12, 16, 17, 19, 20] and pixel dilation method [11, 13].

In most works use fractal analysis to study different CNS structures with visual identification of the boundaries of the studied structures [12, 17] and skeletonization of images [11], which allows to determine the fractal dimension of skeleton images that correspond to the main branches of white matter. The cerebellum is a rather complex structure, so its fractal analysis must be multicomponent and take into account the study of various elements that can be identified using different image segmentation algorithms. In particular, in addition to skeletonization, you can use the determination of the fractal dimension of the external linear contour of the cerebellum and the fractal dimension of cerebellar tissue as a whole, which will objectively assess the morphofunctional state of the cerebellum by quantifying the complexity of the spatial configuration of its cortex. In addition, different anatomical areas of the cerebellum, which have different phylogenetic age, have some differences in structure [18], which in turn may affect the value of the fractal dimension and patterns of their variability.

The aim of the study was to determine the value of fractal dimension of phylogenetically different parts of the cerebellum by studying magnetic resonance imaging of the brain using pixel dilation and to identify sex and age characteristics of individual variability of fractal dimension of the cerebellum and its external linear contour.

Materials and methods

The study was performed on 120 magnetic resonance imaging of the brain of patients aged 18-86 years (mean age - 43.33±1.43 years, 65 women, 55 men), in which no organic pathology of the brain was detected, so the structure of the brain of these patients were considered as a conditional norm.

The study was conducted in compliance with the basic bioethical provisions of the Council of Europe Convention on Human Rights and Biomedicine (04.04.1997), the Helsinki Declaration of the World Medical Association on the ethical principles of scientific medical research with human participation (1964-2008), and the order of Ministry of Health of Ukraine №690 dated 23.09.2009. The conclusion of the Commission on Ethics and Bioethics of Kharkiv National Medical University confirms that the study was conducted in compliance with human rights, in accordance with current legislation in Ukraine, meets international ethical requirements and does not violate ethical standards in science and standards of biomedical research (minutes of the meeting of the commission on ethics and bioethics of KhNMU №10 from 07.11.2018).

Tomograms were obtained using a magnetic resonance imaging Siemens Magnetom Symphony with a magnetic induction value of 1.5 T. T2-weighted images were used for the study. The method of pixel dilatation in the author's modification described earlier was used for fractal analysis [13].

For fractal analysis, a fragment of a digital image of a tomogram containing a tomographic section of the cerebellum was copied and processed in Adobe Photoshop CS5. To study individual lobes from the image, 64x64 pixel sections corresponding to different phylogenetic and anatomical zones of the cerebellum were copied, namely: the upper lobe of the cerebellum, which includes the upper paleocerebellum (lobules I-V), the lower lobe of the cerebellum, which includes neocerebelum (lobules VI-VII), lower paleocerebellum with archicerebellum (lobules VIII-X) (Fig. 1A).

In order to separate the studied structure (cerebellar tissue) from the surrounding, background structures, image segmentation was performed. The image was transformed from halftone to binary format. The binary image consists of pixels of only two colors: black (which has a brightness value of 0 and corresponds to the studied structure) or white (has a brightness value of 255 and corresponds to the background pixels). Segmentation of cerebellar tissue in the image was performed using the tool "Threshold" of Adobe Photoshop CS5, which colors all pixels darker than the specified threshold value into black color, lighter - into white color (Fig. 1B).

For segmentation of tomographic sections of a cerebellum as a whole empirically established threshold value of brightness 100 (Fig. 1B). In order to investigate the outer contour of the cerebellum on a tomographic section, the brightness thresholds of 100 and 90 were empirically selected. Segmentation of digital tomographic images in this range (difference 100-90) allows to detect the outer linear contour of the cerebellum (Fig. 1D).

After segmentation, fractal analysis was performed using the pixel dilation method. To do this, the image resolution was gradually reduced from 64 pixels per inch to 32, 16, 8, 4, and 2 pixels per inch. In order to calculate the individual values of fractal dimension (FD) for the cerebellum as a whole and the contour separately, at each stage the number of segmented pixels corresponding to the studied structure was calculated for the threshold values of brightness 100 (N_1) and 90 (N_2) and their difference ($N_3=N_1 - N_2$). The FD values calculated with the value of N1 correspond to the FD of the tomographic section of the cerebellum as a whole, N_3 - FD contour of the cerebellar tissue.

FD values were determined for tomographic images of the cerebellum, segmented with brightness values 100 (FD_{100}), 90 (FD_{90}) and in the range of 100-90 (FD_{100-90} or fractal dimension of the outer contour of the cerebellum) for its upper and lower lobes, including phylogenetically

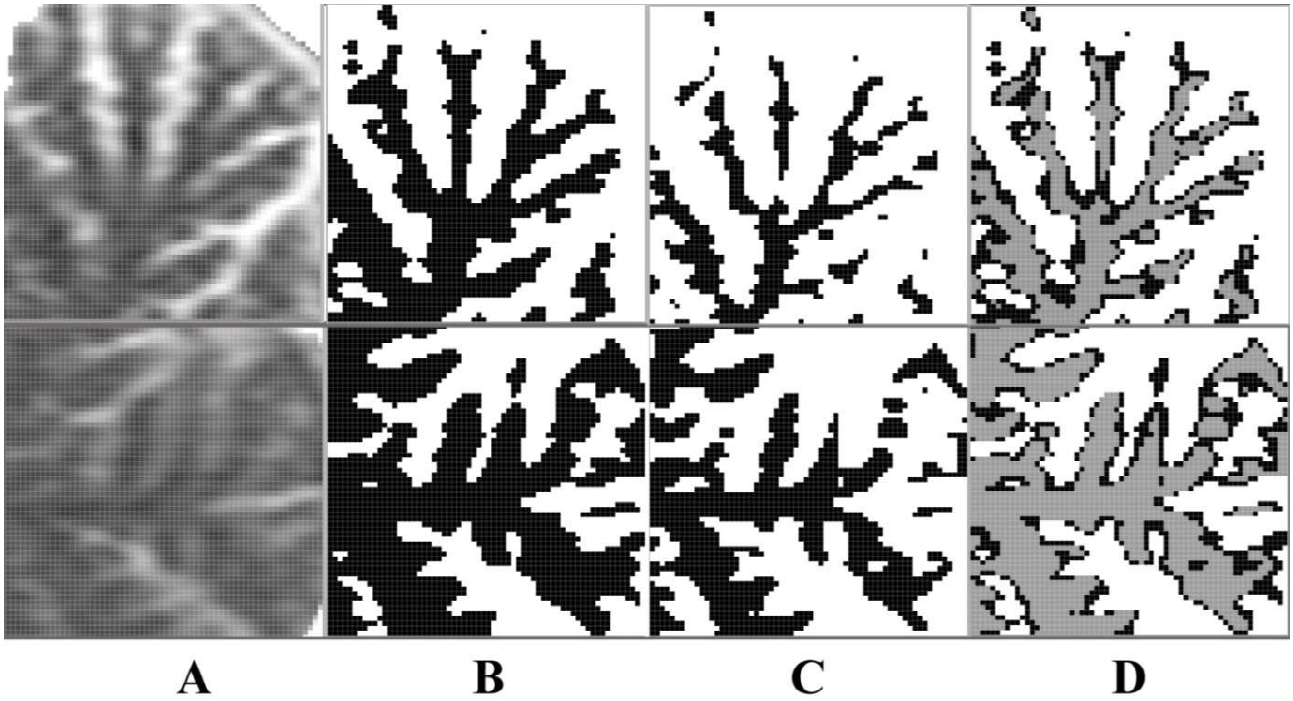

Fig. 1. Segmentation of digital image of magnetic resonance imaging of the human cerebellum. The upper row of images - upper lobe of the cerebellum, the lower row - lower lobe. A - the original image; B - segmentation with a threshold value of brightness 100, C - segmentation with a threshold value of brightness 90, D - the difference between the thresholds 100 and 90, which corresponds to the contour of the cerebellum, is shown in black color.

different zones.

Statistical data processing was performed using Microsoft Excel 2010. The following values were calculated: arithmetic mean (M) and its error (m_M). To determine the distribution of values, the median (Me), the values of the 25th and 75th percentiles, the minimum (min) and maximum (max) values were determined. Pearson's correlation coefficient was calculated to determine the relationship between the values. The significance of statistical differences and the significance of the correlation were assessed using Student's t test.

Results

The average value of FD_{100} of the upper lobe of the cerebellum was 1.816±0.005, the lower lobe - 1.855±0.005. The average value of FD_{90} of the upper lobe of the cerebellum was 1.734±0.009, the lower lobe - 1.768±0.009. The average value of FD_{100-90} of the upper lobe of the cerebellum was 1.370±0.009, the lower lobe - 1.431±0.008. The distribution of fractal dimension values determined for the upper and lower lobes of the cerebellum is shown in Fig. 2.

The highest values are FD of tomographic sections of the cerebellum, segmented with a brightness threshold of 100 (FD_{100}), slightly lower - 90 (FD_{90}). The lowest value has FD of the outer contour of the cerebellum (FD_{100-90}).

FD_{100} has statistically significantly greater values than FD_{90} and in the upper lobe of the cerebellum ($p=9.61e^{-14}$), and in the lower lobe ($p=3.61e^{-15}$), also has statistically significantly greater values than FD_{100-90} in both parts (upper lobe - $p=8.9e^{-113}$; lower lobe - $p=3.7e^{-117}$). In turn, FD_{90} is statistically significantly higher than the value of FD_{100-90} in the upper ($p=1.98e^{-78}$) and lower (p=6.98e-77) lobes of the cerebellum.

All three values of FD of the lower lobe of the cerebellum, which corresponds to the phylogenetically younger areas of the cerebellum (neocerebellum and lower paleocerebellum), are statistically significantly higher than the corresponding values of FD of the lower lobe of the cerebellum, which corresponds to phylogenetically older areas (upper paleocerebelum) (FD_{100} - $p=1.23e^{-7}$; FD_{90} - p=0.009; FD_{100-90} - $p=1.27e^{-6}$). This feature generally reflects the peculiarities of the organization of cerebellar lobules at the micro-macroscopic level: lobules of neocerebellum and lower paleocerebellum, which have a smaller phylogenetic age, generally have a more complex spatial configuration due to more complex and diverse variants of structure and branching of white matter in these lobules, which patterns of individual anatomical variability have been described in our previous studies [18].

The calculated FD values (FD_{100}, FD_{90}, FD_{100-90}) are correlated by different strengths and orientations. Thus, FD_{100} is associated with FD_{90} by a strong positive correlation (upper lobe - r=0.92, $p=2.84e^{-24}$; lower lobe - r=0.96, $p=2.43e^{-35}$). But FD_{100} is associated with FD_{100-90} by negative correlation of weak force in the upper lobe (r=-0.27, p=0.004) and negative correlation of medium force in the lower lobe (r=-0.45, $p=2.12e^{-5}$). FD_{90} is also associated with FD_{100-90} by

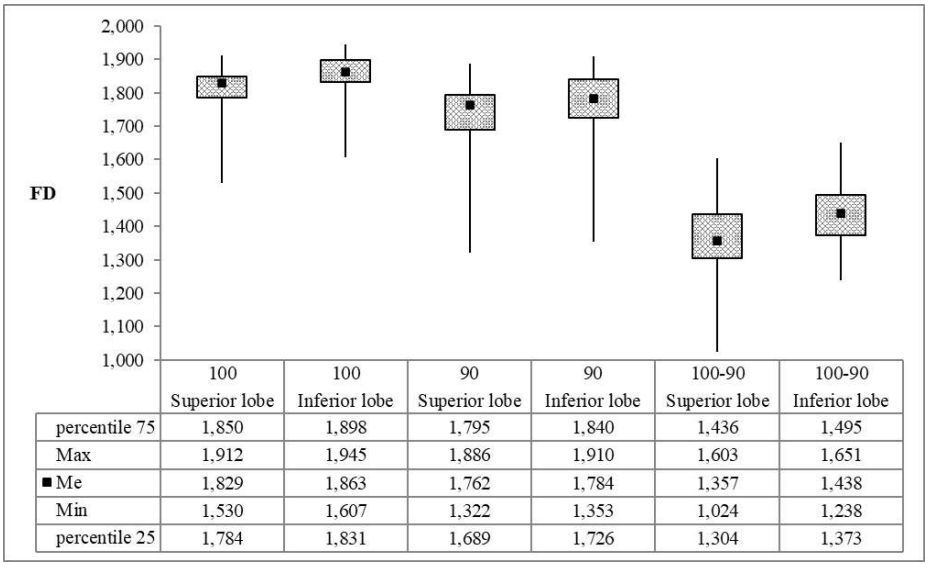

	100 Superior lobe	100 Inferior lobe	90 Superior lobe	90 Inferior lobe	100-90 Superior lobe	100-90 Inferior lobe
percentile 75	1,850	1,898	1,795	1,840	1,436	1,495
Max	1,912	1,945	1,886	1,910	1,603	1,651
■ Me	1,829	1,863	1,762	1,784	1,357	1,438
Min	1,530	1,607	1,322	1,353	1,024	1,238
percentile 25	1,784	1,831	1,689	1,726	1,304	1,373

Fig. 2. Distribution of fractal dimension values (FD_{100}, FD_{90}, FD_{100-90}) of the upper and lower parts of the human cerebellum.

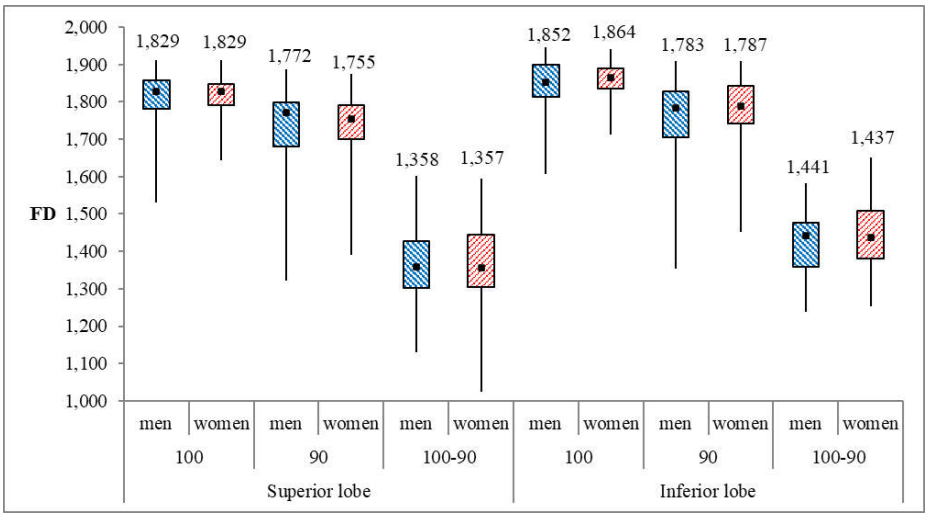

Fig. 3. Distribution of fractal dimension values (FD_{100}, FD_{90}, FD_{100-90}) of the upper and lower lobes of the human cerebellum in men and women.

negative correlation of medium strength in both parts of the cerebellum (upper lobe - r=-0.57, p=2.41e^{-7}; lower lobe - r=-0.65, p=5.34e^{-9}).

Paired values of the FD of the same name of the upper and lower lobes are related by a positive correlation (FD_{100} - r=0.76, p=3.26e^{-12}; FD_{90} - r=0.85, p=9.24e^{-17}; FD_{100-90} - r=0.83, p=1.87e^{-15}).

Sex characteristics were also determined: three FD values for the upper and lower lobes of the cerebellum in men and women were determined. The average value of FD^{100} of the upper lobe of the cerebellum in men was 1.815±0.006, in women - 1.816±0.006, the lower lobe in men - 1.847±0.009, in women - 1.863±0.006. The average value of FD^{90} of the upper lobe of the cerebellum in men was 1.734±0.014, in women - 1.735±0.011, the lower lobe in men - 1.759±0.015, in women - 1.776±0.011. The average value of FD_{100-90} of the upper lobe of the cerebellum in men was 1.366±0.012, in women - 1.372±0.013, the lower lobe in men - 1.422±0.012, in women - 1.438±0.011. The distribution of fractal dimension values (FD_{100}, FD_{90}, FD_{100-90}) in men and women is shown in Fig. 3.

Thus, the values of FD in men and women have almost no difference, statistically significant difference don't have all three fractal indices: FD_{100} (upper lobe - p=0.91; lower lobe - p=0.12), FD_{90} (upper lobe - p=0.99; lower lobe - p=0.34) and FD_{100-90} (upper lobe - p=0.74; lower lobe - p=0.32), which indicates the absence of statistically significant sex differences in the studied indicators.

In addition to sex, the age features of variability of fractal dimension in different parts of the cerebellum were also studied (Fig. 4). It was found that FD_{100} has a positive correlation with age (upper lobe - r=0.29, p=0.002; lower lobe - r=0,41, p=7,61e-5) as well as FD_{90} (upper lobe - r=0.38, p=0.0001; lower lobe - r=0.50, p=3.75e-6). In contrast to these indicators, FD_{100-90} has a negative correlation with age in both lobes (upper lobe - r=-0.44, p=2.94e-5; lower lobe - r=-0.58, p=1.57e-7). At the same time more expressed changes are observed in the lower lobe of a cerebellum (Fig. 3) which has smaller phylogenetic age.

FD_{100-90} characterizes the complexity of the organization of the outer contour of the cerebellum, which in turn characterizes the features of the spatial configuration of the cerebellar cortex. This figure decreases with age in both lobes of the cerebellum, which reflects the process of age-related atrophy of the cerebellum, which is accompanied by a decrease in the degree of convoluting of the cortex, which leads to a decrease in the fractal index of the outer contour of the cerebellum. More pronounced age-related changes are observed in phylogenetically younger areas, which have higher values of fractal dimension in general (which reflects the more complex and diverse structure of these lobules). Thus, areas of the cerebellum that have a more complex spatial configuration of the cortex are characterized by a

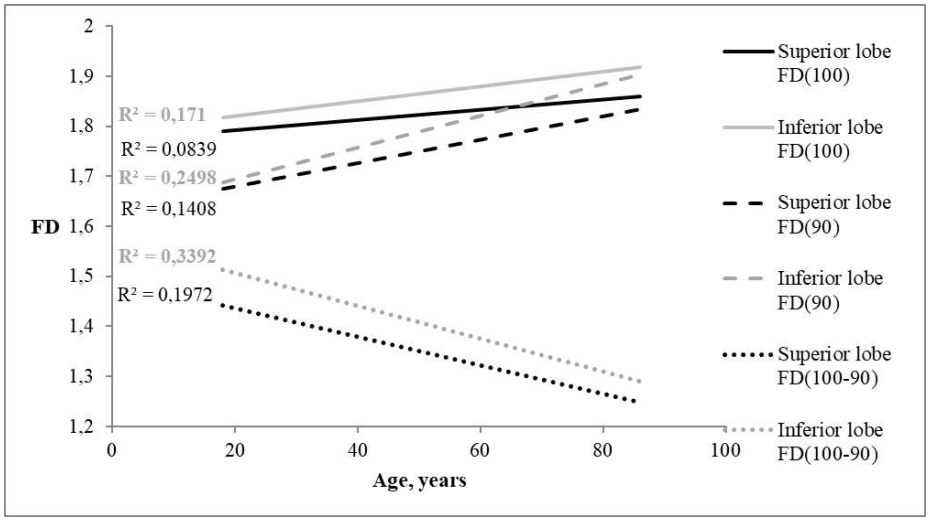

Fig. 4. Values of fractal dimension (FD_{100}, FD_{90}, FD_{100-90}) of the upper and lower lobes of the cerebellum depending on age.

more pronounced decrease in the fractal index with age than areas that have a less complex structure and greater phylogenetic age.

It should be noted that the decrease in this indicator is more pronounced in men (upper lobe - r=-0.54, $p=8.24e^{-6}$; lower lobe - r=-0.67, $p=1.76e^{-8}$) than in women (upper lobe - r=-0.37, lower lobe - p=0.002; r=-0.51, $p=2.60e^{-5}$), which reflects the more pronounced age-related atrophy of the cerebellum, characteristic for men.

Discussion

The values of the fractal dimension obtained in this study exceed the values of the fractal dimension obtained by us earlier in the study of sectional material (1.372±0.006) [16]. This difference is due to the fact that in this study we determined the fractal dimension of tomographic sections of the cerebellum as a whole and its outer linear contour, while on the section material we determined the fractal dimension of the main branches of the white matter of the cerebellum.

Another values of the fractal dimension of the cerebellum have been obtained in the works of other scientists. The values of the fractal dimension of two-dimensional images of the cerebellum, calculated on MR tomograms of 16 relatively healthy patients using the method of counting squares, were 1.49±0.06 and 1.56±0.05 for white and gray matter, respectively [1]. In other works, three-dimensional values of fractal dimension were determined: three-dimensional FD value of white matter was 2.26±0.05 [2] and 2.277±0.045 [19], gray matter - 2.49±0.04 [2] and 2.5267±0.0228 [19]. In these works, the FD values were determined using the method of counting squares. In another work [11], the values of FD of skeletonized branches of the cerebellar white matter were determined using one of the modifications of the pixel dilatation method. The value of the three-dimensional fractal dimension obtained as a result of this study was 2.57±0.01. The difference between the average values of the fractal dimension obtained as a result of our and other studies can be explained by the peculiarities of the method of determining the fractal dimension and the differences of the cerebellar segmentation algorithm into different components of the structure and background.

Fractal analysis of magnetic resonance imaging of the brain can be used to diagnose the condition of the cerebellum as an additional morphometric study in magnetic resonance imaging of the brain. The obtained data and described research algorithms can be used for morphometric examination of the cerebellum using magnetic resonance imaging.

Conclusions

1. As a result of the study of magnetic resonance imaging of the brain with the help of the author's modification of the method of pixel dilatation, the value of the fractal dimension of tomographic sections of the cerebellum as a whole and its external linear contour was determined.

2. All three values of the fractal dimension (FD_{100}, FD_{90}, FD_{100-90}) of the lower lobe, lobules of which have a lower phylogenetic age, statistically significantly exceed the corresponding values of the fractal dimension of the upper lobe and have a more pronounced correlation with age compared to the upper lobe. These features are consistent with the structure of the cerebellar lobules belonging to its lower lobe, and are characterized by a more complex and diverse structure than lobules belonging to the upper lobe of the cerebellum and have a greater phylogenetic age.

References

[1] Akar, E., Kara, S., Akdemir, H., & Kiris, A. (2015). Fractal dimension analysis of cerebellum in Chiari Malformation type I. *Computers in Biology and Medicine*, 64, 179-186. https://doi.org/10.1016/j.compbiomed.2015.06.024

[2] Akar, E., Kara, S., Akdemir, H., & Kiris, A. (2017). 3D structural complexity analysis of cerebellum in Chiari malformation type I. *Medical & Biological Engineering & Computing*, 55(12), 2169-2182. https://doi.org/10.1007/s11517-017-1661-7

[3] Di Ieva, A., Esteban, F. J., Grizzi, F., Klonowski, W., & Martin-Landrove, M. (2015). Fractals in the neurosciences, Part II: clinical applications and future perspectives. *The Neuroscientist: a review journal bringing neurobiology, neurology and psychiatry,* 21(1), 30-43. https://doi.org/10.1177/1073858413513928

[4] Di Ieva, A., Grizzi, F., Jelinek, H., Pellionisz, A. J., & Losa, G. A. (2014). Fractals in the Neurosciences, Part I: General Principles and Basic Neurosciences. *The Neuroscientist: a review journal bringing neurobiology, neurology and psychiatry,* 20(4), 403-417. https://doi.org/10.1177/1073858413513927

[5] Diedrichsen, J., Balsters, J. H., Flavell, J., Cussans, E., & Ramnani, N. (2009). A probabilistic MR atlas of the human cerebellum. *NeuroImage,* 46(1), 39-46. https://doi.org/10.1016/j.neuroimage.2009.01.045

[6] Grizzi, F., Castello, A., Qehajaj, D., Russo, C., & Lopci, E. (2019). The Complexity and Fractal Geometry of Nuclear Medicine Images. *Molecular Imaging and Biology*, 21(3), 401-409. https://doi.org/10.1007/s11307-018-1236-5

[7] He, N., Langley, J., Huddleston, D. E., Ling, H., Xu, H., Liu, C. … Hu, X. P. (2017). Improved Neuroimaging Atlas of the Dentate Nucleus. *Cerebellum,* 16(5-6), 951-956. https://doi.org/10.1007/s12311-017-0872-7

[8] John, A. M., Elfanagely, O., Ayala, C. A., Cohen, M., & Prestigiacomo, C. J. (2015). The utility of fractal analysis in clinical neuroscience. *Reviews in the Neurosciences,* 26(6), 633-645. https://doi.org/10.1515/revneuro-2015-0011

[9] Lee, D. K., Yoon, U., Kwak, K., & Lee, J. M. (2015). Automated Segmentation of Cerebellum Using Brain Mask and Partial Volume Estimation Map. *Computational and Mathematical Methods in Medicine,* 167489. https://doi.org/10.1155/2015/167489

[10] Lehman, V. T., Black, D. F., DeLone, D. R., Blezek, D. J., Kaufmann, T. J., Brinjikji, W., & Welker, K. M. (2020). Current concepts of cross-sectional and functional anatomy of the cerebellum: a pictorial review and atlas. *The British Journal of Radiology*, 93(1106), 20190467. https://doi.org/10.1259/bjr.20190467

[11] Liu, J. Z., Zhang, L. D., & Yue, G. H. (2003). Fractal dimension in human cerebellum measured by magnetic resonance imaging. *Biophysical Journal,* 85(6), 4041-4046. https://doi.org/10.1016/S0006-3495(03)74817-6

[12] Liu, S., Fan, X., Zhang, C., Wang, Z., Li, S., Wang, Y. … Jiang, T. (2019). MR imaging based fractal analysis for differentiating primary CNS lymphoma and glioblastoma. *European Radiology,* 29(3), 1348-1354. https://doi.org/10.1007/s00330-018-5658-x

[13] Maryenko, N. I., & Stepanenko, O. Yu. (2019). Fractal analysis as a morphometric method in morphology: a pixel dilatation technique in the study of digital images of anatomical structures. *Medicine Today and Tomorrow,* 82(1), 8-14. https://doi.org/10.35339/msz.2019.82.01.02

[14] Park, M. T., Pipitone, J., Baer, L. H., Winterburn, J. L., Shah, Y., Chavez, S. … Chakravarty, M. M. (2014). Derivation of high-resolution MRI atlases of the human cerebellum at 3T and segmentation using multiple automatically generated templates. *NeuroImage,* 95, 217-231. https://doi.org/10.1016/j.neuroimage.2014.03.037

[15] Ristanovic, D., & Milosevic, N. T. (2012). Fractal analysis: methodologies for biomedical researchers. *Theoretical Biology Forum,* 105(2), 99-118.

[16] Smitha, K. A., Gupta, A. K., & Jayasree, R. S. (2015). Fractal analysis: fractal dimension and lacunarity from MR images for differentiating the grades of glioma. *Physics in Medicine and Biology,* 60(17), 6937-6947. https://doi.org/10.1088/0031-9155/60/17/6937

[17] Stepanenko, A. Yu., & Maryenko, N. I. (2017). Fractal analysis of the human cerebellum white matter. *World of Medicine and Biology,* 61(3), 145-149. https://doi.org/10.26724/2079-8334-2017-3-61-145-149

[18] Stepanenko, A. Yu., & Maryenko, N. I. (2014). The variants of white matter branches structure of human cerebellum vermis. *Bulletin of Problems in Biology and Medicine,* 4(2), 259-264.

[19] Wu, Y. T., Shyu, K. K., Jao, C. W., Wang, Z. Y., Soong, B. W., Wu, H. M., & Wang, P. S. (2010). Fractal dimension analysis for quantifying cerebellar morphological change of multiple system atrophy of the cerebellar type (MSA-C). *NeuroImage,* 49(1), 539-551. https://doi.org/10.1016/j.neuroimage.2009.07.042

[20] Zaletel, I., Ristanovic, D., Stefanovic, B. D., & Puskas, N. (2015). Modified Richardson's method versus the box-counting method in neuroscience. *Journal of Neuroscience Method*s, 242, 93-96. https://doi.org/10.1016/j.jneumeth.2015.01.013

[21] Zhang, L., Liu, J. Z., Dean, D., Sahgal, V., & Yue, G. H. (2006). A three-dimensional fractal analysis method for quantifying white matter structure in human brain. *Journal of Neuroscience Methods,* 150(2), 242-253. https://doi.org/10.1016/j.jneumeth.2005.06.021

ФРАКТАЛЬНА РОЗМІРНІСТЬ ФІЛОГЕНЕТИЧНО РІЗНИХ ДІЛЯНОК МОЗОЧКА ЛЮДИНИ (ЗА ДАНИМИ ДОСЛІДЖЕННЯ МАГНІТНО-РЕЗОНАНСНИХ ТОМОГРАМ)

Мар'єнко Н.І., Степаненко О.Ю.

Фрактальний аналіз в останні роки все частіше використовують у якості морфометричного методу, що дозволяє оцінювати ступінь складності організації квазифрактальних біологічних структур, у тому числі й мозочка. Мета дослідження - визначити значення фрактальної розмірності філогенетично різних ділянок мозочка шляхом дослідження магнітно-резонансних томограм головного мозку за допомогою методу дилатації пікселів та виявити гендерні та вікові особливості індивідуальної мінливості фрактальної розмірності мозочка та його зовнішнього лінійного контуру. Дослідження проведене на 120 магнітно-резонансних томограмах головного мозку умовно здорових пацієнтів віком 18-86 років (65 жінок, 55 чоловіків). Досліджені Т2 зважені томографічні зображення. Проведений фрактальний аналіз за допомогою методу дилатації пікселів у авторській модифікації. Визначались значення фрактальної розмірності (FD) для томографічних зображень мозочка, сегментованих зі значеннями яскравості 100 (FD_{100}), 90 (FD_{90}) та у діапазоні 100-90 (FD_{100-90} або фрактальна розмірність зовнішнього контуру мозочка) для його верхньої та нижньої часток, що включають філогенетично різні зони. Отримані дані обробляли за допомогою загальноприйнятих статистичних методів. Середнє значення FD_{100} верхньої частки мозочка становило 1,816±0,005, нижньої частки - 1,855±0,005. Середнє значення FD90 верхньої частки мозочка становило 1,734±0,009, нижньої частки - 1,768±0,009. Середнє значення FD_{100-90} верхньої частки мозочка становило 1,370±0,009, нижньої частки - 1,431±0,008. Усі три значення фрактальної розмірності нижньої частки, часточки якої мають менший філогенетичний вік, статистично значуще перевищують відповідні їм значення фрактальної розмірності верхньої частки, мають більш виражений кореляційний зв'язок із віком порівняно з верхньою часткою. Розроблений алгоритм дослідження може бути використаний для діагностики стану мозочка в якості додаткового морфометричного дослідження при проведенні магнітно-резонансної томографії головного мозку.

Ключові слова: *фрактальний аналіз, мозочок, магнітно-резонансна томографія.*

ФРАКТАЛЬНАЯ РАЗМЕРНОСТЬ ФИЛОГЕНЕТИЧЕСКИ РАЗЛИЧНЫХ УЧАСТКОВ МОЗЖЕЧКА ЧЕЛОВЕКА (ПО ДАННЫМ ИССЛЕДОВАНИЯ МАГНИТНО-РЕЗОНАНСНЫХ ТОМОГРАММ)

Марьенко Н.И., Степаненко А.Ю.

Фрактальный анализ в последние годы все чаще используют в качестве морфометрического метода, позволяющего оценивать степень сложности организации квазифрактальных биологических структур, в том числе и мозжечка. Цель исследования - определить значение фрактальной размерности филогенетически различных участков мозжечка путем исследования магнитно-резонансных томограмм головного мозга с помощью метода дилатации пикселей и выявить гендерные и возрастные особенности индивидуальной изменчивости фрактальной размерности мозжечка и его внешнего линейного контура. Исследование проведено на 120 магнитно-резонансных томограммах головного мозга условно здоровых пациентов в возрасте 18-86 лет (65 женщин, 55 мужчин). Исследованы Т2 взвешенные томографические изображения. Проведен фрактальный анализ с помощью метода дилатации пикселей в авторской модификации. Определены значения фрактальной размерности (FD) для томографических изображений мозжечка, сегментированных со значениями яркости 100 (FD_{100}), 90 (FD_{90}) и в диапазоне 100-90 (FD_{100-90} или фрактальная размерность внешнего контура мозжечка) для его верхней и нижней долей, включающих филогенетически различные зоны. Полученные данные обрабатывали с помощью общепринятых статистических методов. Среднее значение FD_{100} верхней доли мозжечка составило 1,816±0,005, нижней доли - 1,855±0,005. Среднее значение FD_{90} верхней доли мозжечка составило 1,734±0,009, нижней доли - 1,768±0,009. Среднее значение FD_{100-90} верхней доли мозжечка составило 1,370±0,009, нижней доли - 1,431±0,008. Все три значения фрактальной размерности нижней доли, дольки которой имеют меньший филогенетический возраст, статистически значимо превышают соответствующие им значения фрактальной размерности верхней доли, с возрастом имеют более выраженную корреляционную связь по сравнению с верхней долей. Разработанный алгоритм исследования может быть использован для диагностики состояния мозжечка в качестве дополнительного морфометрического исследования при проведении магнитно-резонансной томографии головного мозга.

Ключевые слова: *фрактальный анализ, мозжечок, магнитно-резонансная томография.*

Professor Cherkasov Viktor Gavrylovych (05.01.1953 - 20.09.2020)

Morphologists of Ukraine express their sincere condolences to relatives, friends, employees of the O.O. Bogomolets National Medical University on the untimely death of a prominent scientist, talented teacher, sincere man, highly respected Professor Viktor Gavrylovych Cherkasov.

On September 20, 2020, the Ukrainian Morphological School suffered an irreparable loss: a prominent morphologist, wise head of the Department of Anatomy, Encyclopaedical Man, Vice President of the Scientific Society of Anatomists, Histologists, Embryologists and Topographic Anatomists of Ukraine, Academician of the International Academy of Integrative Anthropology, Honored Worker of Science and Technology of Ukraine, Doctor of Medical Sciences, Professor Viktor Gavrylovych Cherkasov died.

Viktor Gavrylovych was born on January 5, 1953 in the city of Kirovograd.

In 1976 he graduated from the Kyiv Medical Institute named after O.O. Bogomolets. For more than 40 years Victor Gavrylovych selflessly served science, having passed the way from the post-graduate student to the head of basic department of anatomy: the post-graduate student (1976), the assistant (1979), the senior teacher, the senior lecturer (1991), the professor (1992), the head of department (2004-2020).

V.G. Cherkasov's scientific worldview was formed under the influence of an outstanding teacher, corresponding member of the National Academy of Pedagogical Sciences of Ukraine, Professor Ivan Ivanovych Bobryk. In the figure of Victor Gavrylovych successfully combined the qualities of a scientist, youth mentor and a talented organizer. Main directions of scientific research: ultrastructural aspects of development of blood and lymphatic vessels; experimental modeling of pathological processes; history of morphology; methodical principles of teaching human anatomy. In 1980 he defended his dissertation "Hemomicrocirculatory tract of the human thymus in the prenatal period of morphogenesis." The doctoral dissertation "Microcirculatory tract of the human immune system in the prenatal period of ontogenesis" was successfully defended in 1990.

He successfully worked as the head of the research sector of the Bogomolets National Medical University (2003-2008).

From 2008 to 2013, Viktor Gavrylovych was the dean of the medical faculty №1. Many graduates remember Cherkasov V.G. as a wise head of the faculty and a reliable assistant to applicants for higher education.

Since 1992, V.G. Cherkasov has been the Vice-President of the Scientific Society of Anatomists, Histologists, Embryologists and Topographic Anatomists of Ukraine, a member of the Academic Council of the Ministry of Health of Ukraine and a member of the Scientific Public Council at the SAC of Ukraine. Meetings with the participation of Viktor Gavrylovych were marked by indifference to the case and understanding of the importance of change for the better.

V.G. Cherkasov - author and co-author of over 300 scientific papers, 12 patents and copyright certificates, 9 monographs, 15 textbooks, 10 books, 3 atlases, was the editor-in-chief of the specialized journal "Bulletin of Morphology" and a member of the editorial boards of scientific journals in Ukraine. Under the supervision of V.G. Cherkasov 6 doctoral and 11 candidate dissertations were completed and successfully defended. Creative approach, in-depth analysis, quality performance of various tasks was in the first place in the activities of the scientist. Victor Gavrylovych was guided by such principles in the work of the specialized academic council at the Bogomolets National Medical University as a secretary, member and chairman of the council. As a member of the specialized academic council at National Pirogov Memorial Medical University, Vinnytsya was remembered by colleagues as a great professional morphologist. Most of Viktor Gavrylovych pupils now are heads of morphological departments in Ukraine.

V.G. Cherkasov performed significant scientific and pedagogical work as the head of the support department. Under

his leadership, programs of the discipline "Human Anatomy" were developed and implemented in Ukraine, which provided the latest organization of the educational process in human anatomy in Ukraine. The support department created the first national textbook "Human Anatomy" in three languages (Ukrainian, Russian, English), which is republished with changes and additions since 2006, gained wide recognition and became basic in human anatomy in higher education in Ukraine. Work on the textbook began with a team consisting of Golovatsky A.S., Sapin M.R., Parakhin A.I. and Kovalchuk O.I. in the early 2000s in order to create a textbook in Ukrainian on the work program of the Department of Anatomy in Ukraine. Victor Gavrylovych manuals on the anatomy of the nervous system and sense organs enjoyed the authority of teachers and students; later expanded and supplemented became the basis of sections of the textbook. Continuous improvement, quality control and additions brought the textbook "Human Anatomy. In three volumes" edited by Golovatsky A.S. and Cherkasov V.G. recognition among the anatomical school of Ukraine and students.

The famous anatomical collection of the Department of Anatomy of the Bogomolets National Medical University was under the special attention of Viktor Gavrylovych and it was on his initiative that the complete cataloging of preparations was carried out. Masterfully possessing historical and morphological data, Professor Cherkasov V.G. could spend hours touring the halls of the department, everyone was delighted with the presentation of information and depth of academic knowledge.

Victor Gavrylovych paid a lot of attention to the study of the history of anatomy, was an active promoter of the activities of Ukrainian morphologists. V.G. Cherkasov studied the creative and scientific path of many historical figures together with his colleagues not only from literary sources, but also visited the places of their birth. A trip to the city of Oster, where Volodymyr Oleksiyovych Betz was born, stood out among them. He walked along Betz Lane and Street, and had an interesting and long discussion with the director of the city's historical museum about the activities of a prominent Ukrainian morphologist. In almost all lectures later, Victor Gavrylovych explained to students how important it is to understand and study the historical aspects in science and education. In addition to the tradition of caring for the graves of employees of the department, at the initiative of V.G. Cherkasov, a memorial service was held on the anniversary of V.O. Betz.

For scientific research of the remains of the sarcophagus of Yaroslav the Wise in St. Sophia Cathedral in 2010 Cherkasov V. G. was awarded a Diploma (National Reserve "Sophia of Kyiv"). During this study, when sarcophagus was opened, bats were found in addition to the remains. In the discussion about their future fate, Viktor Gavrylovych noted "… we have never seen what angels look like - do not touch, let them stay".

Over the years of work at the Bogomolets National Medical University V.G. Cherkasov was formed as an outstanding morphologist, known abroad. Viktor Gavrylovych high professionalism and perseverance in achieving the goal were harmoniously combined with demanding, tactful and responsible. Victor Gavrylovych was a hard-working and demanding specialist, who was appreciated and respected by all who had to communicate and work together.

Viktor Gavrylovych was an extremely responsible and highly professional man, his life path is an example of selfless service to medical education and science. His active social and scientific-pedagogical activity has been awarded many prizes. For significant contribution to the development of health care and high professionalism in 2006 by the Decree of the President of Ukraine V.G. Cherkasov was awarded the Order "For Merit" of the III degree; in 2009 he was awarded the honorary title of "Honored Worker of Science and Technology of Ukraine". Victor Gavrylovych was awarded the Certificate of Appreciation and Diploma of the Ministry of Health of Ukraine, diplomas and awards, "Gold Medal of Betz" AGET of Ukraine.

Victor Gavrylovych will remain a kind and sensitive person in our hearts. Thoughts, scientific plans and achievements will be reproduced in the affairs of his many pupils, who will gratefully leave the memory of their Master in new scientific works, discoveries and history of anatomy.

REQUIREMENTS FOR ARTICLES

For publication, scientific articles are accepted only in English only with translation on Ukrainian or Russian, which contain the following necessary elements: UDC code; title of the article (in English, Ukrainian and Russian); surname, name and patronymic of the authors (in English, Ukrainian and Russian); the official name of the organization (institution) (in English, Ukrainian and Russian); city, country (in English, Ukrainian and Russian); structured annotations (in English, Ukrainian and Russian); keywords (in English, Ukrainian and Russian); introduction; purpose; materials and methods of research; research results; discussion; conclusions; bibliographic references.

The title of the article briefly reflects its contents and contains no more than 15 words.

Abstract. The volume of the annotation is 1800-2500 characters without spaces. The text of an annotation in one paragraph should not contain general phrases, display the main content of the article and be structured. The abstract should contain an introductory sentence reflecting the relevance of the study, the purpose of the study, a brief description of the methods of conducting research (2-3 sentences with the mandatory provision of the applied statistical methods), a description of the main results (50-70% of the volume of the abstract) and a concise conclusion (1 sentence). The abstract should be clear without familiarizing the main content of the article. Use the following expressions: "Detected ...", "Installed ...", "Fixed ...", "Impact assessed ...", "Characterized by regularities ...", etc. In an annotation, use an active rather than passive state.

Keywords: 4-6 words (or phrases).

"Introduction"

The introduction reflects the state of research and the relevance of the problem according to the world scientific literature (at least 15 references to English articles in international journals over the past 5 years). At the end of the entry, the purpose of the article is formulated (contains no more than 2-3 sentences, in which the problem or hypothesis is addressed, which is solved by the author).

"Materials and methods"

The section should allow other researchers to perform similar studies and check the results obtained by the author. If necessary, this section may be divided into subdivisions. Depending on the research objects, the ethical principles of the European Convention for the protection of vertebrate animals must be observed; Helsinki Declaration; informed consent of the surveyed, etc. (for more details, see "Public Ethics and its Conflict"). At the end of this section, a "statistical processing of results" section is required, which specifies the program and methods for processing the results obtained by the automobile.

"Results"

Requirements for writing this section are general, as well as for all international scientific publications. The data is presented clearly, in the form of short descriptions, and must be illustrated by color graphics (no more than 4) or drawings (no more than 8) and tables (no more than 4), the information is not duplicated.

"Discussion"

In the discussion, it is necessary to summarize and analyze the results, as possible, compare them with the data of other researchers. It is necessary to highlight the novelty and possible theoretical or practical significance of the results of the research. You should not repeat the information already listed in the "Introduction" section. At the end of the discussion, a separate paragraph should reflect the prospects for using the results obtained by the author.

"Conclusion"

5-10 sentences that summarize the work done (in the form of paragraphs or solid text).

"Acknowlegements"

Submitted after conclusion before bibliographic references.

"References"

References in the text are indicated by Arabic numerals in square brackets according to the numerology in the list of references. The list of references (made without abbreviations) sorted by alphabet, in accordance with the requirements of APA Style (American Psychological Association Style): with the obligatory referencing of all authors, work titles, journal names, or books (with obligatory publication by the publishing house, and editors when they are available), therefore, numbers or releases and pages. In the Cyrillic alphabets references, give the author's surnames and initials in English (Cyrillic alphabet in brackets), the title of the article or book, and the name of the magazine or the publisher first to be submitted in the original language of the article, and then in square brackets in English. If available, doi indexes must be provided on www.crossref.org (at least 80% of the bibliographic references must have their own doi indexes). Links to online publications, abstracts and dissertations are not welcome.

After the list of references, it is necessary to provide information about all authors (in English, Ukrainian and Russian): last name, first name and patronymic of the author, degree, place of work and position, **ORCID number** (each of the authors of the ORCID personal number if absence - free creation on the official website http://www.orcid.org) to facilitate the readers of this article to refer to your publications in other scientific publications.

The last page of the text should include the surname, name and patronymic of the author, degree, postal address, telephone number and e-mail of the author, with which the editors will maintain contact.

Concluding remarks

The manuscript should be executed in such a way that the number of refinements and revisions during the editorial of the article was minimal.

When submitting the article, please observe the following requirements. The volume of the article - not less than 15 and not more than 25 pages, Times New Roman, 14 pt, line spacing - one and a half, fields - 2 cm, sheet A4. Text materials should be prepared in the MS Word editor (* .docx), without indentations. Math formulas and equations to prepare in the embedded editor; graphics - in MS Excel. Use the units of the International Measurement System. Tables and drawings must contain the name, be numbered, and references to them in the text should be presented as follows: (fig. 1), or (table 1). The drawings should be in the format "jpg" or "tif"; when scanned, the resolution should be at least 800 dpi; when scanning half-tone and color images, the resolution should be at least 300 dpi. All figures must be represented in the CMYK palette. The statistical and other details are given below the table in the notes. Table materials and drawings place at the end of the text of the manuscript. All elements of the text in images (charts, diagrams, diagrams) must have the Times New Roman headset.

Articles are sent to the editorial board only in electronic form (one file) at the e-mail address nila@vnmu.edu.ua

Responsible editor - Gunas Igor Valeryovich (phone number: + 38-067-121-00-05; e-mail: gunas.red@gmail.com).

Signed for print 12.10.2020
Format 60x84/8. Printing offset. Order № 1024. Circulation 100.
Vinnytsia. Printing house “Tvory”, Keleckaya St., 51a
PO Box 8825, 600-Richchya Str., 21, Vinnytsya, 21007
Phone: +38 (0432) 603 000
+38 (096) 97-30-934, +38 (093) 89-13-852
e-mail: tvory2009@gmai.com
http://www.tvoru.com.ua